

In presenting this thesis in partial fulfillment of the requirements for an advanced degree at Idaho State University, I agree that the Library shall make it freely available for inspection. I further state that permission to download and/or print my thesis for scholarly purposes may be granted by the Dean of the Graduate School, Dean of my academic division, or by the University Librarian. It is understood that any copying or publication of this thesis for financial gain shall not be allowed without my written permission.

Signature _____

Date _____

TRACKING LATE DEVONIAN REACTIVATION OF THE TOOELE ARCH WITH
DETRITAL ZIRCON PROVENANCE, GREAT BASIN

Natalie Hollis

A thesis submitted as partial fulfillment
of the requirements for the degree of:

Masters of Science in
Geology

Idaho State University

2015

Committee Approval

To the Graduate Faculty:

The members of the committee appointed to examine the thesis of Natalie Hollis find it satisfactory and recommend that it be accepted.

Leif Tapanila,
Major Advisor

Paul Link,
Committee Member

Kenneth Bosworth,
Graduate Faculty Representative

Acknowledgements

First I would like to thank my advisor, Leif Tapanila, for his guidance throughout this thesis, as well as general life advice and merriment on an approximate weekly basis. Second, I thank committee member Paul Link for being an endless resource of books, knowledge, advice, and encouragement. Third, I'm grateful for my committee member Ken Bosworth for his interest in geology, as well as being great fun in teaching a statistics class.

I would also like to thank David Pearson for brief, but thought provoking conversations of structural geology and sedimentology, which were helpful throughout the development and writing of this thesis. I'm also thankful for him allowing me to use his mineral separation lab and help in creating zircon mounts.

My undergraduate advisor, Diane Clemens-Knott from California State University, Fullerton prepared me for graduate school and supported me throughout my graduate career by being a resource as well as a friend, for which I am very appreciative.

Thank you to Chelsi White, Mark Pecha, Nicky Geisler, and the rest of the staff at the Arizona LaserChron Center who are always extremely helpful and for the use of their lab.

I want to extend extreme gratitude to the agencies that helped to fund this project which include the ISU Geosciences Department Geslin Fund, Northwest Scientific Association, Rocky Mountain Section-SEPM Fluvial Sedimentology Award, and the National Science Foundation EAR 1024843 (P.I. Leif Tapanila).

To Melissa Neiers, Kate Zajanc, Diana Boyack, and Michelle Hughes I want to extend my deepest gratitude for taking care of so many department logistics, for being so welcoming, and for making the transition into graduate school so easy and enjoyable.

Thank you to Lori Tapanila for always being able to make me laugh, for friendship, for lunch dates, for ladies nights, fudge jokes, and making my last semester at ISU so much brighter, especially when I needed it.

Idaho State University would not have been the same without the numerous friends I made so quickly. Thank you to the original Galena Pod (Jess, Connor, Tess, John), but especially to Jessica Meyers, who's friendship came so quickly after the Glacier NP trip and the infamous wine incident.

Thank you to Leif's field vehicle Burbie, who was trusty and did not die on me when alone out in the field, though I am also thankful for Amber Hobbs and John Whiting who were my field partners on separate and brief outings.

A big thank you goes out to a very special border collie mix Mr. Lancey-Pants (and to Dave & Amanda Pearson for letting me borrow him) who provided all the snuggles, stress-relieving, and running a girl could need.

Last, but certainly not least, thank you to my Mom, Dad, and sister who encouraged me and were always there to talk to or listen without whom this project may not have been completed.

TABLE OF CONTENTS

List of Figures.....	vi
List of Tables.....	vii
Abstract.....	viii
Chapter 1: Introduction.....	1
Chapter 2: Geologic Setting.....	3
Great Basin Subsidence.....	3
Tooele Arch.....	3
Taghanic Onlap.....	3
Alamo Impact.....	6
Antler Orogeny.....	6
Stansbury Uplift.....	7
Stratigraphy.....	9
Chapter 3: Methods.....	13
Detrital Zircons.....	13
Isopach Map Reinterpretation.....	13
Chapter 4: Results.....	21
U-Pb Data.....	21
Isopach Maps.....	22
Chapter 5: Discussion.....	24
Model for Sediment Sources.....	24
Tooele Arch Activity.....	27
Antler Sedimentation.....	28
Foreland Basin Modeling.....	32
Timing of Antler Events.....	34
Chapter 6: Conclusions.....	36
References.....	37
Appendices.....	46
Appendix I: Detrital Zircon Data.....	46
Appendix II: Detrital Zircon Photograph.....	64
Appendix III: Petrographic Descriptions.....	65
Appendix IV: Photomicrographs.....	67
Appendix V: Foreland Basin Modelling Parameters.....	72

List of Figures

Figure 2.1 Location map of region of study.....	4
Figure 2.2 Subsidence curves of western Laurentia.....	5
Figure 2.3 Paleogeologic map of the Late Devonian Stansbury uplift.....	8
Figure 2.4 Stratigraphic correlation map.....	10
Figure 2.5 Qm-F-L Diagram of samples from this study.....	12
Figure 3.6 Stacked probability density plots of Late Devonian detrital zircon signatures.....	15
Figure 3.7 Stacked probability density plots of Middle Devonian Oxyoke Formation detrital zircon signatures.....	17
Figure 3.8 Reinterpreted isopach maps.....	19
Figure 5.9 Map of possible provenance from the North American craton.....	25
Figure 5.10 Step-wise progression of flexure and sea level rise as a model for sediment preservation.....	29
Figure 5.11 Modeled foreland basin curves of the Antler and Sevier orogenies.....	33

List of Tables

Table 3.1: Significant (>3 grains) populations of detrital zircons of all Late Devonian samples.....	16
Table 3.2: Significant (>3 grains) populations of detrital zircons of all Middle Devonian Oxyoke Formation samples.....	18

ABSTRACT:

Late Devonian sandstones track backbulge basin migration of the Antler foreland system. Coupled with the timing of subsidence, these backbulge basin sandstones constrain the Antler orogeny as beginning in the Givetian (Middle Devonian) rather than the previously constrained Famennian (Late Devonian). Comparing the approximate age of these sandstones and shortening in Nevada with previous studies, there is evidence for left-lateral migration of the Antler orogeny and associated terranes.

Detrital zircon provenance of these sandstones show populations chiefly >1800 Ma in southern Idaho and northern Utah, while detrital zircon populations of <1765 Ma exist in central Utah and southern Nevada. A signature containing both of these populations exists in north-central Utah and northeastern Nevada. This latitudinal change in detrital zircon signatures corresponds with the Tooele arch and gives evidence for the Tooele arch being a positive topographic into the Late Devonian. It is unknown if the Tooele arch remained active from the Silurian through Early Devonian, but it was likely reactivated in the Middle Devonian by the Antler Orogeny.

1. INTRODUCTION:

The early- to mid-Paleozoic passive margin of western Laurentia was dominated by carbonate production and punctuated by siliciclastic deposition. Since Neoproterozoic rifting of Rodinia, the major events on the west coast of Laurentia include the intermittent activity of the Tooele arch (Neoproterozoic-Ordovician), the Taghanic onlap (Middle-Late Devonian), the Alamo impact (Late Devonian), and the Antler orogeny (Late Devonian-early Mississippian).

The Antler orogeny records the Paleozoic transition from a passive to active collisional margin (Johnson and Pendergast, 1981) and was the first step in building the North American Cordillera. Sedimentary facies and fill patterns in Nevada and Utah allowed Goebel (1991) to identify an east-southeastward migration of the Antler foreland basin from mid-Frasnian (early Late Devonian) through Kinderhookian (late early Mississippian) time, however, basin analysis from Kominz and Bond (1991) shows an increase in flexural subsidence beginning earlier, in Givetian (late Middle Devonian) time.

The earliest flexural signal of the Antler orogeny without crustal shortening will herein be referred to as “early phase flexure” and occurs in the Givetian to early Frasnian time. Secondary mid-Frasnian to Kinderhookian flexure characterized by the migration of the foreland basin and crustal shortening will be referred to as “late phase flexure”. This temporal separation in Antler-related foreland basin flexure leads to confusion in defining the timing of onset of the Antler orogeny.

The Antler orogeny is coincident with the development of the northern Utah Stansbury uplift, a localized eroded antiform on the carbonate shelf that occurred in mid-

to late-Frasnian time (Poole, 1974). The cause of the Stansbury uplift remains unknown, however the timing of deformation suggests an interaction with Antler-related flexure. The Stansbury uplift occurs along the axis of the Tooele arch, an east-west trending arch thought to be inactive in the Devonian. The location of the Stansbury uplift implies that the Tooele arch may have been active, so one of the aims of this paper is to determine if the activity of the Tooele arch can be observed in sedimentary patterns.

To study the Antler orogeny's early phase flexure and the activity of the Tooele arch, detrital zircon provenance of Frasnian and Famennian sandstones were used to identify the source of the siliciclastic sediment: were they sourced from the Antler thrust sheets, the Stansbury uplift, the North American craton, or some other source? The results of this study have implications for the timing of Antler crustal flexure, the longevity of the Tooele arch, and the influence of flexure in the reactivation of preexisting structures.

2. GEOLOGIC SETTING:

The major events of early- to mid-Paleozoic time that affected the western margin of Laurentia include subsidence of the Great Basin, activity of the Tooele arch, the Taghanic Onlap, the Alamo impact, the Antler Orogeny, and the Stansbury uplift. Figure 2.1 shows the present day locations of the record of these events.

Great Basin Subsidence:

Kominz and Bond (1991) established subsidence was rift related, as shown by a prolonged period of thermal subsidence (Figure 2.2). This began in the Cambrian after the rifting of Rodinia and the western margin thermally subsided with a decreasing subsidence rate until the Antler Orogeny. Flexural subsidence is shown as beginning in the Middle to Late Devonian, but quickly slows thereafter.

Tooele Arch:

Intermittently present in the rock record from Neoproterozoic through Ordovician time, the Tooele arch is an east-west trending positive topographic feature. Also known as the Cortez-Uinta axis (Hintze and Kowallis, 2009), it is hypothesized to be a failed rift arm (Kingsbury-Stewart et al., 2013) inverted in the late Proterozoic to become an emergent structure (Roberts et al., 1965; Stewart, 1980). The Tooele arch has not been well documented as being an active feature in the Devonian though some recognition has been given more recently (Morrow and Sandberg, 2008).

Taghanic Onlap:

Beginning in the late Middle Devonian, a widespread transgression known as the Taghanic onlap (Johnson, 1970) transgressed onto the continent. Johnson (1970) concluded that transgression occurred over a short period of time rather than gradually

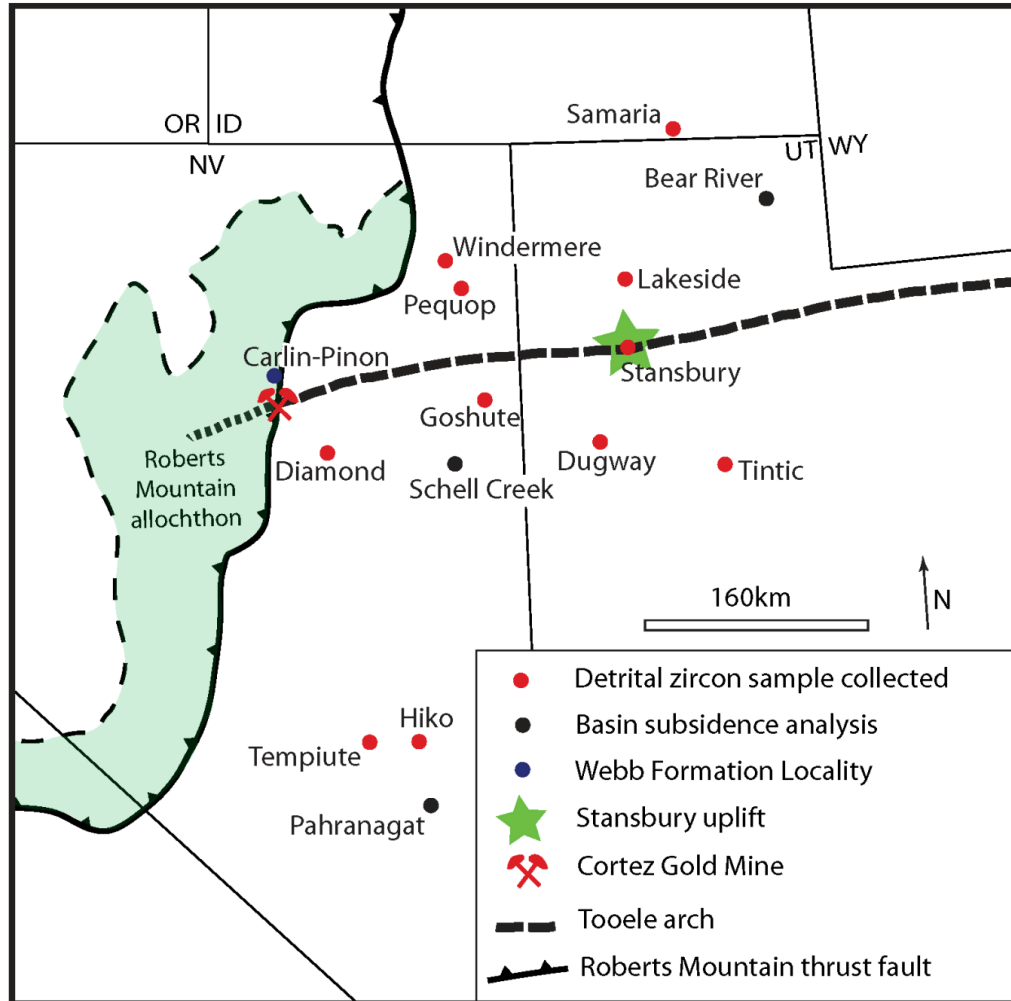


Figure 2.1: Location map showing generalized study area, locations of detrital zircon samples, ranges from which basin analysis was performed, the approximate trace of the Tooele arch, the Stansbury uplift, and the extent of the Roberts Mountain allochthon. Roberts Mountain allochthon and Roberts Mountain thrust fault geometry modified from Burchfiel and Royden (1991). Tooele arch axis modified from Roberts et al. (1965).

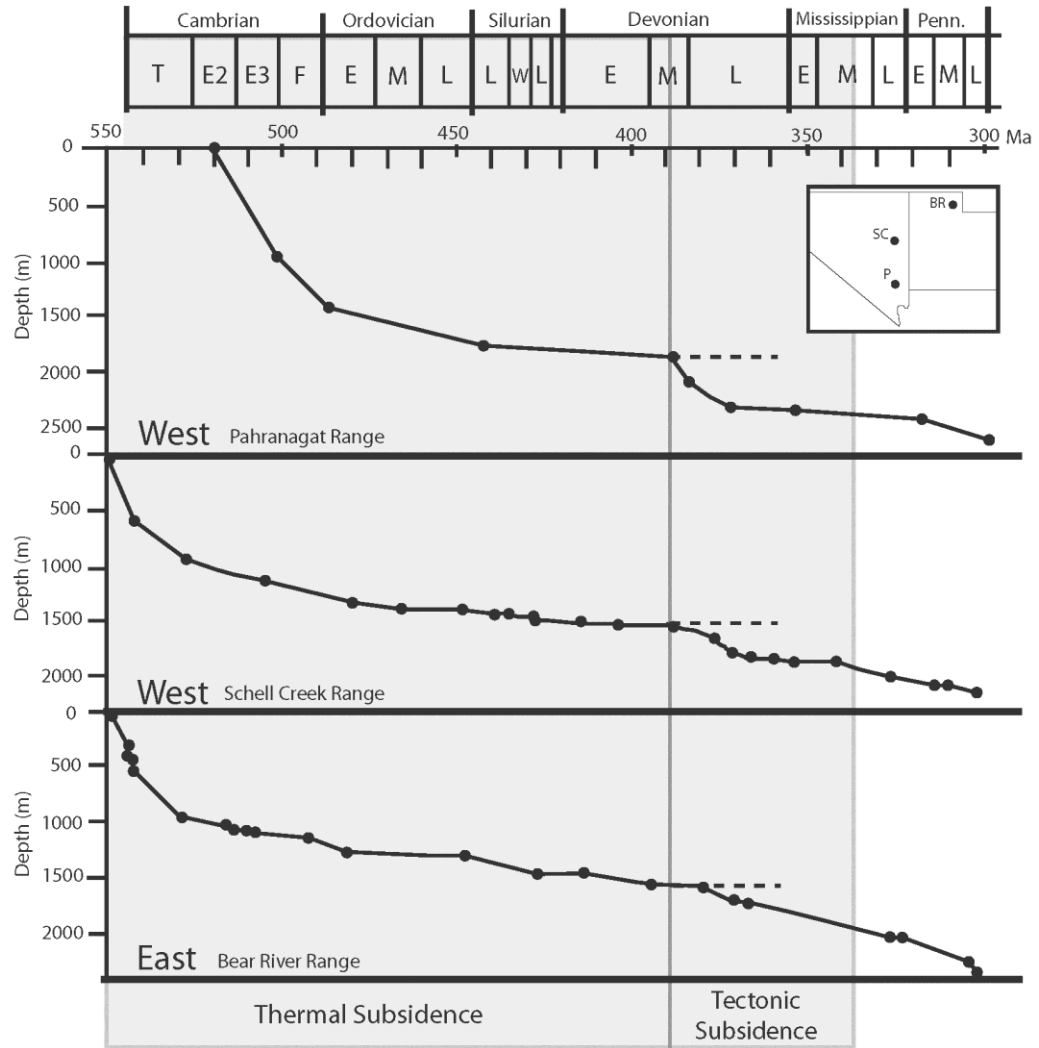


Figure 2.2: Subsidence curves showing both thermal and tectonic subsidence. The western ranges (Pahranaagat and Schell Creek) show subsidence beginning in the Givetian. The eastern range (Bear River) shows subsidence beginning later, in the Frasnian. Flexural subsidence curves have concave down shapes, whereas thermal subsidence from rifting has a concave up shape. The curve from the Schell Creek and the Bear River Range show concave down patterns, consistent with flexure, however the Pahranaagat Range shows a concave up pattern. This is due to the lower resolution of data collected from the Pahranaagat Range. Error bars (not shown), are less than 100m, as the sea level does not have large enough fluctuations to change the curves because the region is all shallow marine deposition. Schell Creek and Bear River Ranges modified from Kominz and Bond (1991); Pahranaagat Range modified from R. Meyers (personal communication, 2015). Dashed lines reflect line trajectory with continued thermal subsidence.

throughout the Late Devonian. This rapid sea level rise drowned the carbonate platform and helped to preserve siliciclastic layers.

Alamo Impact:

The early- to mid-Frasnian Alamo bolide impact in southern Nevada occurred on the carbonate shelf and excavated ~3.5-6 km of rock in forming a 100 km diameter crater (Morrow et al., 2005; Retzler et al., 2015). The impact breccia is contained within the Guilmette Formation, but contains blocks down through Cambrian aged strata (Retzler et al., 2015).

Antler Orogeny:

The Antler orogenic belt extends from southeastern California, north-northeastward through Nevada into central Idaho (Roberts et al., 1965; Link et al., 1996), and continues into British Columbia (Savoy and Mountjoy, 1995; Root, 2001; Colpron and Nelson, 2009). In Nevada, the Antler Orogeny is characterized by the emplacement of the Roberts Mountain allochthon along the Roberts Mountain thrust fault (Figure 2.1). The Roberts Mountain allochthon is composed of Cambrian-Devonian deep-water siliceous and volcanic strata that was emplaced onto coeval, but lithostratigraphically different carbonate and siliciclastic rocks of western Laurentia (Stewart, 1980). This thrusting created highlands from which coarse sediment was shed to the east creating flysch deposits that are now found in south-central Idaho (Link et al., 1996) and Nevada (Poole, 1974;).

The Roberts Mountain allochthon loaded the crust and produced a foreland basin that migrated east-southeastward (Goebel, 1991). The timing of Antler orogeny (mid-Frasnian through Kinderhookian, Johnson and Pendergast, 1981; Smith and Ketner,

1968) is supported by the work of Goebel (1991), who suggests thick foreland basin deposits do not occur prior to mid-Frasnian age. Constraints on the timing of the Roberts Mountain thrust occur within the Carlin-Piñon Range (Figure 1) where the Mississippian Webb Formation overlies both assemblages of autochthonous and allochthonous rocks. The youngest strata in the lower plate is Famennian in age, while the Webb Formation is as old as late Kinderhookian (Smith and Ketner, 1968). This indicates displacement of at least 165 km (Stewart, 1980) of the Roberts Mountain allochthon in ~20 m.y.

The style of faulting of the Roberts Mountain allochthon is enigmatic mainly due to the lack of recorded magmatism. Dominant models for the emplacement of the Roberts Mountain allochthon include (1) a non-collisional model (Burchfiel and Davis, 1972; 1975) (2) a dextral oblique transpressional model (Wright and Wyld, 2006), (3) a sinistral oblique transpressional model (Eisbacher, 1983; Colpron and Nelson, 2009; Housen, 2014), or (4) a controversial model in which the Roberts Mountain is not an allochthon but a large gravity slide of blocks dislodged by the Alamo Impact, sliding westward onto the slope (Ketner, 2012).

Stansbury Uplift:

The Stansbury uplift of northwestern Utah (Figure 2.1) occurred during mid- to late Frasnian time (Poole, 1974) and caused localized erosion of Devonian through Cambrian strata, exposing the Lower Cambrian Tintic Quartzite at its core. Previous research identifies two centers of the uplift as being within the present-day Stansbury Mountains, south of the Great Salt Lake and in Salt Lake City (Figure 2.3; Rigby, 1959). During uplift, detritus eroded to form a coarse-grained, poorly sorted, angular conglomerate known as the Stansbury Formation in the Northern Stansbury Range and

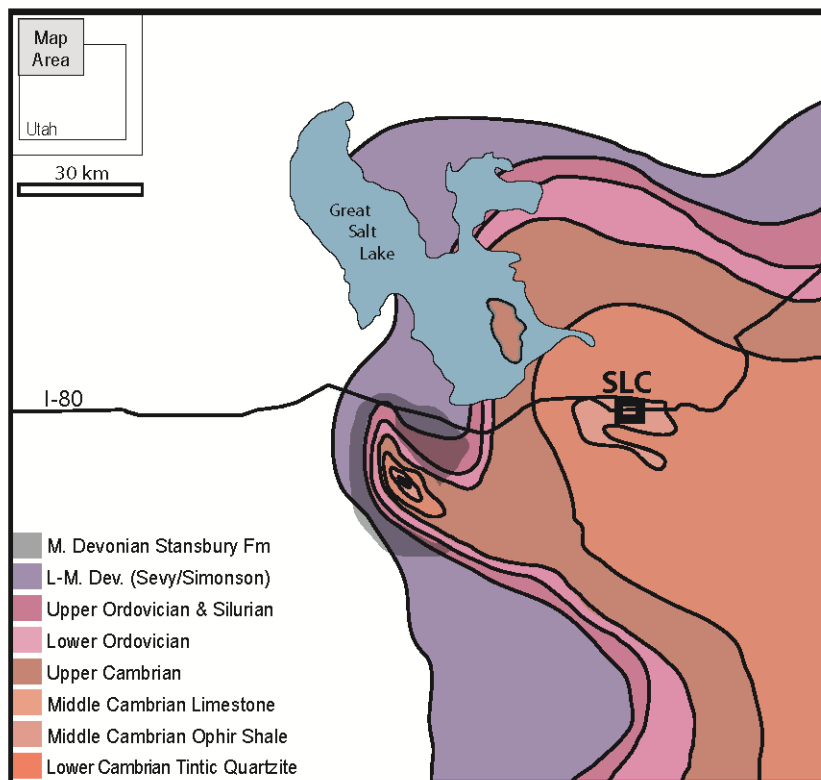


Figure 2.3: Late Devonian paleogeologic map of the Stansbury uplift. The Stansbury uplift is a small, localized event, but with a severe degree of erosion. This map shows two cores of uplift, the western in the Stansbury Range, and the eastern beneath Salt Lake City (SLC). The two cores of uplift line up in an east-west trend, similar to the Tooele arch. Image modified from Rigby (1959).

Stansbury Island. This unit is wedge-shaped and thins away from the center of the uplift (Trexler, 1992).

Stratigraphy:

The early- to mid-Paleozoic shelf was dominated by carbonate production, but punctuated by sandstones in the Middle Ordovician (Eureka Quartzite), Middle Devonian (Oxyoke Formation), and Late Devonian (Guilmette Formation and correlative sandstones). The Late Devonian sandstones, the focus of this study, are found throughout eastern Nevada, western Utah, and southern Idaho.

The Guilmette Formation of Nevada and Utah is correlative with the Jefferson Formation of northern Utah, Idaho and Montana, the Engelmann Formation and Gilson Dolomite of western Utah, and the Bluebell Formation of central Utah (Figure 2.4; Hintze and Kowallis, 2009). Unconformably overlying each of these carbonate units is a sandstone or quartzite member. The upper Guilmette sandstone of Nevada and north-central Utah is lithostratigraphically correlative with the Cove Fort Quartzite or upper Goshoot Sandstone of west-central Utah, the Victoria Quartzite of central Utah, and the Beirdneau Sandstone of northern Utah and southern Idaho (Figure 2.4; Hintze and Kowallis, 2009).

Although these sandstones have been constrained as Late Devonian, the ages of these sandstones (Frasnian or Famennian) are difficult to distinguish. The correlation of sandstones were taken from Hintze and Kowallis (2009), as well as Hellbusch (2012) for the Pequop Range, Goshute after Elrick (1986), Tempiute after Pinto and Warne (2008), Hiko after Thomason (2010), Lakeside after Young (1953),

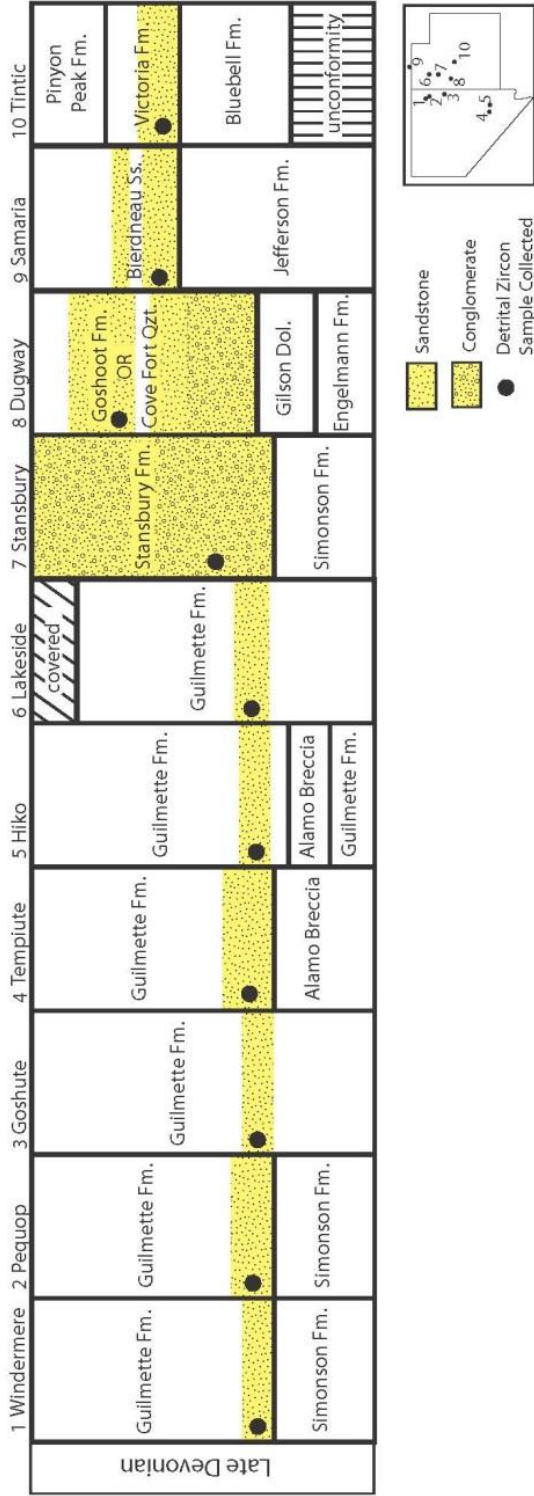


Figure 2.4: Stratigraphic correlation chart of ranges from which detrital zircon samples were collected laid out in a W-E transect. Intervals from which detrital samples were collected are denoted by a black circle.

Stansbury after Pooele (1974), Dugway after Staaz and Carr (1964) and Crosby (1959), Samaria after Walters (2013), Tintic after Morris and Lovering (1961).

These sandstones are 2-15m thick and in any given locality occur in a single bed, or as multiple sandy horizons interbedded with limestone or dolomite. All sample sites that had an exposed base, exhibit some degree of erosion, mostly indicated by localized zones of concentrated rip-up clasts of mudstone or limestone and locally channelized deposits. Some of these sandstone beds contain medium-bedded or massive sandstone, but all collected sandstone samples exhibit (~10-18°) planar crossbedding indicating relatively shallow water (<20m). The upper Guilmette sandstone sample collected from the northern Lakeside Mountains exhibits long wavelength, very low angle (3-5°) crossbeds, indicating a beach depositional environment, while the sandstone in the Goshute range exhibited both moderate to low (8°) and high angle (35°) crossbeds. The upper bound of these sandstones often grade upward into dolomite, or exhibit a sharp contact with an overlying limestone bed.

Thin sections of the sandstones from each locality produced a similar distribution of composition and maturity showing mature calcite-cemented medium- to fine-grained quartz arenites. The sample taken from the Dugway Range is different from the remaining samples and classified as a submature to immature calcite-cemented quartz- and chert-lithic pebble conglomerate (Figure 2.5).

As a result of poor age constraints on the sandstones, brachiopods in the dolomite overlying the upper Guilmette sandstone in the northern Lakeside Mountains were collected. They have been heavily dolomitized, but appear to be *Radiatrypa multicostellata* (J. Day, personal communication 2014). This brachiopod is common in

the Great Basin of the Late Devonian, and would place the sandstone as approximately middle Frasnian in age (Day, 1998).

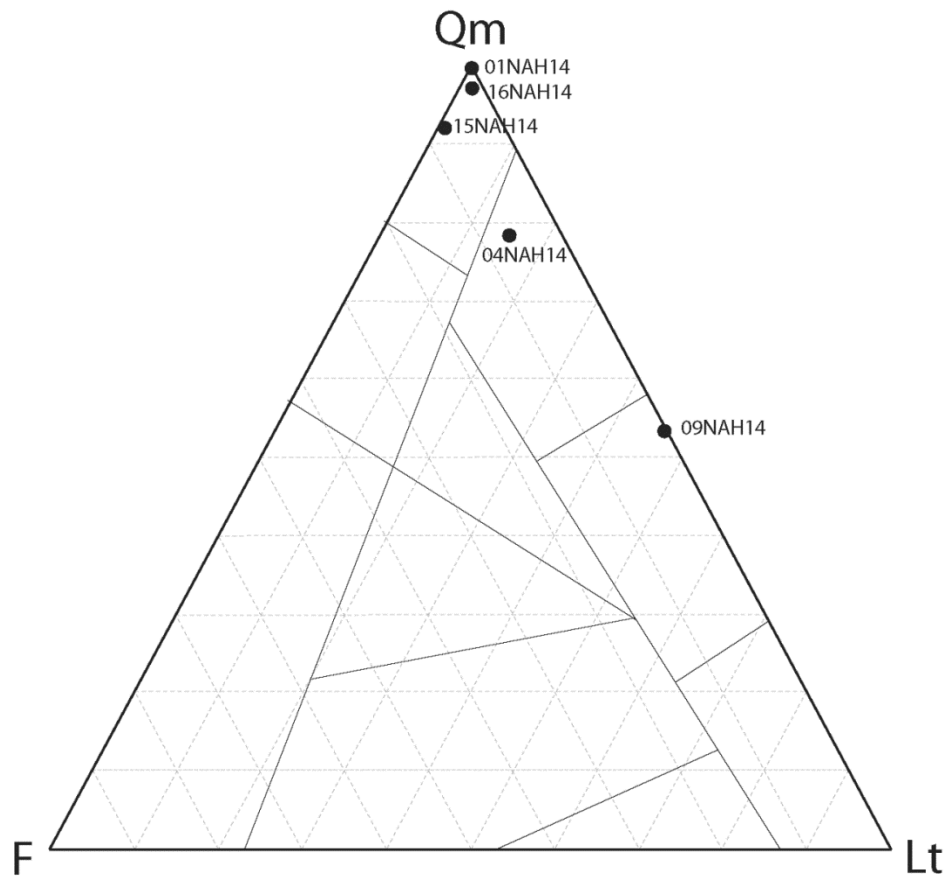


Figure 2.5: Qm-F-L plot of samples from this study. All samples are quartz arenites with the exception of 09NAH14, the sample taken from the Dugway range. This sample was rich in subrounded quartz lithics and chert fragments and is likely derived from the Stansbury uplift and is part of the Stansbury Formation. 01NAH14 – Windermere; 04NAH14 – Lakeside; 09NAH14 – Dugway; 15NAH14 – Goshute; 16NAH14 – Tintic.

3. METHODS:

To test whether the sandstones in this study were derived from the Stansbury uplift, the Antler orogenic thrust sheets, the North American craton, or some other source, detrital zircon provenance analysis was performed on sandstones collected throughout eastern Nevada, western Utah, and southern Idaho (Figure 2.1).

Samples collected for this study underwent zircon separation processes as described in Gehrels et al. (2008). U-Pb analyses of approximately 100 detrital zircon grains were conducted on a Laser Ablation Inductively Coupled Plasma Mass Spectrometer at the Arizona LaserChron Center.

The detrital zircon probability density plots of each sample analyzed from this study were compared with five previously collected and analyzed samples from southeastern Idaho, south to east-central Nevada, and west-central Utah (Figure 3.6; Table 3.1; Anderson, 2008; Thomason, 2010; Nichols et al., 2011; Hellbusch, 2012; Walters, 2012). Two detrital zircon samples of the Eifelian Oxyoke Formation (from Gehrels and Pecha, 2014; Figure 3.7; Table 3.2) were used as a baseline to identify the ambient signatures present in the Middle Devonian before the Alamo Impact and the Antler orogeny. This also helps to determine if a change in population occurred when the Alamo impact excavated the siliciclastic layers of the Middle Devonian and Ordovician (Morrow et al., 2005; Retzler et al., 2015).

Published isopach maps were reinterpreted to determine if a concentric pattern of Devonian strata exists around the Stansbury uplift. This pattern would support the hypothesis of the sandstones collected in this study being derived from the Stansbury uplift. Devonian isopach maps of Poole et al. (1992; Figure 3.8A) and Hintze and Davis

(2003; Figure 3.8B) were digitized and, using the same stratigraphic thickness data, the isopach contours were reinterpreted.

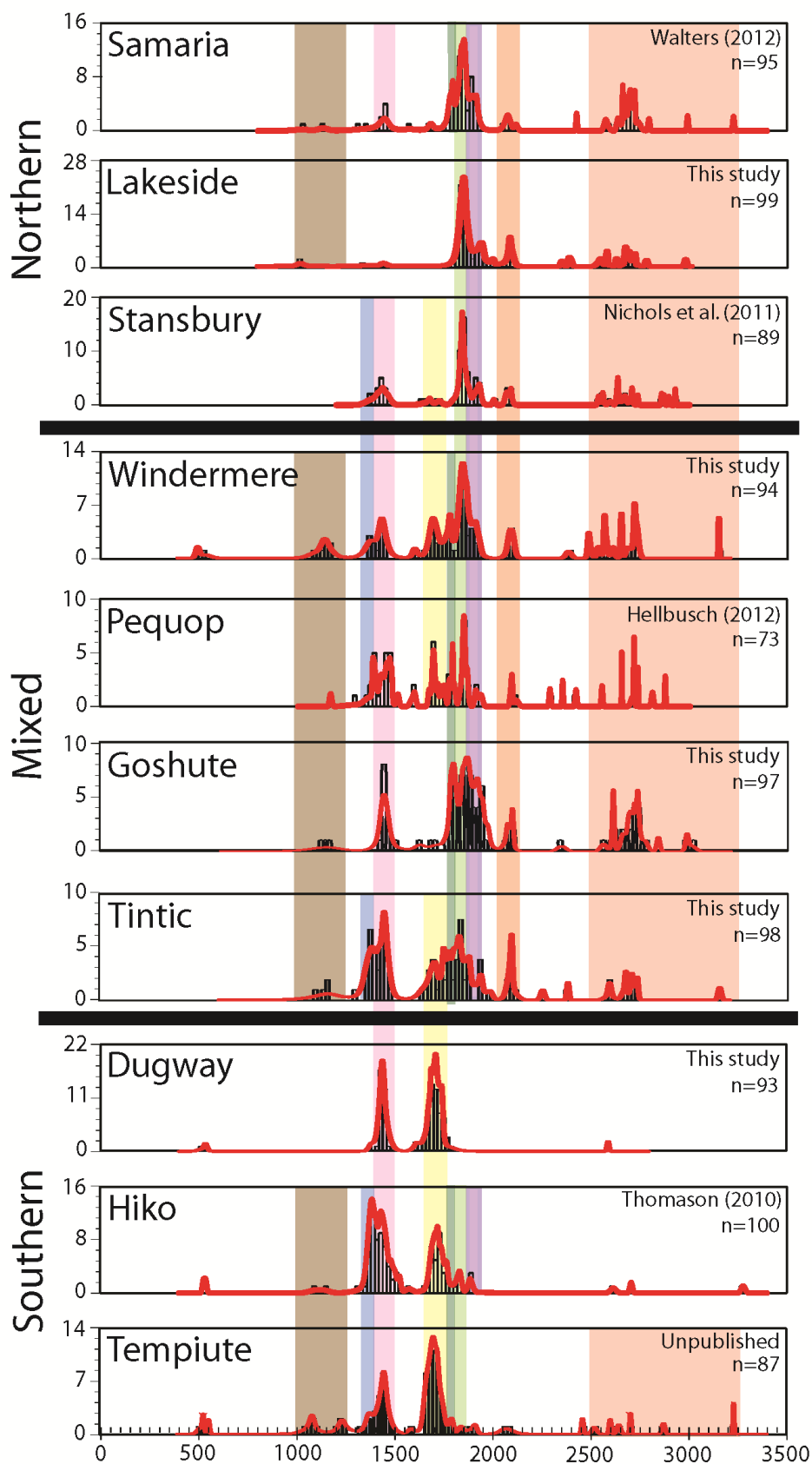


Figure 3.6: Detrital zircon probability density diagrams of Frasnian & Famennian sandstones in Utah and Nevada. Histogram (black) is overlain by a probability density plot (red). Vertical colored bands correlate to the age populations listed in Table 1. The “northern” samples have populations dominantly > 1.8 Ga, whereas the “southern” samples have populations < 1.76 Ga. The “mixed” samples show a spread of both populations of detrital zircons. Colored bands: brown 1000-1250 Ma; blue 1325-1395 Ma; pink 1395-1500 Ma; yellow 1650-1765 Ma; dark green 1765-1800 Ma; light green 1800-1865 Ma; purple 1865-1945 Ma; orange 2025-2145 Ma; light red 2500-3250 Ma.

Signature Type	Sample	n=	~1000-1350Ma	~1350-1410Ma	~1411-1510Ma	~1650-1765Ma	~1765-1800Ma	~1800-1845Ma	~1850-1940Ma	~2050-2120Ma	Archean grains (>2500Ma)
Northern	Samaria	95	3%		6%		8%	20%	27%	5%	21%
	Lakeside	99	3%					37%	26%	8%	16%
	Stansbury	89		5%	13%	3%		38%	10%	6%	18%
Mixed	Windermere	94	7%	5%	10%	12%	4%	12%	19%	5%	15%
	Pequop	73	3%	11%	20%	16%	8%	8%	12%	4%	9%
	Goshute	97	3%		13%		12%	9%	27%	5%	21%
	Tintic	98	5%	18%	14%	15%	6%	9%	10%	7%	8%
Southern	Dugway	93			34%	54%					
	Hiko	100	5%	27%	28%	27%		4%	3%		
	Tempiute	87	11%	5%	21%	42%					6%
	Pahrnagat	74	9%	9%	31%	20%	8%	8%	4%		
	Mt. Irish	90	3%	20%	12%	26%		3%	4%		

Table 3.1: Shows significant populations ($\geq 3\%$) of detrital zircons for each sample locality of Frasnian or Fammenian sandstones. Samples are organized geographically from north to south, corresponding with their signature type of northern, mixed, or southern. Northern samples have lesser populations of grains 1.0-1.76 Ga and are more abundant in 1.76-2.5+ Ga zircons, whereas the southern samples exhibit the opposite pattern with more grains 1.0-1.76 Ga and smaller populations of 1.76-2.5+ Ga grains. The mixed signature type contains an approximately equal spread of grain populations <1.76 and >1.76 Ga.

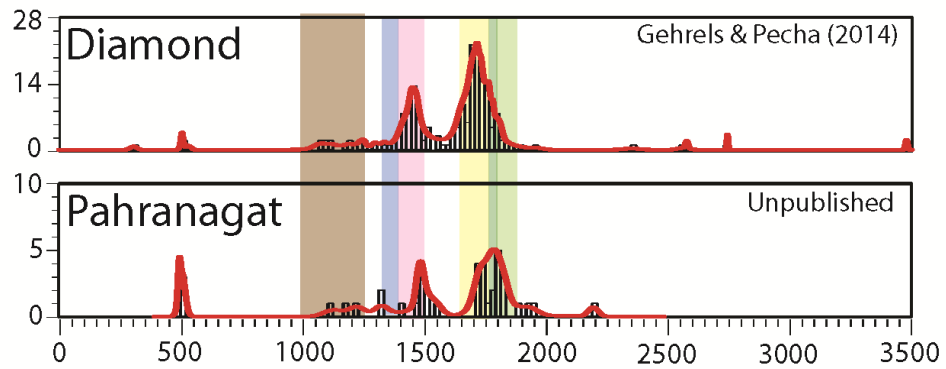


Figure 3.7: Detrital zircon probability density diagrams of sandstones from the Oxyoke Formation. Histogram (black) is overlain by a probability density plot (red). Vertical colored bands are the same as those in Figure 3.6 and correlate to the age populations listed in Table 2. These two samples provide a baseline for the ambient signature present in south to east-central Nevada before Antler tectonism began.

Signature Type	Sample	n=	~1000-1350Ma	~1350-1410Ma	~1411-1510Ma	~1650-1765Ma	~1765-1800Ma	~1800-1845Ma	~1850-1940Ma	~2050-2120Ma	Archean grains (>2500Ma)
Pre-Antler	Diamond	390	5%		9%	22%	3%				
	Pahranagat	82	6%		10%	21%					

Table 3.2: Shows significant populations ($\geq 3\%$) of detrital zircons for each sample locality of the Eifelian Oxyoke Formation. Samples are organized geographically north to south and show a baseline of what the ambient populations of grains are present in the Middle Devonian, before the Antler orogeny.

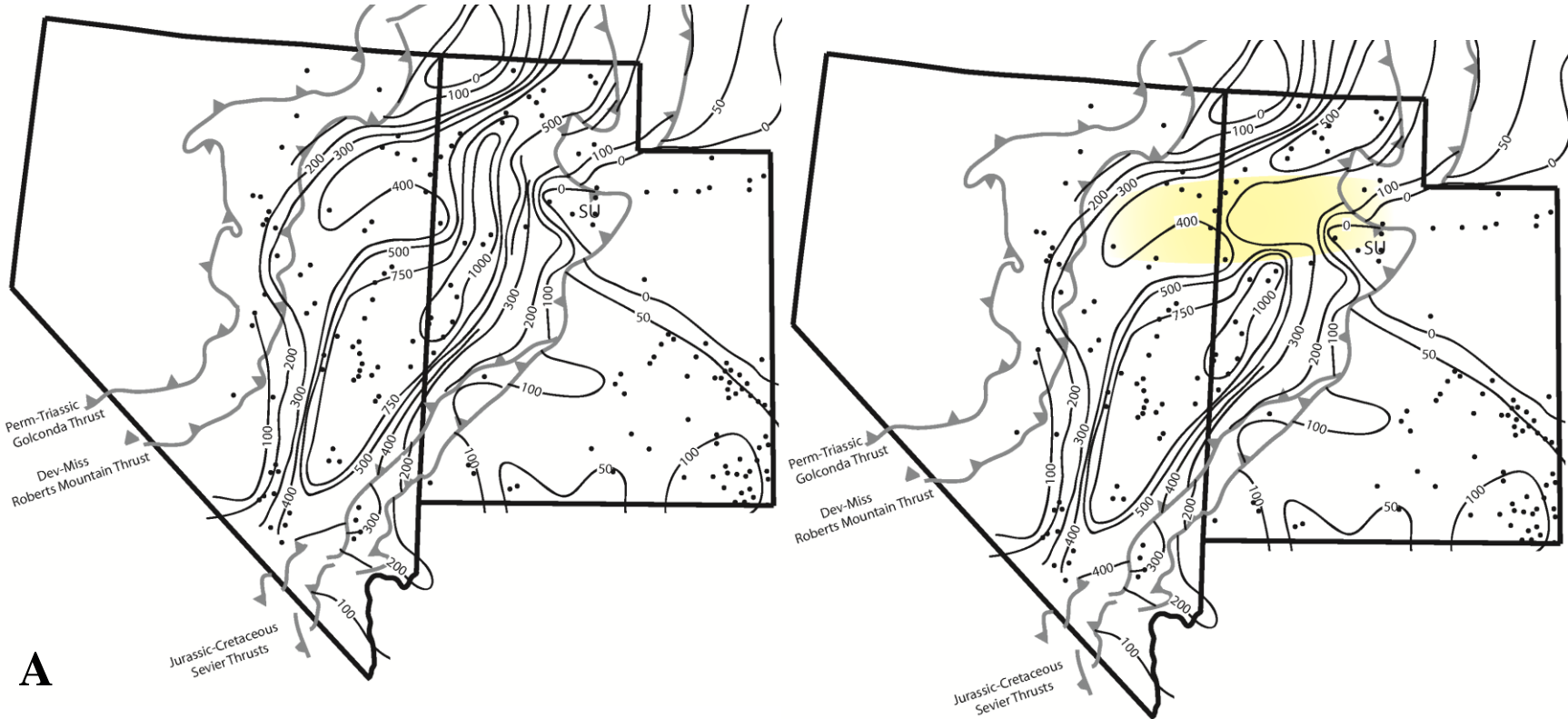
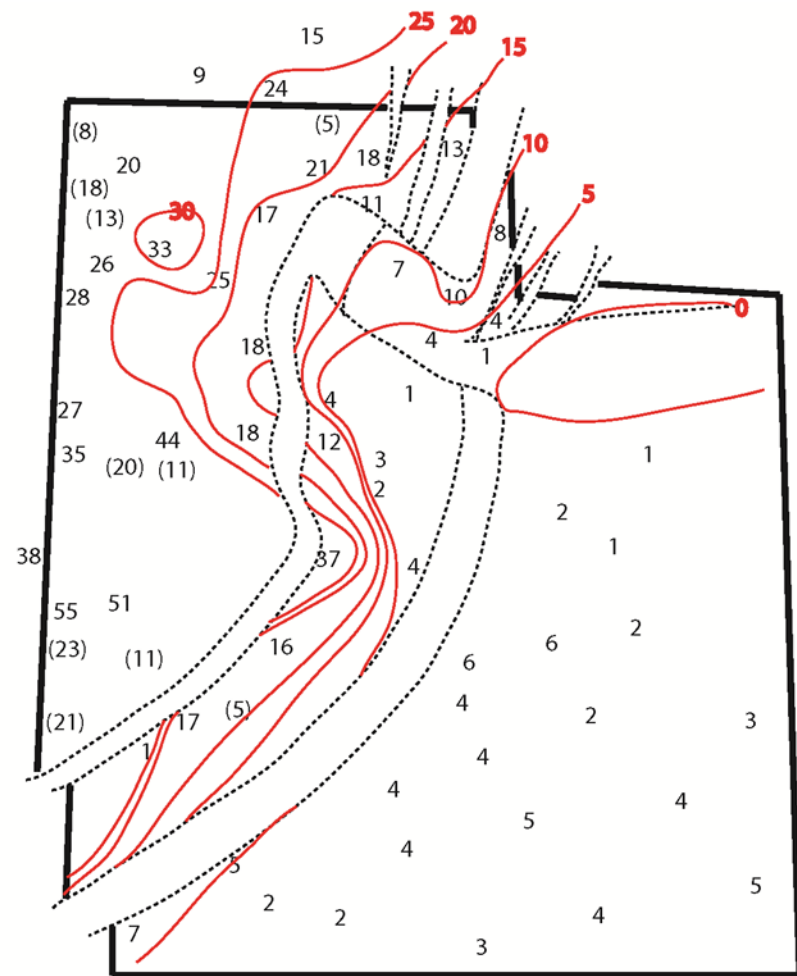
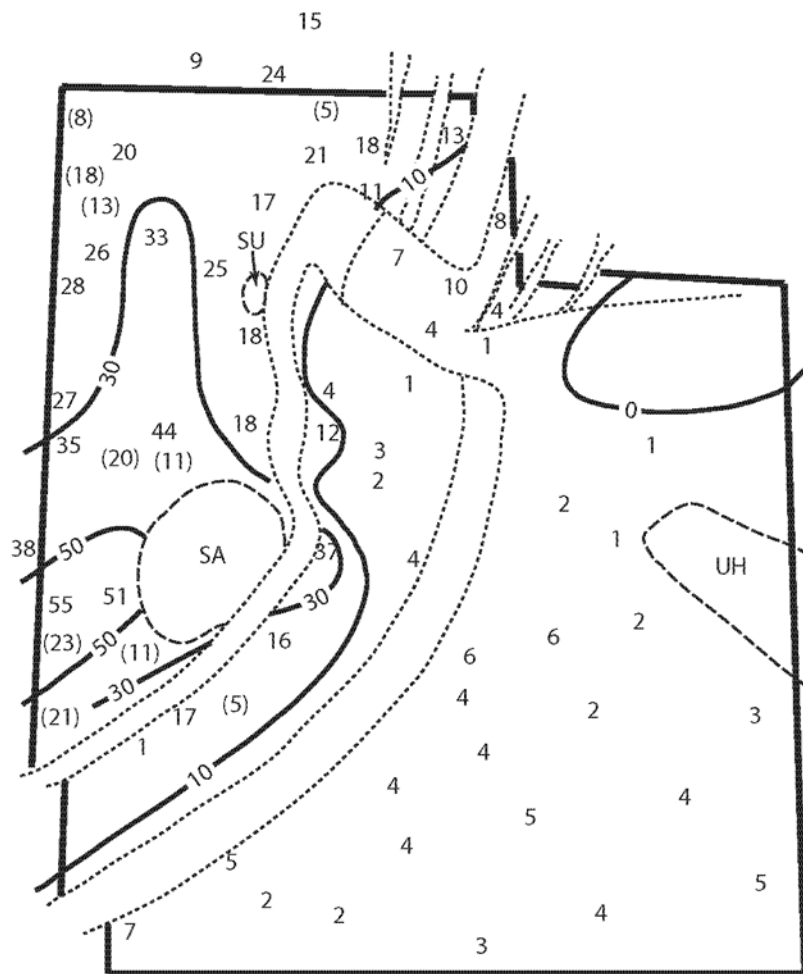


Figure 3.8: Two reconstructed isopach maps of Utah and Nevada (A) and Utah (B). Both original isopach maps (left) have data missing within northwestern Utah, and (A) has data missing in northeastern Nevada. Reinterpreting isopach contours shows a topographically positive, westward plunging feature, the Tooele arch. (A) Modified from Poole et al., (1992); contours in meters; highlighted area in right image shows the approximate trace of the Tooele arch. (B) Modified from Hintze and Davis (2003); thickness and contours in 100s of feet.



B

4. RESULTS:

U-Pb Data:

Figure 3.6 shows stacked probability density plots of all Late Devonian samples. From these plot comparisons, three groups were created (Table 1): (1) a “northern” signature, characterized by large spikes in the data at ~1800-1940Ma accompanied by a spread of Archean grains >~2500Ma, (2) a “southern” signature characterized by major peaks ~1400-1500Ma and ~1650-1765Ma, and (3) a “mixed” signature into which plots containing the major peaks of both the “northern” and the “southern” signatures were grouped. Table 1 compares the significant populations (≥ 3 grains) of age-grouped zircons and shows that the major components in the northern samples are not present in the south, and vice versa.

The following descriptions are of the major populations in each of the ranges discussed in this study and are arranged from north to south. The same data is presented in Table 1. The sample from the Samaria Range has 95 grains analyzed and populations at 1000-1350 Ma, 1411-1510 Ma, 1765-1800 Ma, 1800-1845 Ma, 1850-1940 Ma, 2050-2120 Ma, and 2500+ Ma. The sample from the Lakeside Mountains has 99 grains analyzed and populations at 1000-1350 Ma, 1800-1845 Ma, 1850-1940 Ma, 2050-2120 Ma, and 2500+ Ma. The sample from the Stansbury Mountains has 89 grains analyzed and populations at 1350-1410 Ma, 1411-1510 Ma, 1650-1765 Ma, 1800-1845 Ma, 1850-1940 Ma, 2050-2120 Ma, and 2500+ Ma. The sample from the Windermere Hills has 94 grains analyzed and populations at 1000-1350 Ma, 1350-1410 Ma, 1411-1510 Ma, 1650-1765 Ma, 1765-1800 Ma, 1800-1845 Ma, 1850-1940 Ma, 2050-2120 Ma, and 2500+ Ma. The sample from the Pequop Range has 73 grains analyzed and populations at 1000-1350

Ma, 1350-1410 Ma, 1411-1510 Ma, 1650-1765 Ma, 1765-1800 Ma, 1800-1845 Ma, 1850-1940 Ma, 2050-2120 Ma, and 2500+ Ma. The sample from the Goshute Range has 97 grains analyzed and populations at 1000-1350 Ma, 1411-1510 Ma, 1765-1800 Ma, 1800-1845 Ma, 1850-1940 Ma, 2050-2120 Ma, and 2500+ Ma. The sample from the East Tintic Mountains has 98 grains analyzed and populations at 1000-1350 Ma, 1350-1410 Ma, 1411-1510 Ma, 1650-1765 Ma, 1765-1800 Ma, 1800-1845 Ma, 1850-1940 Ma, 2050-2120 Ma, and 2500+ Ma. The sample from the Dugway Range has 93 grains analyzed and populations at 1411-1510 Ma, and 1650-1765 Ma. The sample from the Hiko Hills has 100 grains analyzed and populations at 1000-1350 Ma, 1350-1410 Ma, 1411-1510 Ma, 1650-1765 Ma, 1800-1845 Ma, and 1850-1940 Ma. The sample from Tempiute Mountain has 87 grains analyzed and populations at 1000-1350 Ma, 1350-1410 Ma, 1411-1510 Ma, 1650-1765 Ma, and 2500+ Ma. The sample from the Pahrangat Range has 74 grains analyzed and populations at 1000-1350 Ma, 1350-1410 Ma, 1411-1510 Ma, 1650-1765 Ma, 1765-1800 Ma, 1800-1845 Ma, and 1850-1940 Ma. The sample from Mount Irish has 90 grains analyzed and populations at 1000-1350 Ma, 1350-1410 Ma, 1411-1510 Ma, 1650-1765 Ma, 1800-1845 Ma, and 1850-1940 Ma.

The Kolmogorov-Smirnov statistic was performed on the data, however due to long-tailed distributions of the populations, the null hypothesis of the sediment being derived from the same populations was rejected in every case.

Isopach Maps:

In both publications, thickness data for Devonian strata is missing in northern Utah, west of the Stansbury uplift (Figure 3.8). Because of this, isopach contours were reinterpreted based on where the sediment signatures are divided in the detrital zircon

signatures: at the boundaries between the northern and mixed and the southern and mixed signatures. This pattern shows that the Tooele arch was likely active in the Late Devonian.

5. DISCUSSION:

Model for Sediment Sources:

Comparing all 10 detrital zircon signatures with possible provenance, the most likely source of the sediment is from the craton interior derived from recycled sandstones (Figure 12), which matches petrographic observation. The southern detrital zircon signatures are consistent with the Yavapai-Mazatzal and Grenville provinces of 0.8-1.8 Ga that exist in the more southerly states (Figure 5.9; Table 1). The northern detrital zircon signatures are consistent with the Archean craton and Trans-Hudson Orogen provinces between 1.8-2.5+ Ga, found in the more northerly states and Canada (Figure 5.9; Table 1). Geographically, there is some overlap with the southerly Yavapai province (1.72-1.8 Ga), which is likely the reason that 8% of the grains found in the sample collected in northeastern Utah in the Samaria Range (a northern sample) are of ages 1.76-1.8 Ga (Table 1).

Although it is not a statistically significant population (<3 grains), >1.8 Ga & Archean zircons, characteristic of the northern samples, exist in all of the southern samples. This suggests there is transport of northern grains southward, likely by longshore drift, but attenuates drastically through central Utah.

It could be argued that the northern grains appearing in the south are due to the exhumation of Ordovician Eureka Quartzite during the Frasnian Alamo impact, however field relations show inclusions of lithified Eureka quartzite in the Alamo breccia, so zircons were not likely liberated from the rock when it was exhumed. It could be expected that the Alamo impact may have contributed some zircons from unlithified sands such as the Eifelian Oxyoke Formation, but the ambient “southern” signature has a

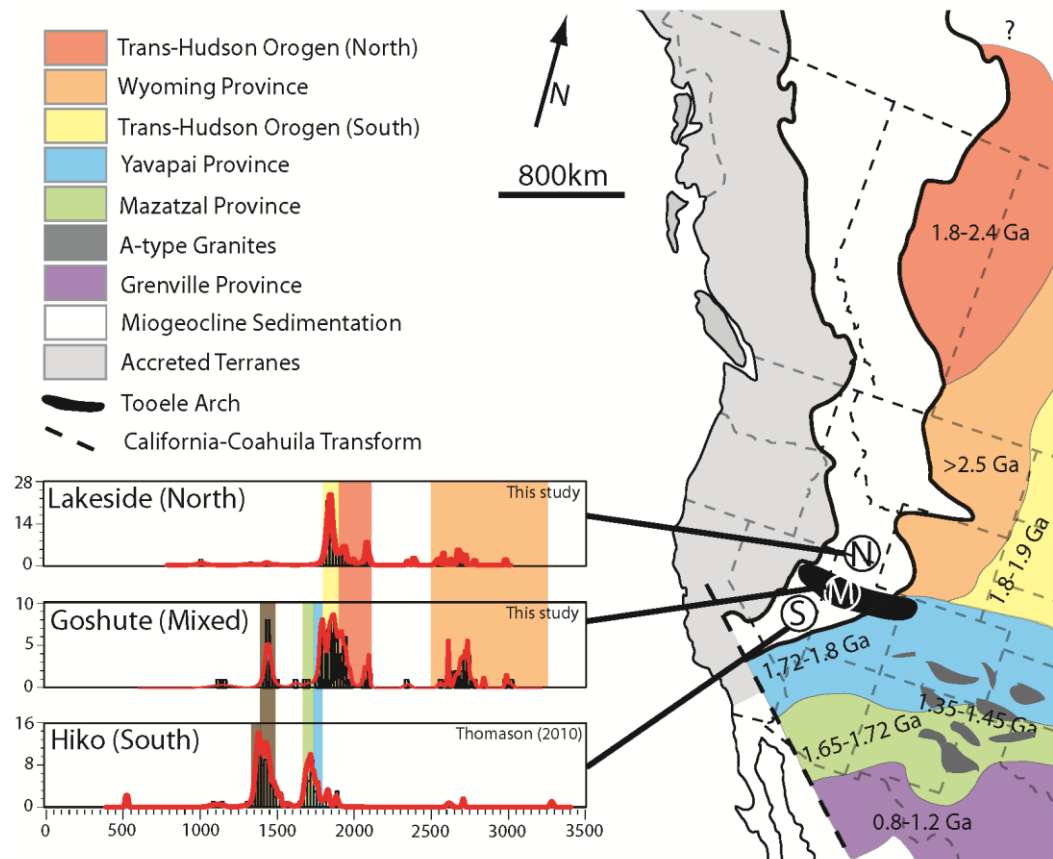


Figure 5.9: Generalized map of basement provinces of western North America and associated age ranges. Modified from Whitmeyer and Karlstrom (2007) and Ross and Villeneuve (2003). Provinces north of the Tooele arch are consistent with the “northern” detrital zircon signatures and provinces south of the Tooele arch are consistent with the “southern” detrital signature. “Mixed” signatures occur along the Tooele arch.

very similar distribution to the Oxyoke Formation, so the distinction cannot be made (Tables 1 and 2). This also indicates that the source of the siliciclastic sediment in the south remained consistent throughout the Middle and Late Devonian.

The Eifelian Oxyoke Formation has been described by Osmond (1954, 1962) and Poole et al. (1992), and they suggest a craton derived-source, similar to those described above of the “southern” samples, however Chamberlain (1999) suggests the Oxyoke Formation was derived from the erosion of the exposed Antler forebulge. The Oxyoke Formation was deposited pre-Antler flexure according to subsidence curves (Figure 2.2), and Chamberlain (1999) offers the exposure and erosion of older Paleozoic sandstones from the forebulge, including the Eureka Quartzite, to be sourcing the sediment of the Oxyoke Formation. The Eureka Quartzite has a dominant >1.8 Ga detrital zircon signature, inconsistent with the lack of >1.8 Ga zircons in either of the Oxyoke Formation sandstone samples (Gehrels and Pecha, 2014; Workman, 2012; Table 2).

The latitudinal change and the location of the mixed signature coincides with the approximate latitude of the Tooele arch. The Tooele arch has not been documented as being an active feature in the Devonian, however the distinct population of detrital zircons shows it either remained an active feature, or was reactivated during early phase flexure in the Givetian. The cause of the Stansbury uplift was likely activated with the Tooele arch also during early phase flexure.

Each of the sample localities is consistent with the distribution of sediment shown in their probability density plots with the exception of the Dugway Range. This sample shows a purely southern distribution, yet lies just on the southern boundary of the

proposed location of the Tooele arch; based on its position, it should have a mixed signature. The granule- to pebble-sized quartz grains and poor sorting are also petrographically inconsistent with the rest of the sandstone samples and implies a very proximal source. One possible explanation is that the sediment is derived from the Stansbury uplift as a distal part of the Stansbury Formation. The Dugway signature does have a very different detrital zircon signature than the more northern to mixed detrital zircon character of the Stansbury Formation detrital zircon sample, but the difference in detrital zircon signatures could represent different periods of uplift and erosion of different strata during the unroofing of the Stansbury uplift. The Stansbury Formation detrital zircon sample was taken from a horizon likely eroded from the Ordovician Eureka quartzite, which is rich in zircons $>1.8\text{Ga}$ (Gehrels and Pecha, 2014; Workman et al., 2012), whereas the sample from the Dugway Range was likely taken from a later unroofing event of lower Cambrian quartzites that contains grains 1.6-1.8 Ga (Reed et al., 2010). Palinspastic reconstruction (Levy and Christie-Blick, 1989; N. Christie-Blick, personal communication, 2014) places the Dugway Range just to the southwest of the Stansbury Range from which the Stansbury Formation was shed, which makes this conclusion plausible.

Tooele Arch Activity:

In Gehrels and Pecha (2014; their Figure 11), a shift in detrital zircon populations occurs in upper Devonian rocks between their Southern British Columbia samples (a northern signature) and their Nevada-Utah samples (a southern signature). It's worth noting all of the rocks sampled for their Nevada-Utah populations were sampled south of

the proposed latitude of the Tooele arch. The most likely explanation for the shift in detrital zircon population would be the continued existence of the Tooele arch.

The Tooele arch has previously been known to be an active feature into the Ordovician-Silurian boundary (Poole et al., 1992), but arch prominence has not been constrained beyond the Silurian. Based on the division of sediment provenance presented in this study, it is likely that the barrier needed to create the Late Devonian separation in signatures was the Tooele arch. If this assumption is correct, the Tooele arch was reactivated as a positive topographic feature in the Middle Devonian until at least Late Devonian time, an additional ~50 m.y. than previously known.

Reinterpreted isopach maps (Figures 3.8) are consistent with a topographically positive feature trending east-west through Utah and Nevada. These maps are consistent with the palinspastically restored isopach map of Stewart (1980).

Antler Sedimentation:

Regional sea level (Morrow and Sandberg, 2008) was compared with the timing of delivery of sandstones to the shelf to determine if eustasy controlled sediment delivery, however the correlation is not obvious. Accommodation space created by a migrating flexural subsidence wave coupled with the eustatic sea level rise caused by the Taghanic onlap likely controlled the preservation of these siliciclastic deposits. Subsidence rate is high enough so that when a local regression occurs, the sandstones are still in submarine conditions. Figure 5.10 shows a time-transgressive model for the preservation of the sandstones in this study. Figure 5.10-T1 shows the carbonate shelf with sea level at a low and sediment being deposited and eroded away during local sea level highs and lows,

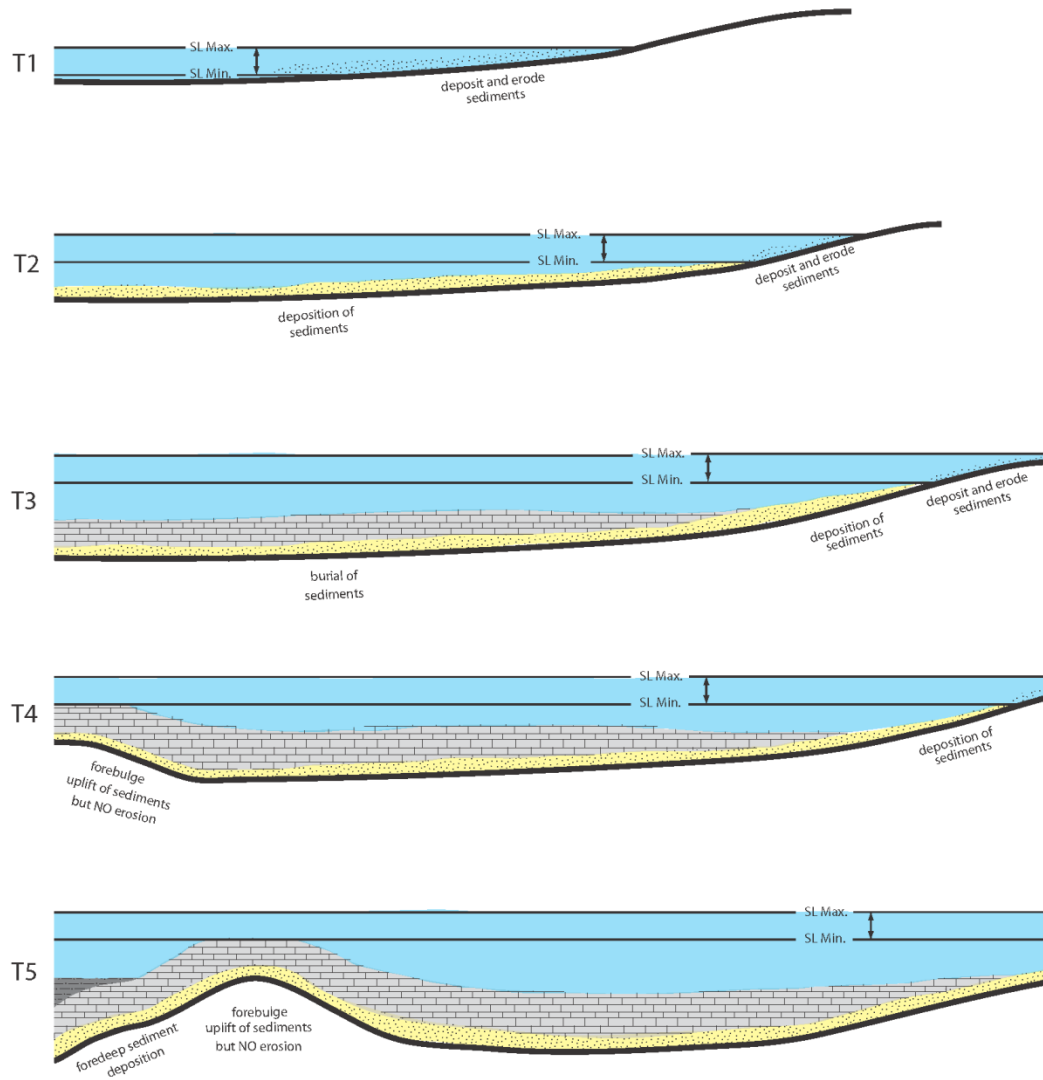


Figure 5.10: Time slices of the eastward progression of subsidence due to the foreland basin migration, and shows the overall transgression through time that favors preservation of backbulge basin sedimentation.

respectively. Figure 5.10-T2 shows eustatic sea level rise and initial eastward propagation of flexure. Because of these two factors, sediment is deposited below the sea level minimum and can be preserved. Figure 5.10-T3 shows the same process, but carbonate production has resumed and buried the sediments. Figure 5.10-T4 shows continued sea level rise and eastward propagation of flexure, and as a result, the forebulge has migrated into the region and uplifted the rock, however it is below sea level minimum, so very little to no erosion has occurred. Lastly, Figure 5.10-T5 exhibits propagation of the forebulge further east, and the foredeep sediments (sand and shale) are deposited and preserved in the foreland basin. This process indicates that the sandstones in this early-phase flexure are preserved backbulge basin siliciclastic preservation as a part of the foreland basin progression.

Early phase flexure is supported by the slope of subsidence curves from Nevada and Utah. Kominz and Bond (1991) presented subsidence curves that show flexure, characterized by a concave down-shaped curve, beginning in the Givetian in the Schell Creek Range of east-central Nevada (Figure 2.2). These data are consistent with values calculated for the Pahrnaghat Range in southern Nevada (Figure 2.2; R. Myers, personal communication, 2015). Flexural subsidence begins later (in the Frasnian) in the Bear River Range of northeastern Utah (Figure 2.2). This record of subsidence is here inferred to be the onset of the Antler orogenic load and suggests the flexure associated with the Antler orogeny in Nevada began in Givetian time, rather than the previously accepted mid-Frasnian (Goebel, 1991; Johnson and Pendergast, 1981). The temporal and spatial differences between the subsidence curve localities show an eastward progression of subsidence through time, consistent with the propagation direction of the foreland basin

of Goebel (1991). Palinspastic reconstruction (Levy and Christie-Blick, 1989, Christie Blick personal communication, 2014) does not significantly change the distance between these two samples, and as a result, the eastward younging pattern is correct. A left- or right-lateral sense of Antler transpression cannot be determined from the data in this study, however Link et al. (1996) show subsidence curves (their Figure 12) of the Copper Basin Group of the Antler flysch deposits in Idaho. The subsidence in the Mississippian is clear, and proposed to be assisted by a normal fault, however flexural subsidence is occurring throughout the Devonian as well. These curves show subsidence beginning by at least early Devonian, before the timing of flexural subsidence in Nevada. The pattern of southward younging flexure again suggests a sinistral sense of slip for the Antler orogeny.

Antler foreland basin sedimentation began in the mid- to late Famennian (late phase flexure; Webb, 1958; Goebel, 1991); thus, the western margin was subsiding before late phase flexure (Antler shortening) began. This brings into question what other researchers define as the onset of orogenesis: is it the first signal of flexure, as identified in this study as early phase flexure and evidence of backbulge basin deposits, or is it the beginning of major crustal shortening when dominant foreland basin sedimentation begins as in late phase flexure? In this case, ~12 m.y. separates these two orogenic signals.

The ~12 m.y. duration between the onset of early and late phase flexure suggests the Antler orogeny had long lived backbulge basin flexure and reached far (~100km) onto the craton, suggesting a long wavelength for the shape for the foreland basin curve. Having such a long-lived backbulge basin suggests the foreland basin took more time to

develop than what is typical of other orogenies. This may be due to the Antler orogeny having a dominantly transpressional motion, rather than orthogonal. The direction of strike slip motion cannot be determined from this study, however Root (2001) documented Antler-related crustal shortening in British Columbia beginning in the Middle Devonian. If Antler crustal shortening in Nevada occurred in the Late Devonian, this would indicate southward younging shortening, and thus sinistral motion.

Foreland Basin Modeling:

Backbulge basin (early phase flexure) sediment deposition and preservation is not commonly preserved in other orogenic events (DeCelles, 2012). One explanation for the preservation of this flexural signature could be the unique characteristics and timing of the Antler orogeny. The Antler orogeny occurred along a passive margin after thermal subsidence had ceased as shown by the subsidence curves (Figure 2.2). This indicates the crust on which the Antler orogeny occurred was cold. Temperature plays a role in how crust will behave when it is deformed; the colder the crust, the more rigid it will act (Jamieson and Beaumont, 2013). As a result, the crust will flex with a longer wavelength if the crust is cold than it would if it were hot (Angevine et al., 1990). In addition to the influence of temperature, the mass of the load placed on the crust will dictate the amplitude of the flexural wave (DeCelles, 2012). A small load, such as the Roberts Mountain allochthon (~3km high), will cause a small amplitude flexural wave, whereas other large orogenic events such as the Sevier orogeny were built on hot crust and had a large volume of loading (~40km high) would have flexural waves with much higher amplitudes. These factors are favorable in preserving horizons that have already been deposited, such as the Frasnian-Famennian sandstones in this study (DeCelles, 2012).

An example of this is shown in Figure 5.11 comparing a model of the foreland basin wave produced by both the Antler and Sevier orogenies. The Sevier orogeny has a longer wavelength, but a higher amplitude than the Antler orogeny. Because the Sevier orogeny has a higher amplitude, when the forebulge migrates through the system, it would erode away any sediments deposited in the backbulge basin. Because the Antler orogeny has a smaller amplitude, and it's in a marine setting, the backbulge basin

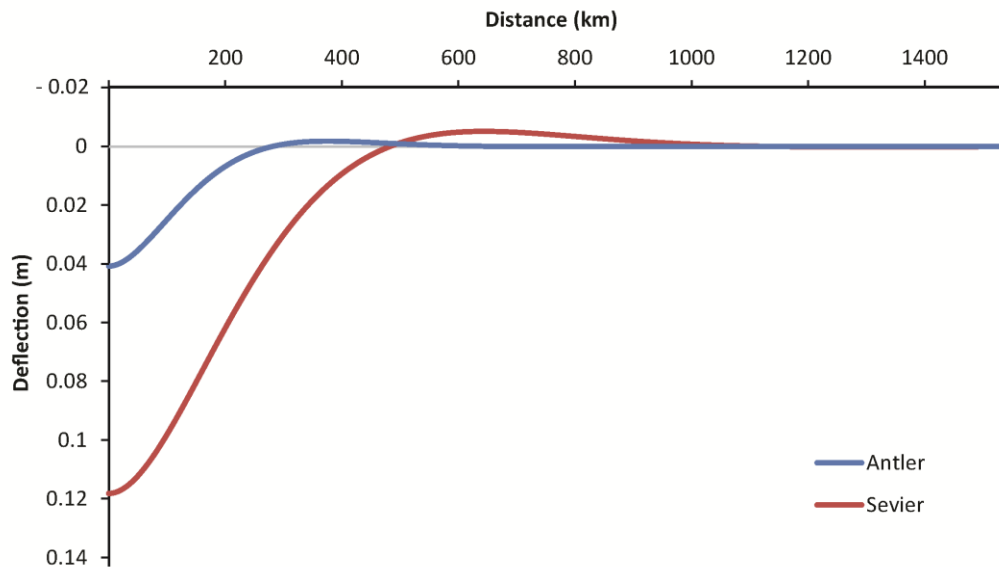


Figure 5.11: A model of two foreland basin waves. Blue curve is the Antler orogeny with a long wavelength and small amplitude. Red curve is the Sevier orogeny with a longer wavelength and a large amplitude. A foreland basin with a higher amplitude would cause the forebulge to have a larger positive deflection and encourage excavation and erosion of previously deposited rock, whereas the lower amplitude of the Antler orogeny does not favor as much uplift or erosion. Data for Antler modeling parameters derived from Speed and Sleep (1982) and Goebel (1991).

siliciclastic layers did not erode away. Figure 5.10-T4 shows the small amplitude forebulge uplifting the sediment deposited in the backbulge basin, but not eroding them.

The unique characteristics of the Antler orogeny (small load emplacement and occurring on cold crust) allowed for this early flexural signature to be preserved and record the earliest signal of the Antler orogeny.

Timing of Antler Events:

Based on the interpretations presented, a timeline of the events associated with the Antler orogeny can be assembled.

1. The sinistral transpressional Antler orogeny's backbulge basin was located in Idaho in the Early Devonian as shown by flexural subsidence curves from Link et al., (1996).
2. In the late Eifelian, Antler crustal shortening was documented in British Columbia by Root (2001).
3. By Givetian time, early phase flexure (the backbulge basin) had migrated southward into Nevada and the westernmost sandstones in this study began deposition as shown by the subsidence curves of the Pahrangat and Schell Creek Ranges.
4. The early- to mid-Frasnian Alamo Impact exhumed detrital zircons from the Oxyoke Formation, but did not alter the populations of detrital zircons present in the southern samples.
5. Flexure migrated eastward into central Utah by the mid-Frasnian as evidenced by the Great Basin brachiopod *Radiatrypa multicostellata* found above the Lakeside sandstone sample.

6. In the mid- to late-Frasnian, shortening from the Antler orogeny caused the Tooele arch to reactivate, and the Stansbury uplift emerged; deposition of the Stansbury Formation began, including the Dugway sample.
7. Late phase flexure began in mid- to late Famennian as Antler shortening began in Nevada and the foreland basin migration analyzed by Goebel (1991), progressed.
8. The Antler orogeny moved to completion by late Kinderhookian as the Early Mississippian Webb Formation was deposited over top both autochthonous and allochthonous rock (Smith and Ketner, 1968).

6. CONCLUSIONS:

Late Devonian laterally extensive sandstone horizons track the earliest onset of Antler orogenic flexure. Further, subsidence curves from Kominz and Bond (1991) show onset of subsidence beginning in the Givetian, even though foreland basin development only begins in the late Frasnian (Goebel, 1991). This early flexure is the result of backbulge basin deposits reaching far onto the continent as a result of prolonged transpression. Backbulge basin deposits are not often preserved in other orogens, likely due to cannibalism by a high amplitude foreland basin curve. The unique qualities of the Antler orogeny with a low amplitude foreland basin curve coupled with the Taghanic Onlap allowed for this sedimentation and record of flexure to be preserved.

The division of detrital zircon provenance with ages $>1.8\text{Ga}$ in the north and $<1.76\text{Ga}$ in the south indicate a distinct topographic barrier, the Tooele arch, prevented the mixing of sediment on the carbonate platform. This extends the longevity of the Tooele arch into the Late Devonian. Although the Tooele arch was likely passively subsiding in the Early Devonian, it was reactivated when crustal shortening began with the onset of the Antler orogeny.

The regional observations of the progression of the Antler orogeny has helped to constrain its motion to being left-lateral, consistent with one of the models of the Antler orogeny (Eisbacher, 1983; Colpron and Nelson, 2009; Housen, 2014, Link et al., in progress).

REFERENCES:

- Anderson, J., 2008, Reconstructing the Aftermath of the Late Devonian Alamo Meteor Impact in the Pahrnagat Range, Southeastern Nevada [Masters Thesis]: Pocatello, Idaho State University, 203 p.
- Angevine, C.L., Heller, P.L., and Paola, C., 1990, Quantitative Sedimentary Basin Modeling: Continuing Education, Course Note Series #32: American Association of Petroleum Geologists, 255 p.
- Burchfiel, B.C., and Davis, G.A., 1972, Structural framework and evolution of the southern part of the Cordilleran orogen, Western United States: American Journal of Science, v. 272, p. 97-118.
- Burchfiel, B.C., and Davis, G.A., 1975, Nature and Controls of Cordilleran Orogenesis, Western United States: Extension of an Earlier Synthesis: American Journal of Science, v. 275-A, p. 363–396.
- Burchfiel, B.C., and Royden, L.H., 1991, Antler orogeny : A Mediterranean-type orogeny: Geology, v. 19, p. 66–69, doi: 10.1130/0091-7613(1991)019<0066.
- Chamberlain, A.K., 1999, Structure and Devonian stratigraphy of the Timpahute Range, Nevada [PhD Thesis]: Golden, Colorado School of Mines, 345 p.
- Colpron, M., and Nelson, J.L., 2009, A Palaeozoic Northwest Passage: incursion of Caledonian, Baltican and Siberian terranes into eastern Panthalassa, and the early

- evolution of the North American Cordillera: Geological Society, London, Special Publications, v. 318, p. 273–307, doi: 10.1144/SP318.10.
- Crosby G.W., 1959, Geology of the South Pavant Range, Millard and Sevier Counties, Utah [Masters Thesis]: Provo, Brigham Young University, 59 p.
- Day, J., 1998, Distribution of latest Givetian-Frasnian Atrypida (Brachiopoda) in central and western North America: *Acta Palaeontologica Polonica*, v. 43, p. 205–240.
- DeCelles, P.G., 2012, Foreland basin systems revisited : variations in response to tectonic settings, *in* Busby, C. and Azor Perez, A. eds., *Tectonics of Sedimentary Basins: Recent Advances*, Blackwell Publishing, p. 405–426.
- Eisbacher, G.H., 1983, Devonian-Mississippian sinistral transcurrent faulting along the cratonic margin of western North America : A hypothesis: *Geology*, v. 11, p. 7–10, doi: 10.1130/0091-7613(1983)11<7.
- Elrick, M., 1986, Depositional and Diagenetic History of the Devonian Guilmette Formation, Southern Goshute Range, Elko County, Nevada [Masters Thesis]: Corvallis, Oregon State University, 109 p.
- Gehrels, G.E., Valencia, V., Ruiz, J., 2008, Enhanced precision, accuracy, efficiency, and spatial resolution of U-Pb ages by laser ablation-multicollector-inductively coupled plasma-mass spectrometry: *Geochemistry, Geophysics, Geosystems*, v. 9, p. 1-13, doi:10.1029/2007GC001805.

- Gehrels, G., and Pecha, M., 2014, Detrital zircon U-Pb geochronology and Hf isotope geochemistry of Paleozoic and Triassic passive margin strata of western North America: *Geosphere*, v. 10, p. 49–65, doi: 10.1130/GES00889.1.
- Goebel, K.A., 1991, Paleogeographic Setting of Late Devonian to Early Mississippian Transition from Passive to Collisional Margin, Antler Foreland, Eastern Nevada and Western Utah, *in* Cooper, J.D., and Stevens, C.H., eds., 1991, *Paleozoic Paleogeography of the Western United States-II: Pacific Section SEPM*, v. 67, p. 401-418.
- Hellbusch, C.A., 2012, Implications for Stratigraphic Omission and Structural Thinning in the Pequop Mountains: Geologic Map of the Devonian Guilmette Formation, Elko County, Nevada [Masters Thesis]: Pocatello, Idaho State University, 107 p.
- Hintze, L.F., and Davis, F.D., 2003, *Geology of Millard County, Utah: Utah Geological Survey Bulletin*, v. 133, 305 p.
- Hintze, L.F., and Kowallis, B.J., 2009, *Geologic History of Utah: Brigham Young University Geology Studies, Special Publication 9*, 202 p.
- Housen, B.A., 2014, Evaluation of paleomagnetic inclination error on paleomagnetic results from the Karheen Formation- Implications for the Devonian paleogeography of the Alexander and associated terranes: *Geological Society of America Abstracts with Programs*, v. 42, no. 6, p. 174

- Johnson, J.G. 1970, The Taghanic onlap and the end of North American Devonian provinciality: Geological Society of America Bulletin, v. 81, p. 2077–2106.
- Johnson, J.G., and Pendergast, A., 1981, Timing and mode of emplacement of the Roberts Mountains allochthon, Antler Timing and mode of emplacement of the Roberts Mountains allochthon, Antler orogeny: Geological Society of America Bulletin, v. 92, p. 648-658, doi: 10.1130/0016-7606(1981)92<648.
- Ketner, K.B., 2012, An Alternative Hypothesis for the Mid-Paleozoic Antler Orogeny in Nevada: United States Geological Survey, Professional Paper 1790, 11 p.
- Kingsbury-Stewart, E.M., Osterhout, S.L., Link, P.K., and Dehler, C.M., 2013, Sequence stratigraphy and formalization of the Middle Uinta Mountain Group (Neoproterozoic), central Uinta Mountains, Utah: A closer look at the western Laurentian Seaway at ca. 750Ma: Precambrian Research, v. 236, p. 65–84, doi: 10.1016/j.precamres.2013.06.015.
- Kominz, M.A., and Bond, G.C., 1991, Unusually large subsidence and sea-level events during middle Paleozoic time : New evidence supporting mantle convection models for supercontinent assembly: Geology, v. 19, p. 56–60, doi: 10.1130/0091-7613(1991)019<0056.
- Levy, M., and Christie-blick, N., 1989, Pre-Mesozoic Palinspastic Reconstruction of the Eastern Great Basin (Western United States): Science, v. 245, p. 1454-1462.

- Link, P.K., Beranek, L.P., Diedesch, T.F., Fanning, C.M., in progress, Provenance of Paleozoic Cordilleran western assemblage and Antler flysch in central Idaho.
- Link, P.K., Warren, I., Preacher, J.M., Skipp, B., 1996, Stratigraphic Analysis and Interpretation of the Mississippian Copper Basin Group, McGowan Creek Formation, and White Knob Limestone, South-Central Idaho *in* M.W. Longman and M.D. Sonnenfeld eds., 1996, Paleozoic Systems of the Rocky Mountain Region, Rocky Mountain Section, SEPM (Society of Sedimentary Geology), p. 117-144.
- Morris, H.T., and Lovering, T.S., 1961, Stratigraphy of the East Tintic Mountains, Utah: USGS Professional Paper no. 361, 145 p.
- Morrow, J.R., and Sandberg, C. a., 2008, Evolution of Devonian carbonate-shelf margin, Nevada: *Geosphere*, v. 4, p. 445–458, doi: 10.1130/GES00134.1.
- Morrow, J.R., Sandberg, C.A., and Harris, A.G., 2005, Late Devonian Alamo Impact, southern Nevada, USA: Evidence of size, marine site, and widespread effects, *in* Kenkmann, T., Hörz, F., and Deutsch, A., eds., Large meteorite impacts III: Geological Society of America Special Paper v. 384, p. 259–280, doi: 10.1130/0-8137-2384-1.259.
- Nichols, J.C., Hellbusch, C.A., Tapanila, L., Link, P.K., 2011, Detrital zircons from the Mississippian sandstones adjacent to the Stansbury Uplift, Northern Utah and Nevada: *Geological Society of America Abstracts with Programs*, v. 43, no. 4, p. 68.

- Osmond, J.C., 1954, Dolomites in Silurian and Devonian of east-central Nevada:
American Association of Petroleum Geologists Bulletin, v. 38, p.1911-1156.
- Osmond, J.C., 1962, Stratigraphy of Devonian Sevy Dolomite in Utah and Nevada:
American Association of Petroleum Geologists Bulletin, v. 46, p. 2033-2056.
- Pinto, J.A., and Warme, J.E., 2008, Alamo Event, Nevada: Crater stratigraphy and impact breccia realms, *in* Evan, K.R., Horton, J.W., Jr., King, D.T., Jr., and Morrow, J.R., eds., The sedimentary record of meteorite impacts: Geological Society of America Special Paper 437, p. 99-137, doi:10.1130/2008.2437(07).
- Poole, F.G., 1974, Flysch deposits of Antler foreland basin, western United States, *in* Dickinson, W.R., ed., Tectonics and sedimentation: Society of Economic paleontologists and Mineralogists Special Publication 22, p. 58-83.
- Poole, F.G., Stewart, J.H., Palmer, A.R., Sandberg, C.A., Madrid, R.J., Ross, R.J., Jr., Hintze, L.F., Miller, E.M., and Wrucke, C.T., 1992, Latest Precambrian to Latest Devonian Time: Development of a Continental Margin, *in* Burchfiel, B. C., Lipman, P.W., and Zoback, M.L., eds., The Cordilleran Orogen: Conterminous U.S.: Boulder, Colorado, Geological Society of America, The Geology of North America, v. G-3, p. 9-56.
- Reed, M., Perry, K., Johnston, S.M., and Gehrels, G., 2010, Detrital zircon provenance of Precambrian–Cambrian miogeoclinal sedimentary rocks, Nevada–Utah border: Geological Society of America Abstracts with Programs, v. 42, no. 4, p. 66

- Retzler, A.J., Tapanila, L., Steenberg, J.R., Johnson, C.J., and Myers, R.A, 2015, Post-impact depositional environments as a proxy for crater morphology, Late Devonian Alamo impact, Nevada: *Geosphere*, v. 11, p. 123–143, doi: 10.1130/GES00964.1.
- Rigby, J.K., 1959, Upper Devonian Unconformity in Central Utah: *Geological Society of America Bulletin*, v. 70, p. 207–218.
- Roberts, R.J., Crittenden Jr., M.D., Tooker, E.W., Morris, H.T., Hose, R.K., and Cheney, T.M., 1965, Pennsylvanian and Permian Basins in Northwestern Utah, Northeastern Nevada and South-Central Idaho: *American Association of Petroleum Geologists Bulletin*, v. 49, p. 1926–1956.
- Root, K.G., 2001, Devonian Antler Fold and Thrust Belt and Foreland Basin Development in the Southern Canadian Cordillera: Implications for the Western Canada Sedimentary Basin: *Bulletin of Canadian Petroleum Geology*, v. 29, no. 1, p. 7-36.
- Ross, G.M., and Villeneuve, M., 2003, Provenance of the Mesoproterozoic (1.45 Ga) Belt basin (western North America): another piece in the pre-Rodinia paleogeographic puzzle: *Geological Society of America Bulletin*, v. 115, p. 1191-1217.
- Savoy L.E., and Mountjoy, E.W., 1995, Cratonic-margin and Antler-age foreland basin strata (Middle Devonian to Lower Carboniferous) of the Southern Canadian Rocky Mountains and adjacent plains *in* Ross, G.M., and Dorobek, S., eds., *Stratigraphic*

Evolution of Foreland Basins, Society for Sedimentary Geology, Special Publication 52, p. 213-231.

Smith J.F., Jr., and Ketner, K.B., 1968, Devonian and Mississippian rocks and the date of the Roberts Mountains thrust in the Carlin-Pinon Range area, Nevada: United States Geological Survey Bulletin 1251-I, 18 p.

Speed, R.C., and Sleep, N.H., 1982, Antler orogeny and foreland basin: A model: Geological Society of America Bulletin, v. 93, p. 815–828, doi: 10.1130/0016-7606(1982)93<815.

Staatz, M., and Carr, W., 1964, Geology and mineral deposits of the Thomas and Dugway Ranges, Juab and Tooele Counties, Utah: Professional Papers of the U.S. Geological Survey, v. 415, 188 p.

Stewart, J.H., 1980, Geology of Nevada: A Discussion to Accompany the Geologic Map of Nevada: Nevada Bureau of Mines and Geology, v. 4, 136 p.

Thomason, C.J., 2010, Recovery of the carbonate platform and fauna in the aftermath of the Late Devonian Alamo Impact, Hiko Hills range, Southeastern Nevada [Masters Thesis]: Pocatello, Idaho State University, 202 p.

Trexler, Jr., J.H., 1992, The Devonian-Mississippian Stansbury Formation at Stansbury Island and in the Northeastern Stansbury Mountains, Utah *in* Wilson, J.R. ed., Field Guide to Geologic Excursions in Utah and Adjacent Areas of Nevada, Idaho, and

- Wyoming: Geological Society of America, Rocky Mountain Section Meeting, p. 161-170.
- Walters, L., 2012, Late Devonian Sea-Level Change: Evidence from the Beirdneau Formation, Southern Idaho/Northern Utah [Masters Thesis]: Moscow, University of Idaho, 130 p.
- Webb, G.W., 1958, Middle Ordovician Stratigraphy in Eastern Nevada and Western Utah: American Association of Petroleum Geologists Bulletin, v. 42, p. 2335–2377.
- Whitmeyer, S.J., Karlstrom, K.E., 2007, Tectonic model for the Proterozoic growth of North America: Geosphere, v. 3, no. 4, p. 220-259, doi: 10.1130/GES00055.1.
- Workman, B., 2012, Sequence Stratigraphy and Detrital Zircon Provenance of the Eureka Quartzite in south-central Nevada and eastern California [Masters Thesis]: Station, Texas A&M University, 51 p.
- Wright, J.E., and Wyld, S.J., 2006, Gondwanan . Iapetan , Cordilleran interactions : A geodynamic model for the Paleozoic tectonic evolution of the North American Cordillera, *in* Haggart, J.W., Enkin R.J., and Monger J.W.H., eds., Paleogeography of the North American Cordillera: Evidence for and against large-scale displacements: Geological Association of Canada, Special Paper 46, p. 377-408.
- Young, J.C., 1953, Geology of the Southern Lakeside Mountains, Utah [Masters Thesis]: Salt Lake City, University of Utah, 90 p.

Appendix I: Detrital zircon data

Age	Sample Number	Fm Name	Range	GPS Zone (NAD 83)	Easting Northing	Outcrop Description
Late Devonian	01NAH14	Guilmette Fm	Windermere Hills, Nevada	11T	0691217 4571317	Light tan to grey weathered, medium grey fresh. Medium- to fine-grained quartz-rich tan sand on a grey calcite matrix. Base of outcrop covered, thickness unknown, but <2m.
	04NAH14	Pinyon Peak Fm	Northern Lakeside Mtns	12T	0341509 4541848	Orange to buff weathered, medium grey fresh. Thick laminated to thinly bedded with very low angle broad cross beds and parallel bedding. Calcite cemented quartz arenite with localized matrix Outcrop ~2-3m thick. Sharp base with channels and rip-up clasts indicating erosional base. Very well rounded, poorly sorted.
	09NAH14	Guilmette Fm/ Goshoot Fm/ Cove Fort Qtzt	Northern Dugway Range	12T	0311276 4430759	Dark pink to burnt rusty brown weathered, light pink fresh. Very coarse-grained sand to pebble quartz conglomerate. Outcrop ~8m thick. Medium bedded with crossbedding. Base of outcrop not exposed. Well rounded, very poorly sorted.
	15NAH14	Guilmette Sandstone	Southern Goshute Mtns	11T	0728094 4480669	Tannish brown weathered, grey fresh with interbedded layers of a light brown. Calcite cemented medium- to coarse-grained, quartz arenite with frosted or glassy quartz grains. Obvious high to intermediate angled crossbedding. 1 to 1.5m thick outcrop, basal unconformity with sparse rip-up clasts. Subrounded to rounded grains with some degree of well sorting.
	16NAH14	Victoria Quartzite/ Pinyon Peak Sandstone Member	East Tintic Range	12S	0408937 4426197	Medium tan to dark brown weathered, medium grey fresh. Dolomite-cemented, very fine-grained quartzite with laminar bedding, minor crenulated bedding, and faint, minor crossbedding. Undulose bedding and channels at base indicated an erosional base or unconformity. 2m thick and grades upward into dolomite. Very well sorted.

Analysis	U	206Pb	U/Th	206Pb*	±	207Pb*	±	206Pb*	±	error	206Pb*	±	207Pb*	±	206Pb*	±	Best age	±	Conc
	(ppm)	204Pb		207Pb*	(%)	235U*	(%)	238U	(%)	corr.	238U*	(Ma)	235U	(Ma)	207Pb*	(Ma)	(Ma)	(Ma)	(%)
01NAH14-1	81	206242	0.9	5.5720	0.3	12.3774	0.5	0.5002	0.4	0.82	2614.7	8.7	2633.5	4.6	2647.9	4.7	2647.9	4.7	98.7
01NAH14-2	49	32374	1.2	11.3982	1.7	2.8975	1.9	0.2395	1.0	0.50	1384.2	11.9	1381.2	14.4	1376.6	31.8	1376.6	31.8	100.6
01NAH14-3	60	53918	1.3	9.5414	1.5	4.4432	1.7	0.3075	0.8	0.45	1728.3	11.8	1720.4	14.2	1710.9	28.1	1710.9	28.1	101.0
01NAH14-5	42	65859	1.2	11.1843	3.1	3.0676	3.3	0.2488	1.1	0.34	1432.4	14.5	1424.6	25.6	1413.0	60.1	1413.0	60.1	101.4
01NAH14-6	160	98604	2.0	9.5212	0.6	4.4018	1.1	0.3040	0.9	0.85	1710.9	13.7	1712.7	8.9	1714.8	10.4	1714.8	10.4	99.8
01NAH14-7	60	123654	1.0	5.8401	0.4	11.7257	1.0	0.4967	0.8	0.89	2599.4	18.2	2582.8	9.0	2569.7	7.4	2569.7	7.4	101.2
01NAH14-8	108	119826	1.9	7.6940	0.5	6.9512	1.0	0.3879	0.9	0.87	2113.0	16.1	2105.2	9.2	2097.6	9.0	2097.6	9.0	100.7
01NAH14-9	86	105422	3.0	11.0912	0.6	3.1748	1.1	0.2554	0.9	0.82	1466.2	11.8	1451.0	8.5	1428.9	11.9	1428.9	11.9	102.6
01NAH14-10	68	106018	1.2	9.6134	0.9	4.3913	1.9	0.3062	1.6	0.86	1721.8	24.3	1710.7	15.4	1697.1	17.4	1697.1	17.4	101.5
01NAH14-11	115	165896	1.9	9.3239	1.1	4.7014	1.5	0.3179	1.1	0.73	1779.6	17.4	1767.5	12.9	1753.2	19.4	1753.2	19.4	101.5
01NAH14-12	71	46718	1.0	9.6530	0.8	4.3116	1.0	0.3019	0.6	0.64	1700.5	9.4	1695.6	8.1	1689.5	14.0	1689.5	14.0	100.7
01NAH14-13	152	379879	2.5	9.2065	0.6	4.7152	1.1	0.3148	1.0	0.87	1764.5	15.1	1769.9	9.4	1776.4	10.1	1776.4	10.1	99.3
01NAH14-14	127	66716	3.3	9.2928	0.7	4.1890	1.9	0.2823	1.8	0.92	1603.1	25.0	1671.9	15.6	1759.3	13.4	1759.3	13.4	91.1
01NAH14-15	114	134284	1.8	6.1482	0.3	10.6198	1.8	0.4735	1.8	0.99	2499.1	37.5	2490.4	17.0	2483.4	4.9	2483.4	4.9	100.6
01NAH14-16	102	61536	3.2	9.2039	0.7	4.8608	1.1	0.3245	0.8	0.75	1811.5	12.7	1795.5	9.0	1776.9	12.8	1776.9	12.8	102.0
01NAH14-17	86	214766	0.7	5.3453	0.2	14.0002	1.0	0.5428	1.0	0.98	2795.0	22.5	2749.7	9.7	2716.7	3.7	2716.7	3.7	102.9
01NAH14-18	18	31801	1.3	9.4474	3.9	4.5218	4.4	0.3098	2.1	0.48	1739.9	32.2	1735.0	36.8	1729.1	71.5	1729.1	71.5	100.6
01NAH14-19	81	92616	3.0	10.9887	1.2	3.1707	1.6	0.2527	1.1	0.68	1452.4	14.2	1450.0	12.3	1446.6	22.2	1446.6	22.2	100.4
01NAH14-20	262	673489	2.7	8.7752	0.3	5.2831	0.6	0.3362	0.6	0.88	1868.5	8.9	1866.1	5.4	1863.4	5.4	1863.4	5.4	100.3
01NAH14-21	62	77392	1.9	8.7517	0.9	5.2616	1.0	0.3340	0.6	0.54	1857.6	9.1	1862.7	8.9	1868.3	15.9	1868.3	15.9	99.4
01NAH14-22	52	22359	3.7	12.7001	3.9	2.0860	4.6	0.1921	2.4	0.53	1132.9	25.1	1144.2	31.5	1165.6	77.1	1165.6	77.1	97.2
01NAH14-23	57	138641	1.2	5.3083	0.4	13.7942	1.0	0.5311	1.0	0.92	2746.0	21.6	2735.7	9.9	2728.1	6.7	2728.1	6.7	100.7
01NAH14-24	59	68759	0.9	8.8036	0.9	5.3139	1.4	0.3393	1.1	0.80	1883.3	18.6	1871.1	12.2	1857.6	15.7	1857.6	15.7	101.4
01NAH14-25	40	23565	0.4	8.6253	1.2	5.4712	1.7	0.3423	1.2	0.72	1897.5	20.0	1896.1	14.5	1894.5	21.2	1894.5	21.2	100.2

01NAH14-26	115	52508	3.4	12.8732	0.8	2.0575	1.3	0.1921	1.0	0.79	1132.7	10.7	1134.8	8.9	1138.7	15.8	1138.7	15.8	99.5
01NAH14-27	168	113826	2.6	10.1277	0.6	3.8436	1.8	0.2823	1.7	0.95	1603.1	23.8	1601.9	14.3	1600.4	10.8	1600.4	10.8	100.2
01NAH14-28	53	69206	0.6	5.3218	0.5	13.6578	2.0	0.5272	1.9	0.97	2729.4	42.6	2726.3	18.7	2723.9	8.0	2723.9	8.0	100.2
01NAH14-29	79	99134	2.9	9.6140	0.6	4.4078	1.6	0.3073	1.4	0.92	1727.6	21.6	1713.8	12.9	1696.9	11.5	1696.9	11.5	101.8
01NAH14-30	166	164159	1.6	8.8882	0.5	5.1742	1.0	0.3335	0.8	0.84	1855.6	13.3	1848.4	8.3	1840.3	9.5	1840.3	9.5	100.8
01NAH14-31	127	237641	1.7	5.8604	0.2	11.3547	0.5	0.4826	0.4	0.91	2538.6	9.1	2552.7	4.4	2563.9	3.3	2563.9	3.3	99.0
01NAH14-32	68	57881	1.4	11.3540	1.2	2.9255	1.4	0.2409	0.8	0.55	1391.4	9.8	1388.5	10.7	1384.1	22.6	1384.1	22.6	100.5
01NAH14-33	36	17425	0.7	5.4595	0.6	13.3594	1.3	0.5290	1.1	0.87	2737.2	24.3	2705.4	11.8	2681.7	10.2	2681.7	10.2	102.1
01NAH14-34	81	129987	3.3	8.9613	0.8	4.9747	1.0	0.3233	0.6	0.62	1805.9	9.9	1815.0	8.5	1825.5	14.2	1825.5	14.2	98.9
01NAH14-35	47	38305	1.1	8.9247	1.7	5.0624	1.9	0.3277	0.8	0.41	1827.1	12.1	1829.8	15.7	1832.9	30.6	1832.9	30.6	99.7
01NAH14-36	20	4106	2.0	18.8495	8.9	0.6301	10.4	0.0861	5.4	0.52	532.7	27.9	496.1	41.0	331.0	202.5	532.7	27.9	160.9
01NAH14-37	147	271934	2.0	8.8393	0.5	5.2099	0.9	0.3340	0.8	0.81	1857.7	12.1	1854.2	7.9	1850.3	9.8	1850.3	9.8	100.4
01NAH14-38	139	169801	1.0	8.4716	0.5	5.5983	2.5	0.3440	2.4	0.98	1905.7	39.9	1915.8	21.3	1926.8	8.6	1926.8	8.6	98.9
01NAH14-39	78	14959	2.6	13.0453	1.8	1.9453	4.7	0.1841	4.4	0.92	1089.1	43.7	1096.8	31.7	1112.2	36.3	1112.2	36.3	97.9
01NAH14-40	221	58980	0.9	8.8940	0.5	5.2367	7.6	0.3378	7.6	1.00	1876.1	123.7	1858.6	65.0	1839.1	9.6	1839.1	9.6	102.0
01NAH14-41	158	147013	1.9	8.8432	0.4	5.2406	0.8	0.3361	0.7	0.88	1867.9	12.0	1859.2	7.2	1849.5	7.3	1849.5	7.3	101.0
01NAH14-42	170	129889	3.8	12.8292	0.9	2.0927	1.2	0.1947	0.8	0.70	1146.9	8.8	1146.4	8.2	1145.5	17.0	1145.5	17.0	100.1
01NAH14-43	56	46759	0.7	8.8838	1.4	5.1441	2.7	0.3314	2.3	0.85	1845.4	36.4	1843.4	22.8	1841.2	25.8	1841.2	25.8	100.2
01NAH14-44	56	120443	0.5	8.6719	1.0	5.3678	1.4	0.3376	0.9	0.66	1875.1	14.7	1879.7	11.6	1884.8	18.3	1884.8	18.3	99.5
01NAH14-45	29	12982	1.2	17.9695	12.4	0.6148	12.5	0.0801	1.9	0.15	496.9	8.9	486.6	48.4	438.4	276.2	496.9	8.9	113.3
01NAH14-46	107	205708	2.7	9.8964	2.9	3.7141	6.9	0.2666	6.3	0.91	1523.4	85.0	1574.4	55.3	1643.4	54.3	1643.4	54.3	92.7
01NAH14-49	242	320723	2.8	4.1016	0.1	20.3852	1.8	0.6064	1.8	1.00	3055.6	44.4	3109.8	17.7	3145.0	2.2	3145.0	2.2	97.2
01NAH14-50	84	65650	1.3	9.4524	1.3	4.3112	1.9	0.2956	1.3	0.70	1669.2	19.4	1695.5	15.5	1728.1	24.5	1728.1	24.5	96.6
01NAH14-51	54	79883	0.7	5.2843	0.6	13.7181	1.4	0.5257	1.3	0.92	2723.5	28.5	2730.4	13.2	2735.6	9.2	2735.6	9.2	99.6
01NAH14-52	71	19092	1.2	8.8474	1.5	5.1563	2.3	0.3309	1.8	0.77	1842.6	28.1	1845.4	19.5	1848.6	26.7	1848.6	26.7	99.7
01NAH14-53	83	33028	1.5	13.1750	1.8	1.9476	2.4	0.1861	1.6	0.67	1100.2	15.9	1097.6	15.8	1092.4	35.3	1092.4	35.3	100.7
01NAH14-54	68	100203	1.2	7.7612	0.5	6.8255	1.0	0.3842	0.8	0.85	2095.9	15.1	2089.0	8.8	2082.3	9.2	2082.3	9.2	100.7

01NAH14-55	54	61418	0.8	8.4897	1.4	5.8386	2.6	0.3595	2.1	0.83	1979.8	36.3	1952.2	22.2	1922.9	25.4	1922.9	25.4	103.0
01NAH14-56	96	52305	1.3	8.9395	0.6	5.2643	1.3	0.3413	1.1	0.89	1893.0	18.5	1863.1	10.8	1829.9	10.6	1829.9	10.6	103.4
01NAH14-57	69	42685	0.7	8.5461	0.5	5.5830	0.8	0.3460	0.7	0.80	1915.7	11.2	1913.5	7.3	1911.1	9.1	1911.1	9.1	100.2
01NAH14-58	54	45072	1.0	11.4638	2.0	2.8728	2.9	0.2389	2.1	0.72	1380.7	26.2	1374.8	22.1	1365.6	39.3	1365.6	39.3	101.1
01NAH14-60	24	9082	0.7	8.8700	3.0	5.1754	5.4	0.3329	4.5	0.83	1852.6	72.7	1848.6	46.1	1844.0	53.9	1844.0	53.9	100.5
01NAH14-61	66	53966	0.7	8.8835	0.6	5.1551	1.3	0.3321	1.2	0.89	1848.8	18.8	1845.2	11.2	1841.3	10.9	1841.3	10.9	100.4
01NAH14-62	83	142145	2.4	8.6809	0.9	5.4029	1.1	0.3402	0.7	0.61	1887.5	11.0	1885.3	9.4	1882.9	15.7	1882.9	15.7	100.2
01NAH14-63	98	86152	2.4	11.0128	1.0	3.2087	1.5	0.2563	1.1	0.73	1470.8	14.4	1459.3	11.6	1442.5	19.6	1442.5	19.6	102.0
01NAH14-64	110	143303	0.6	5.3489	0.4	13.7206	0.7	0.5323	0.6	0.87	2751.0	14.4	2730.6	7.0	2715.5	6.0	2715.5	6.0	101.3
01NAH14-65	75	168645	2.2	8.8004	0.9	5.3444	1.3	0.3411	0.9	0.73	1892.0	15.4	1876.0	10.9	1858.3	15.7	1858.3	15.7	101.8
01NAH14-66	123	154593	2.1	9.6583	0.6	4.3649	1.9	0.3058	1.8	0.95	1719.8	27.7	1705.7	16.0	1688.5	11.3	1688.5	11.3	101.9
01NAH14-66	203	180158	2.5	5.5632	0.2	12.8391	0.7	0.5180	0.7	0.97	2690.9	15.9	2667.9	7.0	2650.6	3.2	2650.6	3.2	101.5
01NAH14-69	76	44058	2.7	12.6890	1.4	2.1584	1.8	0.1986	1.2	0.67	1168.0	13.3	1167.8	12.8	1167.3	27.0	1167.3	27.0	100.1
01NAH14-70	58	80771	2.0	8.7237	1.4	5.4216	1.8	0.3430	1.2	0.66	1901.2	19.9	1888.3	15.6	1874.1	24.6	1874.1	24.6	101.4
01NAH14-71	66	96177	0.6	9.6310	0.9	4.3412	2.0	0.3032	1.8	0.90	1707.3	26.8	1701.2	16.3	1693.7	15.8	1693.7	15.8	100.8
01NAH14-72	65	90453	1.7	7.7689	0.6	6.9478	3.2	0.3915	3.2	0.98	2129.7	57.2	2104.8	28.6	2080.5	11.4	2080.5	11.4	102.4
01NAH14-73	65	56007	1.3	8.9044	0.9	5.1981	1.2	0.3357	0.8	0.70	1865.9	13.6	1852.3	10.3	1837.0	15.7	1837.0	15.7	101.6
01NAH14-74	105	119589	2.8	11.0634	0.8	3.2373	1.6	0.2598	1.4	0.87	1488.6	18.6	1466.1	12.5	1433.7	15.2	1433.7	15.2	103.8
01NAH14-75	84	127298	1.2	7.6878	0.7	7.0671	1.6	0.3940	1.5	0.91	2141.6	27.0	2119.9	14.5	2099.0	11.9	2099.0	11.9	102.0
01NAH14-76	51	114013	0.7	6.5291	0.8	9.5359	1.7	0.4516	1.5	0.88	2402.2	29.3	2391.0	15.3	2381.5	13.7	2381.5	13.7	100.9
01NAH14-77	48	88944	0.9	8.9540	1.6	5.1454	2.8	0.3341	2.4	0.83	1858.4	38.0	1843.6	24.2	1826.9	29.0	1826.9	29.0	101.7
01NAH14-78	107	195575	1.5	8.9124	0.6	5.2981	1.1	0.3425	0.9	0.81	1898.5	14.6	1868.6	9.4	1835.4	11.7	1835.4	11.7	103.4
01NAH14-79	92	79389	0.7	6.1222	0.6	10.8680	4.5	0.4826	4.5	0.99	2538.4	93.7	2511.9	41.9	2490.5	9.5	2490.5	9.5	101.9
01NAH14-80	121	27680	1.2	11.4218	1.0	2.7500	5.4	0.2278	5.3	0.98	1323.0	63.5	1342.1	40.3	1372.7	20.1	1372.7	20.1	96.4
01NAH14-82	121	93095	0.9	8.5701	0.5	5.7379	0.9	0.3566	0.8	0.85	1966.2	13.3	1937.1	7.9	1906.0	8.6	1906.0	8.6	103.2
01NAH14-83	39	67149	1.3	9.1774	2.4	4.9682	3.0	0.3307	1.6	0.56	1841.7	26.4	1813.9	24.9	1782.1	44.6	1782.1	44.6	103.3
01NAH14-84	30	25802	0.6	7.7738	1.2	6.9367	1.7	0.3911	1.2	0.69	2127.9	21.5	2103.4	15.3	2079.4	22.0	2079.4	22.0	102.3

01NAH14-85	83	68628	2.4	11.0810	1.6	3.2203	2.1	0.2588	1.3	0.63	1483.7	17.2	1462.1	16.0	1430.7	30.6	1430.7	30.6	103.7
01NAH14-86	57	66142	1.7	5.8398	0.6	11.8523	1.9	0.5020	1.8	0.95	2622.4	38.1	2592.8	17.5	2569.8	10.1	2569.8	10.1	102.0
01NAH14-87	42	28987	2.8	10.9805	2.3	3.2129	4.1	0.2559	3.4	0.82	1468.7	44.1	1460.3	31.6	1448.1	44.0	1448.1	44.0	101.4
01NAH14-88	191	185452	4.1	9.1891	0.3	4.9178	3.1	0.3278	3.1	1.00	1827.5	48.8	1805.3	26.0	1779.8	5.0	1779.8	5.0	102.7
01NAH14-89	86	55974	2.2	12.7617	1.4	2.1717	1.8	0.2010	1.1	0.62	1180.7	12.3	1172.0	12.8	1156.0	28.7	1156.0	28.7	102.1
01NAH14-90	221	32466	4.5	11.0544	0.6	2.8569	3.3	0.2290	3.3	0.98	1329.5	39.4	1370.6	25.1	1435.3	12.0	1435.3	12.0	92.6
01NAH14-91	59	174391	1.3	5.9678	0.5	11.4966	1.6	0.4976	1.5	0.95	2603.5	32.1	2564.3	14.7	2533.5	7.9	2533.5	7.9	102.8
01NAH14-92	101	20429	2.5	11.0470	1.3	2.9070	1.9	0.2329	1.4	0.75	1349.7	17.3	1383.7	14.3	1436.6	23.9	1436.6	23.9	94.0
01NAH14-93	41	102703	1.1	8.9902	1.0	5.1218	1.5	0.3340	1.1	0.74	1857.5	18.2	1839.7	12.9	1819.6	18.4	1819.6	18.4	102.1
01NAH14-94	56	68115	0.5	5.7099	0.5	11.7583	1.0	0.4869	0.9	0.89	2557.4	19.2	2585.3	9.6	2607.3	7.9	2607.3	7.9	98.1
01NAH14-95	63	204991	1.7	5.3874	0.8	13.2859	2.3	0.5191	2.2	0.94	2695.4	47.4	2700.2	21.7	2703.7	13.1	2703.7	13.1	99.7
01NAH14-96	29	23736	0.6	8.8262	1.7	5.2832	2.6	0.3382	2.0	0.75	1878.0	32.4	1866.2	22.5	1853.0	31.4	1853.0	31.4	101.4
01NAH14-97	97	48260	1.5	9.7556	0.7	3.7044	3.3	0.2621	3.2	0.98	1500.6	43.2	1572.3	26.5	1670.0	13.4	1670.0	13.4	89.9
01NAH14-98	47	52428	0.8	8.6412	1.4	5.5391	2.1	0.3471	1.5	0.74	1920.9	25.4	1906.7	17.9	1891.2	25.3	1891.2	25.3	101.6
01NAH14-99	57	59883	0.9	11.3579	2.4	2.8984	2.9	0.2388	1.7	0.57	1380.2	20.8	1381.5	22.2	1383.4	46.6	1383.4	46.6	99.8
01NAH14-100	66	66471	0.9	8.8210	0.9	5.3724	2.1	0.3437	1.9	0.91	1904.5	31.3	1880.5	17.9	1854.0	15.8	1854.0	15.8	102.7

04NAH14-01	18	31097	1.0	7.9012	1.7	6.7010	2.8	0.3840	2.1	0.78	2094.9	38.3	2072.7	24.4	2050.8	30.7	2050.8	30.7	102.2
04NAH14-02	70	104308	1.0	8.9389	0.8	5.1125	1.3	0.3314	1.0	0.77	1845.4	15.8	1838.2	10.9	1830.0	14.8	1830.0	14.8	100.8
04NAH14-03	33	32477	0.8	8.9883	2.0	5.0542	3.6	0.3295	2.9	0.82	1835.9	46.5	1828.5	30.2	1820.0	37.1	1820.0	37.1	100.9
04NAH14-04	265	73924	1.8	7.7761	0.2	6.6950	1.3	0.3776	1.2	0.99	2065.0	22.0	2072.0	11.1	2078.9	3.6	2078.9	3.6	99.3
04NAH14-05	177	342639	0.8	8.1664	0.3	6.1505	2.1	0.3643	2.0	0.99	2002.4	35.2	1997.4	18.1	1992.3	6.2	1992.3	6.2	100.5
04NAH14-06	83	144975	0.6	8.4611	0.5	5.6253	0.6	0.3452	0.3	0.60	1911.6	5.6	1920.0	4.9	1929.0	8.2	1929.0	8.2	99.1
04NAH14-07	61	52741	1.2	7.7872	0.8	6.7026	2.4	0.3785	2.2	0.94	2069.5	39.4	2073.0	20.9	2076.4	14.1	2076.4	14.1	99.7
04NAH14-08	18	39114	1.3	8.6933	2.2	5.5061	2.4	0.3472	1.0	0.40	1921.0	16.0	1901.6	20.5	1880.3	39.4	1880.3	39.4	102.2
04NAH14-09	34	45088	0.9	8.8103	1.4	5.2014	2.5	0.3324	2.0	0.82	1849.8	32.8	1852.8	21.1	1856.2	25.3	1856.2	25.3	99.7
04NAH14-10	65	76356	1.1	8.9521	1.0	5.0135	1.2	0.3255	0.7	0.57	1816.6	10.7	1821.6	10.1	1827.3	17.8	1827.3	17.8	99.4

04NAH14-11	60	146387	1.5	7.7917	0.8	6.6160	1.1	0.3739	0.8	0.68	2047.6	13.7	2061.5	10.1	2075.4	14.8	2075.4	14.8	98.7
04NAH14-12	35	83120	0.8	8.9563	1.3	5.0539	2.7	0.3283	2.4	0.88	1830.1	38.1	1828.4	23.0	1826.5	23.4	1826.5	23.4	100.2
04NAH14-13	169	459269	4.9	8.4075	0.4	5.9506	1.0	0.3629	0.9	0.93	1995.7	15.5	1968.7	8.5	1940.4	6.4	1940.4	6.4	102.9
04NAH14-14	104	335892	2.1	7.7806	0.4	6.8000	0.6	0.3837	0.5	0.77	2093.7	8.2	2085.7	5.3	2077.9	6.7	2077.9	6.7	100.8
04NAH14-15	80	127611	1.2	8.8908	0.7	5.1470	2.0	0.3319	1.9	0.94	1847.5	30.8	1843.9	17.3	1839.8	12.4	1839.8	12.4	100.4
04NAH14-16	51	46272	1.4	11.6597	2.9	2.7107	5.2	0.2292	4.4	0.83	1330.4	52.4	1331.4	38.9	1332.9	56.2	1332.9	56.2	99.8
04NAH14-17	53	73986	1.5	8.8270	0.8	4.8806	3.4	0.3124	3.4	0.98	1752.8	51.4	1798.9	29.0	1852.8	13.8	1852.8	13.8	94.6
04NAH14-18	73	162854	1.5	7.7482	0.6	6.7867	1.1	0.3814	0.8	0.80	2082.7	15.0	2084.0	9.4	2085.2	11.2	2085.2	11.2	99.9
04NAH14-19	256	134883	2.4	8.9456	0.3	5.0860	1.0	0.3300	1.0	0.97	1838.3	16.0	1833.8	8.8	1828.7	4.9	1828.7	4.9	100.5
04NAH14-20	28	38853	0.9	8.9481	2.1	4.9825	3.1	0.3234	2.3	0.74	1806.1	36.3	1816.4	26.4	1828.1	38.1	1828.1	38.1	98.8
04NAH14-21	58	110122	1.4	5.5152	0.2	12.9106	0.7	0.5164	0.7	0.95	2684.0	14.5	2673.1	6.6	2665.0	3.7	2665.0	3.7	100.7
04NAH14-22	88	21813	1.4	5.3858	0.3	11.8473	1.8	0.4628	1.8	0.98	2451.8	36.2	2592.4	16.9	2704.2	5.5	2704.2	5.5	90.7
04NAH14-23	107	146116	1.9	8.8610	0.3	5.1017	1.3	0.3279	1.2	0.96	1828.0	19.9	1836.4	11.0	1845.9	6.2	1845.9	6.2	99.0
04NAH14-24	86	15774	2.0	8.8590	0.8	4.8529	3.6	0.3118	3.5	0.97	1749.6	53.9	1794.1	30.4	1846.3	14.9	1846.3	14.9	94.8
04NAH14-25	76	51253	1.5	8.9086	1.2	4.8889	2.1	0.3159	1.8	0.84	1769.6	27.4	1800.3	17.9	1836.2	21.1	1836.2	21.1	96.4
04NAH14-26	96	441586	0.9	8.9599	0.6	5.0102	1.7	0.3256	1.5	0.93	1816.9	24.5	1821.0	14.0	1825.8	10.7	1825.8	10.7	99.5
04NAH14-27	95	372396	1.9	8.8990	0.5	5.1134	0.8	0.3300	0.5	0.70	1838.5	8.5	1838.3	6.5	1838.1	9.8	1838.1	9.8	100.0
04NAH14-28	18	39902	0.5	5.3764	1.6	13.5645	2.8	0.5289	2.3	0.83	2736.9	51.2	2719.8	26.3	2707.1	25.8	2707.1	25.8	101.1
04NAH14-29	42	79550	1.2	8.8618	1.5	5.2288	3.8	0.3361	3.5	0.91	1867.7	56.1	1857.3	32.3	1845.7	27.8	1845.7	27.8	101.2
04NAH14-30	54	72845	1.2	5.4975	0.3	13.0721	0.9	0.5212	0.9	0.93	2704.3	19.3	2684.9	8.8	2670.3	5.5	2670.3	5.5	101.3
04NAH14-31	120	79536	2.0	13.6994	0.8	1.7715	1.4	0.1760	1.2	0.85	1045.2	11.8	1035.1	9.3	1013.8	15.5	1013.8	15.5	103.1
04NAH14-32	101	4348	1.5	5.1679	0.4	12.1989	7.4	0.4572	7.4	1.00	2427.3	148.9	2619.8	69.3	2772.1	5.8	2772.1	5.8	87.6
04NAH14-33	34	61298	0.9	8.9400	2.1	5.1446	4.3	0.3336	3.7	0.87	1855.7	60.2	1843.5	36.5	1829.8	38.4	1829.8	38.4	101.4
04NAH14-34	51	64177	0.4	8.3078	1.3	5.7446	2.5	0.3461	2.1	0.84	1916.1	34.6	1938.1	21.5	1961.7	24.0	1961.7	24.0	97.7
04NAH14-35	55	69096	1.3	8.9440	1.3	4.9620	1.5	0.3219	0.7	0.45	1798.9	10.5	1812.9	12.5	1829.0	23.8	1829.0	23.8	98.4
04NAH14-36	99	327263	1.3	5.9441	0.4	11.0837	2.1	0.4778	2.1	0.98	2517.8	43.9	2530.2	20.0	2540.2	6.8	2540.2	6.8	99.1
04NAH14-37	167	224708	2.0	8.8662	0.4	5.1624	1.4	0.3320	1.3	0.96	1847.9	21.5	1846.4	11.8	1844.8	6.9	1844.8	6.9	100.2

04NAH14-38	29	82746	1.9	5.9896	0.6	10.9593	1.3	0.4761	1.2	0.88	2510.2	24.4	2519.7	12.4	2527.3	10.6	2527.3	10.6	99.3
04NAH14-39	128	382021	1.6	8.8532	0.4	5.2842	1.0	0.3393	0.9	0.93	1883.3	15.4	1866.3	8.6	1847.5	6.5	1847.5	6.5	101.9
04NAH14-40	66	4306	0.7	8.9273	2.5	4.1008	3.6	0.2655	2.7	0.74	1518.0	36.4	1654.5	29.7	1832.4	44.4	1832.4	44.4	82.8
04NAH14-41	56	50165	1.1	13.6740	2.9	1.7538	3.1	0.1739	1.0	0.32	1033.7	9.5	1028.6	20.0	1017.6	59.3	1017.6	59.3	101.6
04NAH14-42	80	114443	0.6	8.7199	0.7	5.2264	0.9	0.3305	0.6	0.61	1841.0	9.2	1856.9	8.0	1874.8	13.4	1874.8	13.4	98.2
04NAH14-43	65	190206	1.0	5.4710	0.4	12.7743	0.9	0.5069	0.9	0.92	2643.3	18.9	2663.2	8.9	2678.2	6.0	2678.2	6.0	98.7
04NAH14-44	29	32775	0.4	8.0115	1.4	6.3511	2.6	0.3690	2.3	0.86	2024.8	39.3	2025.5	23.2	2026.2	24.2	2026.2	24.2	99.9
04NAH14-45	84	135457	0.6	6.6769	0.4	9.0556	1.0	0.4385	0.9	0.92	2344.0	17.8	2343.6	9.0	2343.3	6.7	2343.3	6.7	100.0
04NAH14-46	214	601092	1.3	8.8658	0.3	5.1730	1.3	0.3326	1.3	0.96	1851.1	20.5	1848.2	11.2	1844.9	6.3	1844.9	6.3	100.3
04NAH14-47	160	143367	2.0	8.8708	0.4	5.2707	1.2	0.3391	1.1	0.93	1882.4	18.1	1864.1	10.2	1843.9	8.0	1843.9	8.0	102.1
04NAH14-48	62	13862	0.7	8.8652	0.7	4.5071	2.6	0.2898	2.5	0.96	1640.5	36.1	1732.3	21.5	1845.0	12.6	1845.0	12.6	88.9
04NAH14-49	65	133387	1.1	8.9553	1.4	5.1828	3.1	0.3366	2.8	0.90	1870.4	44.7	1849.8	26.2	1826.7	24.7	1826.7	24.7	102.4
04NAH14-50	235	77602	1.8	8.4398	0.5	5.5058	0.8	0.3370	0.6	0.79	1872.3	10.5	1901.5	7.1	1933.5	9.1	1933.5	9.1	96.8
04NAH14-51	53	85015	1.1	8.4466	0.7	5.7815	1.6	0.3542	1.4	0.88	1954.5	23.2	1943.7	13.6	1932.1	13.4	1932.1	13.4	101.2
04NAH14-52	139	131848	2.3	11.0534	0.7	3.2167	1.3	0.2579	1.1	0.83	1479.0	14.4	1461.2	10.1	1435.5	13.8	1435.5	13.8	103.0
04NAH14-53	26	33024	1.0	8.4997	1.0	5.6525	2.8	0.3485	2.6	0.93	1927.2	43.2	1924.1	24.0	1920.8	17.9	1920.8	17.9	100.3
04NAH14-54	21	23529	0.9	9.0861	3.1	5.1152	4.6	0.3371	3.4	0.74	1872.6	55.8	1838.6	39.2	1800.3	56.0	1800.3	56.0	104.0
04NAH14-55	38	65451	0.9	8.5249	1.1	5.7211	1.3	0.3537	0.7	0.52	1952.4	11.5	1934.6	11.4	1915.5	20.2	1915.5	20.2	101.9
04NAH14-56	119	215901	1.3	5.8324	0.2	11.5712	0.5	0.4895	0.5	0.96	2568.4	10.7	2570.4	4.9	2571.9	2.5	2571.9	2.5	99.9
04NAH14-57	101	181294	1.8	8.9170	0.7	5.1813	0.8	0.3351	0.4	0.55	1863.0	7.2	1849.5	6.9	1834.4	12.3	1834.4	12.3	101.6
04NAH14-58	97	188004	0.8	8.9183	0.8	5.2560	1.3	0.3400	1.1	0.81	1886.5	17.2	1861.7	11.1	1834.2	14.0	1834.2	14.0	102.9
04NAH14-59	148	69482	1.7	8.8296	0.8	5.2843	1.1	0.3384	0.8	0.70	1879.0	12.6	1866.3	9.4	1852.3	14.3	1852.3	14.3	101.4
04NAH14-60	50	153801	1.0	7.7995	1.1	7.0746	3.4	0.4002	3.2	0.95	2169.9	59.1	2120.9	30.1	2073.6	18.9	2073.6	18.9	104.6
04NAH14-61	63	81947	2.1	8.8831	1.0	5.2354	2.8	0.3373	2.6	0.93	1873.7	42.6	1858.4	24.0	1841.3	18.6	1841.3	18.6	101.8
04NAH14-62	49	65060	1.1	8.8576	1.4	5.2890	2.0	0.3398	1.4	0.71	1885.6	23.4	1867.1	17.3	1846.6	25.9	1846.6	25.9	102.1
04NAH14-63	109	314769	1.1	6.5398	0.3	9.7266	2.0	0.4613	2.0	0.99	2445.5	41.0	2409.2	18.7	2378.7	5.0	2378.7	5.0	102.8
04NAH14-64	81	206793	0.4	8.4362	0.9	5.7429	1.0	0.3514	0.5	0.51	1941.2	8.7	1937.8	8.8	1934.3	15.6	1934.3	15.6	100.4

04NAH14-65	55	62001	1.2	8.8445	1.8	5.2981	2.4	0.3399	1.6	0.66	1885.9	26.4	1868.6	20.9	1849.2	33.3	1849.2	33.3	102.0
04NAH14-66	38	54807	1.2	8.7938	1.1	5.3201	1.3	0.3393	0.8	0.60	1883.3	13.0	1872.1	11.3	1859.6	19.0	1859.6	19.0	101.3
04NAH14-67	29	50495	0.8	5.4778	0.8	12.7978	1.7	0.5084	1.5	0.89	2650.0	33.2	2664.9	16.2	2676.2	12.9	2676.2	12.9	99.0
04NAH14-68	75	91644	1.9	7.7548	0.8	7.0226	2.0	0.3950	1.9	0.92	2145.9	34.1	2114.3	18.1	2083.7	14.0	2083.7	14.0	103.0
04NAH14-69	95	147382	1.5	8.9805	0.6	5.1213	1.0	0.3336	0.8	0.82	1855.6	13.6	1839.6	8.7	1821.6	10.6	1821.6	10.6	101.9
04NAH14-70	143	202459	2.3	8.7760	0.4	5.4189	1.4	0.3449	1.3	0.96	1910.2	21.9	1887.8	11.8	1863.3	7.1	1863.3	7.1	102.5
04NAH14-71	71	107466	0.8	8.9370	0.9	5.0676	1.2	0.3285	0.7	0.62	1831.0	11.9	1830.7	10.2	1830.4	17.1	1830.4	17.1	100.0
04NAH14-72	61	153953	0.9	7.7224	0.6	6.8230	2.0	0.3821	1.9	0.95	2086.3	33.3	2088.7	17.4	2091.1	10.4	2091.1	10.4	99.8
04NAH14-73	30	37445	1.0	8.4861	1.4	5.6943	2.2	0.3505	1.6	0.75	1936.8	27.2	1930.5	18.8	1923.7	25.8	1923.7	25.8	100.7
04NAH14-74	103	162458	1.2	8.8875	0.5	5.3335	1.7	0.3438	1.6	0.95	1904.9	26.7	1874.3	14.5	1840.5	9.3	1840.5	9.3	103.5
04NAH14-75	130	267288	1.7	6.5030	0.4	9.2420	1.1	0.4359	1.0	0.94	2332.2	19.5	2362.3	9.7	2388.3	6.2	2388.3	6.2	97.7
04NAH14-76	83	142894	1.1	5.6664	0.3	12.6829	1.8	0.5212	1.8	0.99	2704.4	39.8	2656.4	17.2	2620.0	4.6	2620.0	4.6	103.2
04NAH14-77	74	100812	1.6	5.4459	0.3	13.5719	1.4	0.5361	1.4	0.98	2766.9	30.8	2720.3	13.2	2685.9	4.8	2685.9	4.8	103.0
04NAH14-78	46	59113	2.8	8.2919	0.9	6.0358	1.1	0.3630	0.7	0.60	1996.3	11.5	1981.0	9.7	1965.1	15.7	1965.1	15.7	101.6
04NAH14-80	62	100516	1.8	8.9156	0.8	5.2137	1.0	0.3371	0.7	0.67	1872.8	11.3	1854.9	8.8	1834.7	13.8	1834.7	13.8	102.1
04NAH14-81	27	30982	0.8	5.5188	0.9	13.1255	1.5	0.5254	1.2	0.79	2721.9	25.8	2688.7	13.9	2663.9	14.9	2663.9	14.9	102.2
04NAH14-82	72	71356	1.1	8.9509	1.1	5.2205	1.4	0.3389	0.9	0.63	1881.4	14.1	1856.0	11.7	1827.6	19.2	1827.6	19.2	102.9
04NAH14-83	82	155756	2.7	8.7666	0.7	5.3029	1.6	0.3372	1.4	0.88	1873.0	22.6	1869.3	13.4	1865.2	13.3	1865.2	13.3	100.4
04NAH14-84	68	99141	0.6	8.6887	1.6	5.3593	3.3	0.3377	3.0	0.88	1875.7	48.1	1878.4	28.6	1881.3	28.2	1881.3	28.2	99.7
04NAH14-85	51	47282	1.9	9.0018	1.1	4.9798	1.4	0.3251	0.9	0.63	1814.7	14.0	1815.9	11.9	1817.3	19.8	1817.3	19.8	99.9
04NAH14-86	52	66798	0.9	8.9226	1.0	5.2134	1.5	0.3374	1.1	0.74	1874.0	18.5	1854.8	13.1	1833.3	18.8	1833.3	18.8	102.2
04NAH14-87	54	80753	1.8	5.8584	1.4	11.3853	3.1	0.4838	2.7	0.89	2543.6	57.4	2555.2	28.6	2564.5	23.1	2564.5	23.1	99.2
04NAH14-88	86	240425	0.9	8.5944	0.5	5.5586	1.2	0.3465	1.1	0.91	1917.8	18.2	1909.7	10.4	1900.9	9.1	1900.9	9.1	100.9
04NAH14-89	109	27578	1.0	10.9359	3.5	2.8432	5.6	0.2255	4.4	0.79	1310.9	52.1	1367.0	42.1	1455.8	65.9	1455.8	65.9	90.0
04NAH14-90	102	143791	1.9	5.3539	0.2	13.8201	0.8	0.5366	0.8	0.96	2769.4	17.1	2737.5	7.5	2714.0	3.4	2714.0	3.4	102.0
04NAH14-91	10	20974	0.5	9.2175	8.4	4.8741	9.9	0.3258	5.2	0.52	1818.2	82.2	1797.8	83.5	1774.2	153.8	1774.2	153.8	102.5
04NAH14-92	100	155103	2.0	8.6958	0.8	5.5505	1.6	0.3501	1.4	0.86	1934.9	22.8	1908.5	13.6	1879.8	14.3	1879.8	14.3	102.9

04NAH14-93	117	172941	1.7	8.8983	0.9	5.2963	2.9	0.3418	2.8	0.95	1895.4	45.6	1868.3	25.0	1838.3	16.6	1838.3	16.6	103.1
04NAH14-94	60	64522	1.8	4.5714	0.3	16.3864	1.3	0.5433	1.3	0.97	2797.2	29.2	2899.6	12.7	2971.5	5.1	2971.5	5.1	94.1
04NAH14-95	65	69473	1.1	8.5286	0.8	5.6068	1.6	0.3468	1.5	0.88	1919.4	24.1	1917.2	14.1	1914.8	13.7	1914.8	13.7	100.2
04NAH14-96	57	84727	1.9	8.8422	0.8	5.2195	1.2	0.3347	0.9	0.75	1861.2	14.7	1855.8	10.3	1849.7	14.5	1849.7	14.5	100.6
04NAH14-97	38	73503	1.9	8.8295	1.1	5.3128	1.8	0.3402	1.4	0.78	1887.7	22.9	1870.9	15.4	1852.3	20.5	1852.3	20.5	101.9
04NAH14-98	86	112492	1.2	8.5040	0.8	5.5804	1.0	0.3442	0.6	0.57	1906.8	9.3	1913.1	8.5	1919.9	14.7	1919.9	14.7	99.3
04NAH14-99	122	135517	1.2	8.8652	0.5	5.2586	1.2	0.3381	1.1	0.92	1877.6	17.6	1862.2	10.0	1845.0	8.4	1845.0	8.4	101.8
04NAH14-100	43	73875	1.0	8.8651	1.1	5.1118	2.0	0.3287	1.7	0.85	1831.9	27.8	1838.1	17.4	1845.0	19.3	1845.0	19.3	99.3

09NAH14-01	46	35871	1.0	10.9171	2.5	3.2309	3.3	0.2558	2.2	0.65	1468.4	28.4	1464.6	25.9	1459.1	48.5	1459.1	48.5	100.6
09NAH14-02	95	108406	1.7	11.0848	1.1	3.1718	2.8	0.2550	2.6	0.92	1464.2	34.2	1450.3	21.9	1430.0	21.0	1430.0	21.0	102.4
09NAH14-03	162	277017	2.7	9.7055	0.5	4.2572	1.1	0.2997	0.9	0.89	1689.7	14.0	1685.1	8.7	1679.5	9.0	1679.5	9.0	100.6
09NAH14-04	121	519476	2.3	9.7121	0.6	4.2056	1.3	0.2962	1.1	0.86	1672.6	16.3	1675.1	10.5	1678.2	12.0	1678.2	12.0	99.7
09NAH14-05	183	37028	1.7	5.7573	0.3	11.9887	2.7	0.5006	2.7	0.99	2616.4	58.0	2603.5	25.5	2593.5	5.2	2593.5	5.2	100.9
09NAH14-06	249	189209	1.1	11.0894	0.6	3.0249	1.1	0.2433	0.9	0.83	1403.8	11.3	1413.9	8.3	1429.2	11.7	1429.2	11.7	98.2
09NAH14-07	93	93140	1.3	9.4516	0.6	4.5039	1.4	0.3087	1.3	0.90	1734.5	19.6	1731.7	11.9	1728.3	11.5	1728.3	11.5	100.4
09NAH14-08	141	58128	2.9	9.6318	0.7	4.2844	2.7	0.2993	2.6	0.96	1687.8	39.0	1690.4	22.4	1693.5	13.4	1693.5	13.4	99.7
09NAH14-09	229	203727	3.9	9.6222	0.4	4.3770	0.9	0.3055	0.8	0.88	1718.3	11.9	1708.0	7.4	1695.4	7.9	1695.4	7.9	101.4
09NAH14-10	186	346669	4.2	9.5326	0.3	4.2143	0.6	0.2914	0.5	0.88	1648.3	7.2	1676.8	4.6	1712.6	5.0	1712.6	5.0	96.2
09NAH14-11	115	64815	0.8	11.0011	1.1	3.1753	2.7	0.2534	2.5	0.91	1455.7	32.6	1451.2	21.2	1444.5	21.6	1444.5	21.6	100.8
09NAH14-12	117	140532	3.3	9.6264	0.7	4.2800	2.1	0.2988	2.0	0.94	1685.4	29.1	1689.5	17.1	1694.6	12.8	1694.6	12.8	99.5
09NAH14-13	58	85164	1.4	9.6910	1.5	4.2642	2.5	0.2997	2.0	0.81	1689.9	29.7	1686.5	20.3	1682.2	26.8	1682.2	26.8	100.5
09NAH14-14	145	143850	1.7	9.5242	0.5	4.3926	1.2	0.3034	1.1	0.90	1708.3	16.8	1710.9	10.3	1714.2	10.1	1714.2	10.1	99.7
09NAH14-15	206	37058	3.5	9.7941	0.9	4.0906	2.3	0.2906	2.1	0.92	1644.4	30.3	1652.4	18.5	1662.7	16.2	1662.7	16.2	98.9
09NAH14-16	152	174450	1.3	9.6812	0.8	4.1385	2.3	0.2906	2.1	0.93	1644.4	30.9	1661.9	18.7	1684.1	15.4	1684.1	15.4	97.6
09NAH14-17	51	35950	0.7	10.9624	2.2	3.0987	2.6	0.2464	1.3	0.50	1419.7	16.5	1432.4	19.9	1451.2	42.7	1451.2	42.7	97.8
09NAH14-18	219	329953	5.1	9.5848	0.6	4.4261	1.8	0.3077	1.7	0.94	1729.3	25.5	1717.2	14.8	1702.6	11.1	1702.6	11.1	101.6

09NAH14-19	171	154818	2.1	9.5772	0.4	4.4937	2.3	0.3121	2.3	0.98	1751.2	35.4	1729.8	19.5	1704.0	7.8	1704.0	7.8	102.8
09NAH14-21	81	67772	1.5	10.9958	1.2	3.1621	1.8	0.2522	1.4	0.75	1449.7	17.9	1448.0	14.1	1445.4	22.8	1445.4	22.8	100.3
09NAH14-22	75	87718	4.1	9.5699	0.8	4.3303	1.0	0.3006	0.6	0.61	1694.1	9.5	1699.2	8.6	1705.4	15.2	1705.4	15.2	99.3
09NAH14-24	119	109951	2.1	11.0585	0.8	3.1398	2.0	0.2518	1.9	0.92	1447.9	24.5	1442.5	15.8	1434.6	14.8	1434.6	14.8	100.9
09NAH14-25	214	351775	1.7	11.0241	0.6	3.1601	0.7	0.2527	0.5	0.66	1452.2	6.3	1447.5	5.7	1440.5	10.6	1440.5	10.6	100.8
09NAH14-26	108	137275	0.9	11.0572	0.9	3.0893	1.8	0.2477	1.5	0.85	1426.8	19.0	1430.0	13.4	1434.8	17.8	1434.8	17.8	99.4
09NAH14-27	81	238973	1.9	9.6524	1.2	4.3141	2.4	0.3020	2.1	0.88	1701.3	31.7	1696.1	19.9	1689.6	21.5	1689.6	21.5	100.7
09NAH14-28	110	169807	1.3	11.0320	1.2	3.1788	2.2	0.2543	1.9	0.85	1460.8	24.9	1452.0	17.4	1439.1	22.8	1439.1	22.8	101.5
09NAH14-29	323	544818	3.8	9.5983	0.3	4.3297	1.1	0.3014	1.0	0.97	1698.3	15.6	1699.0	8.9	1700.0	4.9	1700.0	4.9	99.9
09NAH14-30	125	103435	0.9	11.0771	0.5	3.2458	2.4	0.2608	2.4	0.98	1493.7	31.4	1468.2	18.7	1431.4	9.9	1431.4	9.9	104.4
09NAH14-31	128	121655	2.0	11.1039	0.7	3.0401	1.1	0.2448	0.8	0.72	1411.7	9.8	1417.7	8.1	1426.8	14.0	1426.8	14.0	98.9
09NAH14-32	380	42342	1.7	9.4350	0.3	4.2040	5.4	0.2877	5.4	1.00	1629.9	78.3	1674.8	44.7	1731.5	5.4	1731.5	5.4	94.1
09NAH14-33	99	171983	1.3	10.9681	0.8	3.1813	1.9	0.2531	1.7	0.91	1454.3	22.6	1452.6	14.7	1450.2	14.8	1450.2	14.8	100.3
09NAH14-35	175	243039	3.1	9.4482	0.6	4.4138	2.7	0.3025	2.6	0.97	1703.5	38.9	1714.9	22.1	1728.9	11.6	1728.9	11.6	98.5
09NAH14-36	63	18226	2.2	17.6423	5.7	0.6723	6.0	0.0860	1.6	0.27	532.0	8.3	522.1	24.3	479.2	126.8	532.0	8.3	111.0
09NAH14-38	39	10534	1.2	19.2077	11.6	0.5970	12.5	0.0832	4.6	0.37	515.0	22.8	475.3	47.5	288.2	266.3	515.0	22.8	178.7
09NAH14-39	121	164206	2.5	9.3711	0.7	4.6549	1.2	0.3164	1.0	0.79	1772.0	15.1	1759.2	10.3	1744.0	13.7	1744.0	13.7	101.6
09NAH14-41	151	168622	1.9	9.4768	0.5	4.4629	1.0	0.3067	0.9	0.88	1724.7	13.2	1724.1	8.2	1723.4	8.6	1723.4	8.6	100.1
09NAH14-42	198	54009	1.4	11.1000	0.8	2.8828	2.4	0.2321	2.3	0.94	1345.4	27.9	1377.4	18.4	1427.4	15.7	1427.4	15.7	94.3
09NAH14-43	166	184919	2.6	9.4936	0.4	4.5226	1.2	0.3114	1.2	0.95	1747.6	17.9	1735.1	10.2	1720.1	6.7	1720.1	6.7	101.6
09NAH14-44	47	29730	1.2	11.1729	2.2	3.0811	2.3	0.2497	0.7	0.32	1436.8	9.6	1428.0	17.8	1414.9	42.0	1414.9	42.0	101.5
09NAH14-46	59	148318	2.0	9.5682	0.9	4.4237	1.5	0.3070	1.3	0.83	1725.9	19.4	1716.8	12.8	1705.7	16.0	1705.7	16.0	101.2
09NAH14-47	36	44760	1.6	9.7671	2.0	4.3141	3.9	0.3056	3.3	0.86	1719.0	49.8	1696.1	31.8	1667.8	36.8	1667.8	36.8	103.1
09NAH14-48	91	74758	1.0	10.9480	1.1	3.1264	1.4	0.2482	0.9	0.60	1429.4	11.0	1439.2	11.0	1453.7	21.8	1453.7	21.8	98.3
09NAH14-49	493	36750	2.0	9.4614	0.4	4.2344	3.7	0.2906	3.7	1.00	1644.4	53.3	1680.7	30.3	1726.4	6.7	1726.4	6.7	95.2
09NAH14-50	249	237452	1.6	11.0433	0.4	3.1578	3.0	0.2529	3.0	0.99	1453.5	39.2	1446.9	23.5	1437.2	7.5	1437.2	7.5	101.1
09NAH14-51	111	34713	3.0	10.1041	1.2	4.0080	2.9	0.2937	2.6	0.91	1660.0	38.0	1635.8	23.2	1604.8	22.0	1604.8	22.0	103.4

09NAH14-52	129	53118	1.2	11.0213	0.4	3.1487	1.1	0.2517	1.0	0.92	1447.2	12.7	1444.7	8.2	1441.0	8.1	1441.0	8.1	100.4
09NAH14-53	585	85822	1.5	9.6624	0.2	4.0785	2.3	0.2858	2.3	1.00	1620.6	33.1	1650.0	18.9	1687.7	2.9	1687.7	2.9	96.0
09NAH14-54	186	191722	2.8	9.3819	0.3	4.5211	1.6	0.3076	1.6	0.98	1729.0	23.8	1734.9	13.3	1741.9	6.2	1741.9	6.2	99.3
09NAH14-55	187	23944	0.9	9.8103	0.7	3.4343	2.7	0.2444	2.6	0.97	1409.3	33.0	1512.3	21.2	1659.6	12.8	1659.6	12.8	84.9
09NAH14-56	21	33824	3.3	9.2767	2.3	4.5919	2.8	0.3089	1.6	0.58	1735.5	24.4	1747.8	23.2	1762.5	41.6	1762.5	41.6	98.5
09NAH14-57	213	245427	2.6	9.6648	0.5	4.3324	0.9	0.3037	0.8	0.84	1709.5	11.5	1699.5	7.6	1687.2	9.3	1687.2	9.3	101.3
09NAH14-58	79	69218	1.5	11.0428	1.7	3.0999	2.7	0.2483	2.2	0.80	1429.5	27.9	1432.7	21.0	1437.3	31.6	1437.3	31.6	99.5
09NAH14-59	137	104148	1.4	9.5450	0.4	4.4756	1.9	0.3098	1.9	0.98	1739.9	28.9	1726.5	16.1	1710.2	7.0	1710.2	7.0	101.7
09NAH14-60	134	143453	1.3	9.4601	0.7	4.4607	1.1	0.3061	0.9	0.82	1721.2	14.2	1723.7	9.5	1726.6	12.0	1726.6	12.0	99.7
09NAH14-61	245	204792	2.4	9.3781	0.3	4.5896	0.9	0.3122	0.9	0.96	1751.4	13.4	1747.4	7.6	1742.6	4.8	1742.6	4.8	100.5
09NAH14-62	174	44165	2.3	9.6375	0.6	4.2559	1.1	0.2975	1.0	0.86	1678.8	14.6	1684.9	9.4	1692.4	10.7	1692.4	10.7	99.2
09NAH14-64	40	51592	1.0	9.7702	2.0	4.2054	2.4	0.2980	1.4	0.58	1681.4	20.9	1675.1	19.8	1667.2	36.2	1667.2	36.2	100.9
09NAH14-65	98	144290	1.6	10.9063	1.1	3.2484	1.5	0.2569	1.0	0.69	1474.2	13.7	1468.8	11.6	1461.0	20.5	1461.0	20.5	100.9
09NAH14-66	44	41241	3.6	9.2374	2.3	4.8051	2.8	0.3219	1.6	0.58	1799.1	25.1	1785.8	23.3	1770.3	41.3	1770.3	41.3	101.6
09NAH14-67	248	260812	2.9	11.0077	0.4	3.0681	2.2	0.2449	2.1	0.99	1412.3	27.2	1424.8	16.6	1443.3	6.8	1443.3	6.8	97.9
09NAH14-68	92	173005	0.9	11.0206	1.5	3.1852	2.1	0.2546	1.5	0.72	1462.1	19.8	1453.6	16.3	1441.1	27.8	1441.1	27.8	101.5
09NAH14-69	239	59361	2.8	9.5455	0.3	4.4326	3.9	0.3069	3.9	1.00	1725.3	59.4	1718.5	32.6	1710.1	5.5	1710.1	5.5	100.9
09NAH14-70	112	16159	0.6	10.9264	1.8	3.2531	2.3	0.2578	1.5	0.64	1478.6	19.4	1469.9	17.9	1457.5	33.7	1457.5	33.7	101.4
09NAH14-71	67	97005	1.7	9.5289	0.8	4.4027	1.1	0.3043	0.8	0.73	1712.5	12.6	1712.8	9.4	1713.3	14.2	1713.3	14.2	99.9
09NAH14-72	170	118114	2.5	9.3783	0.4	4.6217	1.5	0.3144	1.4	0.97	1762.1	21.6	1753.2	12.1	1742.6	7.0	1742.6	7.0	101.1
09NAH14-73	101	367482	2.8	9.4327	0.6	4.4392	1.1	0.3037	1.0	0.85	1709.6	14.5	1719.7	9.4	1731.9	10.8	1731.9	10.8	98.7
09NAH14-74	134	154302	2.0	9.6333	0.5	4.3715	3.3	0.3054	3.3	0.99	1718.2	49.0	1707.0	27.2	1693.2	8.9	1693.2	8.9	101.5
09NAH14-75	277	257794	4.4	11.0655	0.4	2.9980	2.9	0.2406	2.8	0.99	1389.8	35.6	1407.1	21.9	1433.4	7.6	1433.4	7.6	97.0
09NAH14-76	125	99218	1.9	10.9675	1.0	3.1662	1.6	0.2518	1.3	0.80	1448.0	17.0	1448.9	12.6	1450.3	18.4	1450.3	18.4	99.8
09NAH14-77	220	204755	2.5	9.6848	0.4	4.3361	2.8	0.3046	2.8	0.99	1713.9	41.8	1700.3	23.2	1683.4	8.0	1683.4	8.0	101.8
09NAH14-78	361	665678	2.8	9.5487	0.3	4.4901	1.5	0.3110	1.5	0.98	1745.4	23.2	1729.1	12.8	1709.5	5.3	1709.5	5.3	102.1
09NAH14-79	107	143859	3.0	9.5435	0.6	4.4467	1.2	0.3078	1.1	0.88	1729.8	16.1	1721.1	10.0	1710.5	10.7	1710.5	10.7	101.1

09NAH14-80	50	34021	1.6	9.7571	1.6	4.3820	4.8	0.3101	4.5	0.94	1741.2	69.4	1709.0	40.0	1669.7	30.4	1669.7	30.4	104.3
09NAH14-81	108	131850	1.9	11.0252	0.6	3.1597	1.3	0.2527	1.2	0.89	1452.2	15.5	1447.4	10.4	1440.3	11.6	1440.3	11.6	100.8
09NAH14-82	32	43566	2.8	9.2556	1.7	4.7657	2.1	0.3199	1.3	0.61	1789.3	20.1	1778.9	17.7	1766.7	30.5	1766.7	30.5	101.3
09NAH14-83	196	176914	3.2	11.3839	0.6	2.8941	1.2	0.2389	1.0	0.88	1381.2	13.0	1380.4	9.0	1379.0	11.0	1379.0	11.0	100.2
09NAH14-84	292	279631	2.4	9.3771	0.4	4.5453	2.4	0.3091	2.3	0.99	1736.4	35.3	1739.3	19.6	1742.8	7.4	1742.8	7.4	99.6
09NAH14-85	224	200447	4.7	9.5112	0.3	4.5018	3.3	0.3105	3.3	0.99	1743.4	49.9	1731.3	27.3	1716.7	6.4	1716.7	6.4	101.6
09NAH14-86	79	75438	1.4	11.0510	1.1	3.2093	1.8	0.2572	1.4	0.80	1475.6	19.0	1459.4	13.9	1435.9	20.6	1435.9	20.6	102.8
09NAH14-87	89	164690	2.2	9.6437	1.3	4.4935	3.9	0.3143	3.7	0.94	1761.8	56.8	1729.8	32.5	1691.3	24.4	1691.3	24.4	104.2
09NAH14-88	108	82451	2.1	9.6306	0.5	4.3671	2.6	0.3050	2.5	0.98	1716.2	37.9	1706.1	21.2	1693.8	9.7	1693.8	9.7	101.3
09NAH14-89	81	45430	0.9	11.0485	1.5	3.1510	2.9	0.2525	2.5	0.85	1451.3	31.9	1445.3	22.1	1436.3	28.4	1436.3	28.4	101.0
09NAH14-90	88	107424	0.9	11.0352	1.6	3.2204	2.2	0.2577	1.4	0.64	1478.3	18.2	1462.1	16.7	1438.6	31.4	1438.6	31.4	102.8
09NAH14-91	65	79454	1.4	9.5314	0.8	4.4450	1.9	0.3073	1.7	0.90	1727.3	26.0	1720.8	15.8	1712.8	15.2	1712.8	15.2	100.8
09NAH14-92	63	25508	0.9	11.0492	1.7	3.1433	2.6	0.2519	2.1	0.78	1448.2	26.8	1443.4	20.4	1436.2	31.6	1436.2	31.6	100.8
09NAH14-93	202	235514	1.9	9.3839	0.4	4.5398	2.4	0.3090	2.3	0.98	1735.6	35.6	1738.3	19.8	1741.5	8.1	1741.5	8.1	99.7
09NAH14-94	187	237745	1.2	11.0439	0.4	3.2366	4.2	0.2592	4.1	0.99	1486.0	54.9	1466.0	32.3	1437.1	8.4	1437.1	8.4	103.4
09NAH14-96	135	84199	1.1	11.0621	0.9	3.1710	1.3	0.2544	1.0	0.75	1461.2	12.9	1450.1	10.2	1433.9	16.6	1433.9	16.6	101.9
09NAH14-96	140	190566	3.1	9.3832	0.6	4.6791	1.2	0.3184	1.0	0.86	1782.1	15.9	1763.5	10.0	1741.6	11.3	1741.6	11.3	102.3
09NAH14-99	269	11780	1.1	10.0494	0.6	3.3027	4.1	0.2407	4.0	0.99	1390.4	50.3	1481.7	31.7	1614.9	11.5	1614.9	11.5	86.1
09NAH14-100	362	97283	5.9	9.7411	0.3	4.0601	1.2	0.2868	1.2	0.96	1625.7	17.2	1646.3	10.1	1672.7	6.1	1672.7	6.1	97.2
09NAH14-102	62	44282	1.6	9.8963	1.6	4.0835	2.6	0.2931	2.1	0.80	1657.0	30.9	1651.0	21.5	1643.4	29.2	1643.4	29.2	100.8
09NAH14-103	239	70592	3.3	9.1251	3.7	3.8850	5.0	0.2571	3.2	0.66	1475.1	42.8	1610.6	40.0	1792.6	68.1	1792.6	68.1	82.3

15NAH14-1	87	87216	2.3	9.3603	1.0	4.6609	1.5	0.3164	1.1	0.73	1772.2	16.7	1760.2	12.4	1746.1	18.8	1746.1	18.8	101.5
15NAH14-2	168	22964	2.1	8.9403	0.3	4.2884	3.6	0.2781	3.6	1.00	1581.6	50.4	1691.1	29.7	1829.7	6.2	1829.7	6.2	86.4
15NAH14-3	40	99875	0.8	5.5492	1.1	13.0366	1.5	0.5247	1.0	0.67	2719.0	22.3	2682.3	14.2	2654.7	18.7	2654.7	18.7	102.4
15NAH14-4	107	106616	1.7	8.4357	0.4	5.8373	2.5	0.3571	2.4	0.99	1968.6	41.2	1952.0	21.3	1934.4	6.9	1934.4	6.9	101.8
15NAH14-5	36	41256	2.0	8.6048	1.3	5.4794	1.6	0.3420	0.8	0.55	1896.1	14.0	1897.4	13.4	1898.8	23.4	1898.8	23.4	99.9

15NAH14-6	108	52399	2.8	11.0313	1.2	3.1784	1.4	0.2543	0.7	0.53	1460.6	9.7	1451.9	10.9	1439.3	22.8	1439.3	22.8	101.5
15NAH14-7	181	408766	1.7	11.0049	0.7	3.0850	1.7	0.2462	1.6	0.91	1419.0	19.9	1429.0	13.1	1443.8	13.2	1443.8	13.2	98.3
15NAH14-8	38	86473	0.8	5.4647	0.9	13.2175	1.4	0.5239	1.0	0.76	2715.5	23.2	2695.3	13.0	2680.2	14.8	2680.2	14.8	101.3
15NAH14-9	106	107824	1.7	11.1624	1.7	3.1610	2.1	0.2559	1.3	0.60	1468.9	16.5	1447.7	16.2	1416.7	32.2	1416.7	32.2	103.7
15NAH14-10	87	79805	2.0	9.1843	1.2	4.8076	1.3	0.3202	0.6	0.42	1790.9	8.9	1786.2	11.3	1780.8	22.3	1780.8	22.3	100.6
15NAH14-11	45	119871	1.3	4.9855	0.5	15.3325	0.7	0.5544	0.5	0.73	2843.4	11.7	2836.1	6.7	2830.9	7.9	2830.9	7.9	100.4
15NAH14-12	43	43044	1.4	8.8325	1.7	5.2271	2.2	0.3348	1.4	0.64	1861.8	22.8	1857.0	18.8	1851.7	30.7	1851.7	30.7	100.5
15NAH14-13	60	31401	2.0	12.8588	3.1	2.0821	3.3	0.1942	1.2	0.36	1144.0	12.6	1142.9	22.9	1141.0	61.8	1141.0	61.8	100.3
15NAH14-14	166	243972	2.9	9.1522	0.5	4.8651	0.8	0.3229	0.6	0.79	1804.1	9.9	1796.2	6.7	1787.1	8.8	1787.1	8.8	100.9
15NAH14-15	22	63726	0.7	8.9413	3.2	5.0726	3.9	0.3289	2.4	0.60	1833.3	37.6	1831.5	33.4	1829.5	57.1	1829.5	57.1	100.2
15NAH14-16	69	95685	2.4	9.1381	0.9	4.8803	1.5	0.3234	1.1	0.77	1806.5	17.8	1798.9	12.4	1790.0	17.1	1790.0	17.1	100.9
15NAH14-17	116	84179	1.8	8.7790	0.6	5.1382	1.7	0.3272	1.6	0.94	1824.6	25.6	1842.4	14.5	1862.7	10.2	1862.7	10.2	98.0
15NAH14-18	84	186357	1.0	5.4671	0.4	13.2450	1.2	0.5252	1.2	0.94	2721.1	26.0	2697.3	11.7	2679.5	6.8	2679.5	6.8	101.6
15NAH14-19	20	52238	1.4	5.3505	1.5	13.8106	2.1	0.5359	1.5	0.70	2766.4	32.8	2736.8	19.8	2715.1	24.7	2715.1	24.7	101.9
15NAH14-20	25	5671	0.9	8.3251	4.6	5.7403	5.4	0.3466	2.8	0.52	1918.3	47.0	1937.5	46.8	1958.0	82.2	1958.0	82.2	98.0
15NAH14-21	48	36447	0.4	7.7883	1.1	6.8858	1.5	0.3889	1.1	0.71	2117.9	19.8	2096.8	13.7	2076.1	19.2	2076.1	19.2	102.0
15NAH14-22	76	119104	1.8	7.7397	0.3	6.8080	0.7	0.3822	0.7	0.93	2086.4	11.7	2086.8	6.2	2087.2	4.6	2087.2	4.6	100.0
15NAH14-23	142	124365	2.7	8.8321	0.5	5.2561	2.4	0.3367	2.4	0.98	1870.7	38.8	1861.8	20.8	1851.8	8.6	1851.8	8.6	101.0
15NAH14-24	100	55373	2.6	11.1035	0.7	3.1715	1.0	0.2554	0.7	0.72	1466.3	9.4	1450.3	7.7	1426.8	13.2	1426.8	13.2	102.8
15NAH14-25	40	43542	1.0	8.8726	1.2	5.2505	1.7	0.3379	1.2	0.68	1876.4	19.1	1860.8	14.6	1843.5	22.6	1843.5	22.6	101.8
15NAH14-26	98	93248	2.1	8.8967	1.1	5.2117	1.5	0.3363	0.9	0.62	1868.8	14.8	1854.5	12.4	1838.6	20.6	1838.6	20.6	101.6
15NAH14-27	144	176259	1.6	8.5183	0.6	5.6389	1.1	0.3484	1.0	0.87	1926.8	16.3	1922.1	9.7	1916.9	10.0	1916.9	10.0	100.5
15NAH14-28	33	57300	1.3	4.5553	0.5	18.0433	1.2	0.5961	1.1	0.92	3014.1	25.8	2992.0	11.2	2977.2	7.5	2977.2	7.5	101.2
15NAH14-29	129	35607	2.5	11.1098	0.9	3.0613	1.2	0.2467	0.9	0.71	1421.2	10.8	1423.1	9.2	1425.7	16.2	1425.7	16.2	99.7
15NAH14-30	58	175495	1.3	8.8580	1.4	5.2967	1.8	0.3403	1.1	0.62	1888.0	18.2	1868.3	15.2	1846.5	25.2	1846.5	25.2	102.3
15NAH14-31	20	33488	1.2	8.7620	3.4	5.2075	4.6	0.3309	3.0	0.66	1842.9	48.4	1853.8	38.8	1866.2	61.6	1866.2	61.6	98.8
15NAH14-32	38	40074	1.2	10.9519	3.3	3.0846	3.6	0.2450	1.4	0.38	1412.7	17.5	1428.9	27.4	1453.0	62.9	1453.0	62.9	97.2

15NAH14-34	51	115145	3.4	12.8888	4.7	2.1355	4.9	0.1996	1.3	0.26	1173.3	13.7	1160.4	33.6	1136.3	93.3	1136.3	93.3	103.3
15NAH14-35	108	137077	1.5	8.8062	0.9	5.3389	1.1	0.3410	0.7	0.63	1891.4	11.2	1875.1	9.3	1857.1	15.4	1857.1	15.4	101.8
15NAH14-36	31	46368	0.8	8.4397	2.8	5.9405	3.3	0.3636	1.8	0.53	1999.3	30.1	1967.2	28.7	1933.5	50.0	1933.5	50.0	103.4
15NAH14-37	34	54703	1.0	6.7024	1.3	9.1206	1.8	0.4434	1.2	0.70	2365.6	24.7	2350.2	16.3	2336.8	21.6	2336.8	21.6	101.2
15NAH14-38	39	79985	0.9	8.5173	1.9	5.8809	3.2	0.3633	2.7	0.82	1997.7	45.5	1958.4	28.1	1917.1	33.4	1917.1	33.4	104.2
15NAH14-39	42	38775	1.3	8.9071	1.6	5.2922	2.3	0.3419	1.6	0.71	1895.7	26.5	1867.6	19.5	1836.5	29.2	1836.5	29.2	103.2
15NAH14-40	46	42287	3.8	8.7638	1.8	5.3118	2.0	0.3376	0.8	0.42	1875.2	13.5	1870.8	16.7	1865.8	32.0	1865.8	32.0	100.5
15NAH14-41	113	130648	2.7	9.1297	0.7	4.8771	0.9	0.3229	0.6	0.64	1804.0	9.1	1798.3	7.6	1791.6	12.7	1791.6	12.7	100.7
15NAH14-42	127	144349	0.6	7.7633	0.4	7.0565	1.2	0.3973	1.1	0.94	2156.7	21.0	2118.6	10.8	2081.8	7.5	2081.8	7.5	103.6
15NAH14-43	270	224876	3.2	11.1332	0.7	2.6904	1.3	0.2172	1.1	0.83	1267.3	12.3	1325.8	9.6	1421.7	13.9	1421.7	13.9	89.1
15NAH14-44	25	27733	0.5	5.3675	1.6	13.6173	3.2	0.5301	2.7	0.86	2741.9	60.9	2723.5	29.9	2709.8	26.4	2709.8	26.4	101.2
15NAH14-45	77	24818	1.0	5.4246	0.4	13.3978	0.9	0.5271	0.8	0.88	2729.3	18.5	2708.1	8.9	2692.3	7.3	2692.3	7.3	101.4
15NAH14-47	79	51249	0.8	8.6602	0.6	5.5275	0.9	0.3472	0.7	0.73	1921.1	11.0	1904.9	7.8	1887.2	11.3	1887.2	11.3	101.8
15NAH14-48	66	69979	1.7	8.5996	0.7	5.5833	1.4	0.3482	1.3	0.87	1926.1	21.0	1913.5	12.4	1899.9	12.6	1899.9	12.6	101.4
15NAH14-49	76	60229	0.8	11.0672	1.1	3.1547	1.9	0.2532	1.5	0.81	1455.1	19.8	1446.2	14.4	1433.1	20.8	1433.1	20.8	101.5
15NAH14-50	261	262666	5.7	9.2363	0.3	4.7408	0.7	0.3176	0.6	0.90	1777.9	10.0	1774.5	6.0	1770.5	5.7	1770.5	5.7	100.4
15NAH14-51	60	225817	0.8	5.3962	0.5	13.7552	1.0	0.5383	0.9	0.85	2776.5	19.3	2733.0	9.5	2701.0	8.6	2701.0	8.6	102.8
15NAH14-52	191	247132	1.0	8.3145	0.5	6.1442	1.1	0.3705	1.0	0.89	2031.8	17.2	1996.6	9.7	1960.2	9.1	1960.2	9.1	103.7
15NAH14-53	30	36143	0.8	8.4770	2.1	5.6156	5.4	0.3453	5.0	0.92	1911.9	82.3	1918.5	46.4	1925.6	37.0	1925.6	37.0	99.3
15NAH14-54	72	51208	1.6	8.9754	0.9	5.1318	1.0	0.3341	0.5	0.51	1858.0	8.4	1841.4	8.6	1822.6	15.7	1822.6	15.7	101.9
15NAH14-55	82	79530	1.6	9.1939	0.9	4.8617	1.1	0.3242	0.6	0.53	1810.1	9.2	1795.6	9.2	1778.9	16.9	1778.9	16.9	101.8
15NAH14-56	205	290362	1.9	8.5644	0.4	5.8049	0.8	0.3606	0.7	0.86	1984.9	11.9	1947.1	7.0	1907.2	7.5	1907.2	7.5	104.1
15NAH14-58	150	173559	3.1	9.1656	0.5	5.0435	1.0	0.3353	0.8	0.87	1863.8	13.7	1826.6	8.2	1784.5	8.8	1784.5	8.8	104.4
15NAH14-59	53	112387	1.1	5.3102	0.3	13.9185	0.8	0.5360	0.7	0.90	2766.9	15.9	2744.2	7.5	2727.5	5.7	2727.5	5.7	101.4
15NAH14-60	63	138040	1.2	5.1935	0.8	14.5765	1.5	0.5490	1.3	0.83	2821.2	28.9	2788.0	14.4	2764.1	13.8	2764.1	13.8	102.1
15NAH14-61	44	23515	3.4	13.0548	5.4	2.0784	5.5	0.1968	0.8	0.14	1158.0	8.3	1141.7	37.4	1110.8	107.9	1110.8	107.9	104.3
15NAH14-62	131	210169	1.6	5.7268	0.3	12.1927	1.1	0.5064	1.1	0.96	2641.3	22.9	2619.3	10.3	2602.4	4.9	2602.4	4.9	101.5

15NAH14-63	77	138399	0.7	5.3226	0.3	13.7983	0.6	0.5327	0.5	0.86	2752.6	11.1	2736.0	5.4	2723.7	4.8	2723.7	4.8	101.1
15NAH14-64	112	115681	6.5	9.1813	0.9	4.8653	1.7	0.3240	1.4	0.85	1809.1	22.6	1796.3	14.2	1781.4	16.1	1781.4	16.1	101.6
15NAH14-65	85	139902	2.9	8.7207	1.4	5.3846	1.8	0.3406	1.1	0.59	1889.4	17.3	1882.4	15.3	1874.7	26.0	1874.7	26.0	100.8
15NAH14-66	133	116504	2.2	8.8801	0.5	5.2114	2.4	0.3356	2.3	0.98	1865.6	37.4	1854.5	20.1	1842.0	8.7	1842.0	8.7	101.3
15NAH14-67	99	147217	2.3	8.7748	0.5	5.2987	1.0	0.3372	0.9	0.87	1873.3	14.5	1868.7	8.7	1863.5	9.0	1863.5	9.0	100.5
15NAH14-68	76	116003	3.4	8.8077	1.3	5.2222	1.5	0.3336	0.8	0.56	1855.8	13.7	1856.2	12.9	1856.8	22.6	1856.8	22.6	99.9
15NAH14-69	82	127710	3.3	9.0866	1.0	4.8417	1.3	0.3191	0.9	0.67	1785.2	13.8	1792.2	11.2	1800.2	18.1	1800.2	18.1	99.2
15NAH14-70	50	38801	1.7	11.1307	3.5	3.0802	3.6	0.2487	0.7	0.20	1431.6	9.5	1427.8	27.7	1422.1	67.7	1422.1	67.7	100.7
15NAH14-71	26	27613	1.7	9.7420	3.4	4.2651	3.9	0.3014	1.9	0.49	1698.0	28.7	1686.7	32.0	1672.5	62.5	1672.5	62.5	101.5
15NAH14-72	38	69242	1.2	8.6231	1.3	5.6123	1.8	0.3510	1.2	0.67	1939.4	20.1	1918.0	15.4	1894.9	23.8	1894.9	23.8	102.3
15NAH14-73	102	252889	1.8	5.7339	0.3	12.1550	0.9	0.5055	0.9	0.96	2637.3	19.1	2616.4	8.6	2600.3	4.2	2600.3	4.2	101.4
15NAH14-74	44	79413	1.4	10.0532	1.3	3.8621	1.6	0.2816	1.0	0.63	1599.4	14.7	1605.8	13.3	1614.2	23.7	1614.2	23.7	99.1
15NAH14-75	17	26050	1.2	5.3315	2.0	13.6250	2.9	0.5268	2.2	0.74	2728.2	48.7	2724.0	27.8	2720.9	32.3	2720.9	32.3	100.3
15NAH14-76	49	64543	1.3	8.5909	1.4	5.5459	2.8	0.3456	2.5	0.88	1913.3	40.7	1907.7	24.1	1901.7	24.3	1901.7	24.3	100.6
15NAH14-77	26	38785	1.3	8.9137	1.9	5.1352	2.4	0.3320	1.4	0.60	1848.0	23.2	1841.9	20.3	1835.1	34.4	1835.1	34.4	100.7
15NAH14-78	130	181357	2.8	11.0553	1.0	3.1158	1.7	0.2498	1.4	0.82	1437.6	17.4	1436.6	12.8	1435.1	18.3	1435.1	18.3	100.2
15NAH14-79	22	25663	1.4	5.9060	0.9	11.2449	2.4	0.4817	2.2	0.93	2534.5	47.0	2543.6	22.6	2550.9	15.3	2550.9	15.3	99.4
15NAH14-80	106	84231	1.7	8.9053	0.6	5.1457	1.6	0.3323	1.5	0.93	1849.8	24.5	1843.7	14.0	1836.8	11.3	1836.8	11.3	100.7
15NAH14-81	60	55147	1.8	8.4697	1.2	5.7681	3.0	0.3543	2.7	0.92	1955.2	46.0	1941.6	25.7	1927.2	21.0	1927.2	21.0	101.5
15NAH14-82	43	61013	0.7	8.4608	1.1	5.6183	3.0	0.3448	2.8	0.93	1909.5	46.4	1918.9	26.0	1929.1	20.0	1929.1	20.0	99.0
15NAH14-83	140	61501	1.6	9.1966	0.7	4.2997	1.3	0.2868	1.1	0.82	1625.5	15.3	1693.3	10.7	1778.3	13.5	1778.3	13.5	91.4
15NAH14-84	75	171472	2.9	8.7511	1.1	5.3952	1.9	0.3424	1.6	0.81	1898.3	25.5	1884.1	16.4	1868.4	20.2	1868.4	20.2	101.6
15NAH14-85	93	153287	0.5	5.7397	0.5	12.2636	3.0	0.5105	3.0	0.99	2658.8	65.4	2624.8	28.5	2598.6	7.8	2598.6	7.8	102.3
15NAH14-86	19	48221	1.4	4.4900	1.3	18.4574	1.8	0.6011	1.2	0.70	3034.1	29.6	3013.9	17.0	3000.4	20.3	3000.4	20.3	101.1
15NAH14-87	49	71027	1.7	5.2977	0.6	14.0268	1.3	0.5389	1.2	0.90	2779.1	26.3	2751.5	12.3	2731.4	9.3	2731.4	9.3	101.7
15NAH14-88	16	15060	2.1	10.7127	4.6	3.2576	5.2	0.2531	2.4	0.46	1454.5	30.9	1471.0	40.4	1494.9	87.6	1494.9	87.6	97.3
15NAH14-89	65	61892	1.5	8.4547	1.3	5.8022	1.6	0.3558	1.0	0.61	1962.2	16.2	1946.7	13.7	1930.3	22.5	1930.3	22.5	101.6

15NAH14-90	135	330377	0.5	5.3658	0.3	13.3592	0.6	0.5199	0.5	0.89	2698.7	11.3	2705.4	5.4	2710.3	4.3	2710.3	4.3	99.6
15NAH14-91	108	82814	3.0	11.1258	1.5	3.1062	1.7	0.2506	0.9	0.54	1441.8	12.1	1434.2	13.3	1423.0	28.0	1423.0	28.0	101.3
15NAH14-92	68	165815	1.0	5.5657	0.7	12.5416	3.0	0.5063	2.9	0.98	2640.6	63.1	2645.8	28.1	2649.8	11.0	2649.8	11.0	99.7
15NAH14-93	26	15520	0.7	8.7430	3.8	5.5572	4.5	0.3524	2.5	0.56	1946.0	42.7	1909.5	39.1	1870.1	68.0	1870.1	68.0	104.1
15NAH14-94	77	90899	1.7	9.1943	1.1	4.8698	1.7	0.3247	1.3	0.74	1812.8	19.8	1797.0	14.3	1778.8	20.9	1778.8	20.9	101.9
15NAH14-95	71	70667	2.8	10.9849	1.2	3.1588	1.4	0.2517	0.7	0.52	1447.1	9.5	1447.2	10.9	1447.3	23.1	1447.3	23.1	100.0
15NAH14-96	49	92990	1.6	9.6166	1.4	4.3579	1.6	0.3039	0.7	0.45	1710.8	11.0	1704.4	13.4	1696.4	26.7	1696.4	26.7	100.8
15NAH14-97	145	211955	2.4	7.8494	0.4	6.6554	0.6	0.3789	0.5	0.78	2071.1	8.4	2066.7	5.4	2062.4	6.7	2062.4	6.7	100.4
15NAH14-98	96	289977	1.9	9.1976	0.9	4.8267	1.2	0.3220	0.7	0.62	1799.3	11.6	1789.6	10.0	1778.1	17.1	1778.1	17.1	101.2
15NAH14-99	55	68243	2.1	7.8876	0.9	6.6809	1.3	0.3822	0.9	0.68	2086.5	15.9	2070.1	11.5	2053.8	16.8	2053.8	16.8	101.6
15NAH14-100	54	49487	1.2	8.8278	2.0	5.2387	2.3	0.3354	1.2	0.51	1864.6	19.0	1858.9	19.7	1852.7	36.0	1852.7	36.0	100.6

16NAH14-1	75	72627	1.2	8.7909	0.9	5.2539	3.5	0.3350	3.4	0.96	1862.5	54.2	1861.4	29.7	1860.2	16.6	1860.2	16.6	100.1
16NAH14-2	67	42227	1.0	11.4197	3.1	2.9133	3.4	0.2413	1.4	0.40	1393.4	17.1	1385.4	25.9	1373.0	60.5	1373.0	60.5	101.5
16NAH14-3	34	26479	1.9	9.6517	2.0	4.2616	2.5	0.2983	1.5	0.60	1682.9	21.8	1686.0	20.3	1689.7	36.5	1689.7	36.5	99.6
16NAH14-4	142	96457	2.4	10.9340	1.0	3.1988	1.4	0.2537	0.9	0.69	1457.4	12.3	1456.9	10.6	1456.1	19.0	1456.1	19.0	100.1
16NAH14-5	40	51106	1.7	9.7082	2.9	4.3104	3.4	0.3035	1.8	0.53	1708.6	26.8	1695.3	27.7	1679.0	52.7	1679.0	52.7	101.8
16NAH14-6	29	37059	3.1	8.8353	1.8	5.2223	2.7	0.3346	2.0	0.75	1860.9	32.5	1856.3	22.7	1851.1	31.7	1851.1	31.7	100.5
16NAH14-7	59	85803	1.2	11.2091	2.2	3.0459	2.5	0.2476	1.2	0.47	1426.2	15.0	1419.2	19.2	1408.7	42.6	1408.7	42.6	101.2
16NAH14-8	52	70466	1.0	11.3078	2.0	2.8720	2.6	0.2355	1.7	0.65	1363.5	20.8	1374.6	19.5	1391.9	37.6	1391.9	37.6	98.0
16NAH14-9	157	112889	2.0	9.1309	0.7	4.7982	1.0	0.3178	0.7	0.72	1778.7	11.1	1784.6	8.3	1791.4	12.4	1791.4	12.4	99.3
16NAH14-10	186	299037	3.9	9.2582	0.5	4.6390	0.8	0.3115	0.6	0.80	1748.1	9.9	1756.3	6.8	1766.1	8.9	1766.1	8.9	99.0
16NAH14-11	163	106855	2.1	9.5753	0.5	4.0820	1.4	0.2835	1.3	0.93	1608.9	18.1	1650.7	11.1	1704.4	9.3	1704.4	9.3	94.4
16NAH14-12	65	62736	1.3	9.2037	0.9	4.7629	1.4	0.3179	1.1	0.78	1779.6	17.6	1778.4	12.2	1776.9	16.4	1776.9	16.4	100.2
16NAH14-13	131	101441	1.9	11.0191	0.5	3.1404	0.9	0.2510	0.8	0.82	1443.5	10.1	1442.7	7.3	1441.4	10.3	1441.4	10.3	100.1
16NAH14-14	19	24734	1.4	9.0108	4.8	4.9353	5.2	0.3225	2.1	0.41	1802.1	33.4	1808.3	44.2	1815.5	86.9	1815.5	86.9	99.3
16NAH14-15	41	100656	1.1	5.5254	0.7	12.5313	1.1	0.5022	0.9	0.76	2623.2	18.7	2645.1	10.7	2661.9	12.3	2661.9	12.3	98.5

16NAH14-16	116	7922	1.7	9.8896	1.2	3.9729	1.6	0.2850	1.1	0.66	1616.3	15.2	1628.7	13.1	1644.7	22.7	1644.7	22.7	98.3
16NAH14-17	33	12931	0.8	8.7539	1.5	5.3506	3.2	0.3397	2.8	0.88	1885.2	45.8	1877.0	27.3	1867.8	27.4	1867.8	27.4	100.9
16NAH14-18	77	77808	0.6	5.3621	0.6	13.3853	0.8	0.5206	0.6	0.74	2701.5	13.8	2707.2	8.0	2711.5	9.3	2711.5	9.3	99.6
16NAH14-19	35	50429	0.4	4.0877	0.5	21.3089	0.9	0.6317	0.7	0.81	3156.4	17.9	3152.8	8.6	3150.4	8.2	3150.4	8.2	100.2
16NAH14-20	117	102381	2.3	9.6474	0.7	4.3351	1.1	0.3033	0.9	0.78	1707.8	13.2	1700.1	9.4	1690.6	13.2	1690.6	13.2	101.0
16NAH14-21	33	75511	0.6	8.9469	1.8	4.9881	2.5	0.3237	1.7	0.68	1807.6	26.6	1817.3	21.0	1828.4	32.9	1828.4	32.9	98.9
16NAH14-22	240	274514	2.1	11.1966	0.5	3.0644	1.3	0.2488	1.2	0.93	1432.5	15.1	1423.8	9.7	1410.9	9.2	1410.9	9.2	101.5
16NAH14-23	94	159960	1.2	5.3025	0.3	13.8192	1.1	0.5314	1.0	0.96	2747.6	22.5	2737.4	10.0	2729.9	5.1	2729.9	5.1	100.6
16NAH14-24	111	70797	1.1	11.4673	1.4	2.9093	1.5	0.2420	0.6	0.41	1396.9	7.8	1384.3	11.4	1365.0	26.5	1365.0	26.5	102.3
16NAH14-25	108	158016	2.1	8.7816	0.7	5.3519	1.3	0.3409	1.1	0.83	1890.8	17.2	1877.2	10.8	1862.1	12.6	1862.1	12.6	101.5
16NAH14-26	65	4347	0.3	8.9171	1.4	5.0914	1.9	0.3293	1.3	0.68	1834.9	20.3	1834.7	15.9	1834.4	25.0	1834.4	25.0	100.0
16NAH14-27	102	49564	1.3	11.5410	1.1	2.8412	1.6	0.2378	1.2	0.75	1375.4	15.2	1366.5	12.2	1352.6	20.5	1352.6	20.5	101.7
16NAH14-28	129	88227	1.0	11.5240	0.9	2.8135	1.2	0.2352	0.7	0.62	1361.4	8.9	1359.1	8.8	1355.5	17.8	1355.5	17.8	100.4
16NAH14-29	85	137796	2.4	5.7723	0.5	11.9429	1.2	0.5000	1.1	0.92	2613.7	24.3	2599.9	11.5	2589.2	7.8	2589.2	7.8	100.9
16NAH14-30	252	241697	3.5	7.7428	0.3	6.4583	3.8	0.3627	3.8	1.00	1994.8	65.5	2040.2	33.7	2086.4	5.6	2086.4	5.6	95.6
16NAH14-31	126	174455	2.7	9.1023	0.5	4.8569	1.2	0.3206	1.1	0.90	1792.8	16.8	1794.8	10.1	1797.1	9.6	1797.1	9.6	99.8
16NAH14-32	106	76143	1.7	11.0540	1.4	3.1033	1.6	0.2488	0.6	0.38	1432.2	7.6	1433.5	12.0	1435.3	27.5	1435.3	27.5	99.8
16NAH14-33	145	32521	1.9	11.0538	0.9	3.1534	1.1	0.2528	0.7	0.61	1452.9	9.0	1445.8	8.8	1435.4	17.3	1435.4	17.3	101.2
16NAH14-34	118	63582	4.1	11.0277	0.8	3.2247	1.6	0.2579	1.3	0.86	1479.1	17.7	1463.1	12.2	1439.9	15.5	1439.9	15.5	102.7
16NAH14-35	123	126815	1.3	9.7295	0.8	4.2232	2.4	0.2980	2.2	0.95	1681.4	33.1	1678.5	19.4	1674.9	14.0	1674.9	14.0	100.4
16NAH14-36	133	286434	1.3	8.4398	0.4	5.7788	1.0	0.3537	0.9	0.90	1952.4	15.7	1943.2	8.9	1933.5	7.9	1933.5	7.9	101.0
16NAH14-37	134	97007	1.1	7.0600	0.6	7.6373	1.5	0.3911	1.4	0.93	2127.7	25.9	2189.3	13.9	2247.4	10.1	2247.4	10.1	94.7
16NAH14-38	162	101168	2.8	10.9728	1.0	3.1386	1.5	0.2498	1.1	0.73	1437.3	14.2	1442.2	11.7	1449.4	19.8	1449.4	19.8	99.2
16NAH14-39	59	54618	1.0	11.3866	2.1	2.9763	2.7	0.2458	1.7	0.63	1416.8	21.2	1401.6	20.2	1378.6	39.6	1378.6	39.6	102.8
16NAH14-40	108	160670	1.8	8.7232	0.3	5.3852	0.9	0.3407	0.8	0.92	1890.0	13.7	1882.5	7.7	1874.2	6.3	1874.2	6.3	100.8
16NAH14-41	69	72381	2.2	8.2266	0.7	6.1808	1.4	0.3688	1.2	0.85	2023.6	20.3	2001.7	12.0	1979.2	13.0	1979.2	13.0	102.2
16NAH14-42	40	42827	3.5	5.3981	1.3	14.1029	4.0	0.5521	3.8	0.95	2834.1	87.0	2756.7	38.0	2700.4	21.2	2700.4	21.2	104.9

16NAH14-43	58	64434	1.1	9.9436	2.0	4.0498	2.1	0.2921	0.6	0.31	1651.8	9.2	1644.2	16.9	1634.6	36.7	1634.6	36.7	101.1
16NAH14-44	189	123770	4.0	11.0170	0.5	3.1373	0.8	0.2507	0.6	0.73	1442.0	7.2	1441.9	5.9	1441.7	9.9	1441.7	9.9	100.0
16NAH14-45	132	125793	1.2	8.9651	0.6	5.0456	0.6	0.3281	0.3	0.49	1829.0	5.1	1827.0	5.5	1824.7	10.3	1824.7	10.3	100.2
16NAH14-46	92	101146	1.3	7.7478	0.6	6.8186	1.0	0.3832	0.8	0.79	2091.0	13.9	2088.1	8.8	2085.3	10.7	2085.3	10.7	100.3
16NAH14-47	17	19929	0.5	9.4029	3.0	4.7622	4.8	0.3248	3.8	0.78	1812.9	59.9	1778.3	40.7	1737.8	55.5	1737.8	55.5	104.3
16NAH14-48	23	27617	1.0	11.5158	7.2	2.8088	7.6	0.2346	2.4	0.31	1358.5	29.2	1357.9	57.1	1356.9	139.6	1356.9	139.6	100.1
16NAH14-49	110	132101	1.2	11.2957	1.4	2.8568	1.7	0.2340	0.9	0.51	1355.6	10.5	1370.6	12.5	1394.0	27.4	1394.0	27.4	97.3
16NAH14-50	141	72435	2.9	11.1071	1.1	2.6680	1.3	0.2149	0.8	0.57	1255.0	8.7	1319.6	9.9	1426.2	21.1	1426.2	21.1	88.0
16NAH14-51	74	129397	1.3	11.3442	1.7	2.9422	2.4	0.2421	1.8	0.72	1397.5	22.0	1392.8	18.5	1385.8	32.4	1385.8	32.4	100.8
16NAH14-52	107	99978	2.1	10.9127	0.9	3.1741	1.2	0.2512	0.8	0.66	1444.8	10.7	1450.9	9.6	1459.8	17.7	1459.8	17.7	99.0
16NAH14-53	118	156557	2.0	7.7950	0.8	6.7730	1.2	0.3829	0.8	0.73	2089.9	15.1	2082.2	10.2	2074.6	13.8	2074.6	13.8	100.7
16NAH14-54	24	17828	1.3	11.8713	5.1	2.7251	5.6	0.2346	2.4	0.42	1358.7	28.8	1335.3	41.7	1298.0	99.1	1298.0	99.1	104.7
16NAH14-55	65	125404	0.9	5.7810	1.4	10.8102	1.9	0.4532	1.3	0.68	2409.7	26.6	2506.9	18.1	2586.7	23.7	2586.7	23.7	93.2
16NAH14-56	212	213691	3.4	9.3757	0.3	4.6821	1.0	0.3184	0.9	0.96	1781.8	14.5	1764.0	8.1	1743.1	4.7	1743.1	4.7	102.2
16NAH14-57	38	20349	3.3	12.9277	3.0	2.1143	3.6	0.1982	1.9	0.53	1165.9	20.3	1153.5	24.7	1130.3	60.4	1130.3	60.4	103.1
16NAH14-58	81	65504	1.1	9.1917	1.2	4.9346	1.5	0.3290	0.9	0.62	1833.4	15.1	1808.2	12.8	1779.3	21.7	1779.3	21.7	103.0
16NAH14-59	72	59494	1.4	11.4464	1.2	2.9248	1.8	0.2428	1.3	0.74	1401.3	16.6	1388.3	13.5	1368.5	23.2	1368.5	23.2	102.4
16NAH14-60	96	94240	1.0	8.9626	1.1	5.1196	1.8	0.3328	1.5	0.80	1851.9	23.8	1839.4	15.7	1825.2	20.0	1825.2	20.0	101.5
16NAH14-61	196	357440	1.3	8.9759	0.4	5.0779	0.7	0.3306	0.6	0.81	1841.1	9.5	1832.4	6.2	1822.5	7.9	1822.5	7.9	101.0
16NAH14-62	142	145611	3.2	9.4166	0.6	4.5384	1.9	0.3100	1.8	0.95	1740.5	27.9	1738.0	16.1	1735.1	11.5	1735.1	11.5	100.3
16NAH14-63	55	44517	1.2	9.7685	1.8	4.2456	2.1	0.3008	1.1	0.53	1695.2	16.9	1682.9	17.5	1667.5	33.3	1667.5	33.3	101.7
16NAH14-64	136	177450	2.9	9.2350	1.0	4.8143	1.8	0.3225	1.5	0.85	1801.7	24.3	1787.4	15.3	1770.7	17.6	1770.7	17.6	101.7
16NAH14-65	64	57893	0.9	9.0654	1.0	5.1306	1.2	0.3373	0.6	0.48	1873.8	9.4	1841.2	10.1	1804.5	18.9	1804.5	18.9	103.8
16NAH14-66	108	168450	2.4	11.3442	1.7	2.9182	1.9	0.2401	0.8	0.45	1387.2	10.4	1386.6	14.1	1385.8	32.0	1385.8	32.0	100.1
16NAH14-67	94	102048	1.3	11.4809	1.9	2.8451	2.3	0.2369	1.4	0.58	1370.6	16.7	1367.5	17.6	1362.7	37.0	1362.7	37.0	100.6
16NAH14-68	115	189226	1.0	5.4916	0.3	13.2540	1.2	0.5279	1.2	0.97	2732.6	26.5	2697.9	11.5	2672.0	4.8	2672.0	4.8	102.3
16NAH14-69	36	32093	0.4	7.7676	1.8	6.8707	2.3	0.3871	1.4	0.60	2109.2	24.7	2094.9	20.3	2080.8	32.2	2080.8	32.2	101.4

16NAH14-70	120	101007	1.0	5.3996	0.4	12.4818	1.3	0.4888	1.2	0.96	2565.5	25.3	2641.4	11.8	2700.0	6.1	2700.0	6.1	95.0
16NAH14-71	50	46605	0.9	8.4559	1.8	5.7291	2.2	0.3514	1.2	0.56	1941.0	20.4	1935.8	18.7	1930.1	32.1	1930.1	32.1	100.6
16NAH14-72	90	124634	1.0	7.7854	0.8	6.7589	1.3	0.3816	1.0	0.79	2083.9	18.0	2080.4	11.3	2076.8	13.9	2076.8	13.9	100.3
16NAH14-73	86	90671	0.9	11.2015	2.3	3.0895	2.8	0.2510	1.5	0.55	1443.6	20.0	1430.1	21.4	1410.0	44.4	1410.0	44.4	102.4
16NAH14-74	50	47339	0.9	8.4743	1.3	5.8379	3.2	0.3588	2.9	0.91	1976.5	48.8	1952.1	27.4	1926.2	23.8	1926.2	23.8	102.6
16NAH14-75	38	20764	3.4	12.8574	5.8	2.1148	5.9	0.1972	1.5	0.25	1160.3	15.5	1153.6	41.0	1141.1	114.8	1141.1	114.8	101.7
16NAH14-76	63	45550	2.0	8.8304	1.4	5.2572	1.8	0.3367	1.1	0.60	1870.7	17.4	1861.9	15.1	1852.1	25.6	1852.1	25.6	101.0
16NAH14-77	153	96115	0.8	9.6260	0.7	4.2475	1.2	0.2965	0.9	0.79	1674.1	13.5	1683.3	9.5	1694.6	13.1	1694.6	13.1	98.8
16NAH14-78	185	129898	1.6	11.0402	0.4	3.1806	2.0	0.2547	2.0	0.98	1462.6	25.5	1452.5	15.4	1437.7	7.6	1437.7	7.6	101.7
16NAH14-79	125	88516	2.7	10.9418	0.8	3.1730	1.1	0.2518	0.7	0.67	1447.8	9.5	1450.6	8.4	1454.8	15.4	1454.8	15.4	99.5
16NAH14-80	163	237432	1.3	11.3690	0.6	2.9319	1.4	0.2417	1.3	0.91	1395.8	16.0	1390.2	10.7	1381.6	11.4	1381.6	11.4	101.0
16NAH14-81	28	31969	4.8	10.8072	3.6	3.2195	4.1	0.2523	1.8	0.45	1450.6	23.6	1461.9	31.5	1478.3	68.8	1478.3	68.8	98.1
16NAH14-82	52	61111	1.1	8.9902	0.8	5.0866	1.8	0.3317	1.6	0.89	1846.4	26.4	1833.9	15.7	1819.6	15.2	1819.6	15.2	101.5
16NAH14-83	58	80207	0.5	8.4991	1.0	5.6191	1.2	0.3464	0.7	0.54	1917.2	11.2	1919.0	10.7	1921.0	18.8	1921.0	18.8	99.8
16NAH14-84	80	89131	1.1	7.6732	1.3	7.2875	2.2	0.4056	1.8	0.82	2194.6	33.8	2147.3	19.8	2102.3	22.4	2102.3	22.4	104.4
16NAH14-85	33	59166	1.5	8.8919	2.4	5.2632	2.5	0.3394	0.8	0.33	1883.9	13.5	1862.9	21.6	1839.6	43.4	1839.6	43.4	102.4
16NAH14-86	148	179134	1.2	6.5468	0.3	9.6511	0.9	0.4583	0.8	0.92	2431.8	15.8	2402.1	7.8	2376.9	5.7	2376.9	5.7	102.3
16NAH14-87	26	25730	0.7	8.9259	2.8	5.2306	3.7	0.3386	2.4	0.65	1880.0	39.0	1857.6	31.3	1832.7	50.3	1832.7	50.3	102.6
16NAH14-88	39	31987	2.9	12.7448	2.2	2.1423	3.3	0.1980	2.5	0.75	1164.7	26.4	1162.6	22.8	1158.6	42.9	1158.6	42.9	100.5
16NAH14-89	43	64110	0.8	8.9594	1.6	5.1460	1.9	0.3344	0.9	0.49	1859.6	14.6	1843.7	15.9	1825.9	29.6	1825.9	29.6	101.8
16NAH14-90	107	83608	1.6	9.6237	1.2	4.2530	1.5	0.2968	0.9	0.62	1675.7	13.6	1684.3	12.2	1695.1	21.5	1695.1	21.5	98.9
16NAH14-91	138	156130	1.9	7.7248	0.2	6.7838	2.5	0.3801	2.4	1.00	2076.6	43.5	2083.6	21.8	2090.5	3.7	2090.5	3.7	99.3
16NAH14-92	69	46129	0.8	9.0471	0.9	5.0554	1.3	0.3317	0.9	0.72	1846.7	15.0	1828.7	11.0	1808.2	16.4	1808.2	16.4	102.1
16NAH14-93	140	221024	1.4	11.4126	1.1	2.9773	3.8	0.2464	3.6	0.96	1420.1	46.5	1401.9	28.9	1374.2	20.5	1374.2	20.5	103.3
16NAH14-94	196	222627	2.3	9.2774	0.5	4.6720	0.6	0.3144	0.4	0.65	1762.1	6.3	1762.2	5.2	1762.4	8.7	1762.4	8.7	100.0
16NAH14-95	110	39407	1.2	11.4135	1.9	2.5244	3.9	0.2090	3.5	0.88	1223.3	38.6	1279.1	28.7	1374.1	35.9	1374.1	35.9	89.0
16NAH14-96	122	105548	2.5	11.0664	0.9	3.1375	1.1	0.2518	0.5	0.44	1447.9	6.0	1441.9	8.1	1433.2	18.1	1433.2	18.1	101.0

16NAH14-97	91	86912	1.5	11.0721	1.3	3.1673	1.6	0.2543	0.9	0.58	1460.8	12.4	1449.2	12.5	1432.2	25.2	1432.2	25.2	102.0
16NAH14-98	87	106624	2.0	9.3944	0.7	4.6617	0.8	0.3176	0.3	0.42	1778.1	5.1	1760.4	6.6	1739.4	13.1	1739.4	13.1	102.2
16NAH14-99	30	15151	3.4	13.1944	5.0	2.0087	5.2	0.1922	1.6	0.31	1133.4	16.8	1118.5	35.5	1089.5	99.8	1089.5	99.8	104.0
16NAH14-100	117	10812	2.9	9.3420	0.8	4.1648	1.6	0.2822	1.4	0.86	1602.4	19.7	1667.1	13.2	1749.7	15.1	1749.7	15.1	91.6

Appendix II: Detrital zircon picture

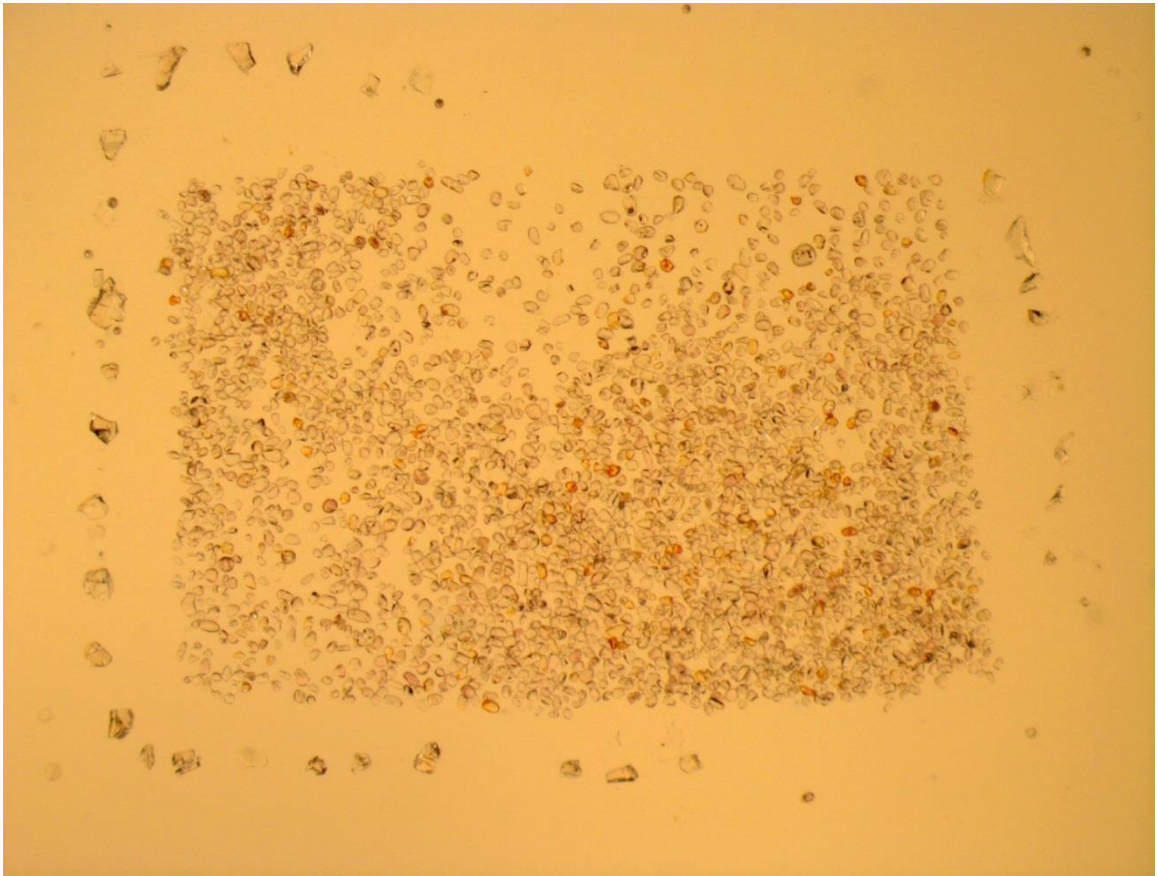


Photo showing grain mount of zircons for sample 16NAH14 with zircon standards for use during U-Pb analysis. Image is 3mm across.

Appendix III: Petrographic Descriptions

01NAH14: Dark tan to grey, submature, fine to medium-grained, peloidal-lithic-rich, ooid-bearing quartz arenite in a calcitic cement.

Quartz grains are well rounded to subrounded; two distributions of grain size depending on bedding layers; larger grains are well rounded to rounded while smaller grains are round to subrounded; very few exhibit undulose extinction, most have normal extinction. No feldspar exists in the sample. Most lithics are subrounded peloids, <1% of sedimentary lithics present and are all mudstones. Dolomitized ooids are sparse, but present in some beds.

Some quartz grains show radial isopached calcite rims (secondary) on opposing sides of the grains, so they are not fully encompassed, and rims are generally oriented 30° from bedding. This may indicate a secondary compaction direction with precipitation of this calcite. Otherwise, the cement is purely calcite with sparry calcite veins up to 1mm in thickness

04NAH14: Grey, submature, medium to fine-grained, lithic-bearing, calcite-cemented quartz arenite.

Quartz grains are subrounded to subangular; there is a small range in grain size which corresponds with bedding; some grains appear to be to have an extinction that looks similar to microcline's tartan twinning, but were uniaxial positive using the Bertand Lens. Small proportions of feldspar were present; slightly more plagioclase than k-spar – both showing cleavage, and k-spar showing small amounts of perthite texture; subrounded grains. Medium- to fine-grained mudstone lithics were also present; fine- to very fine-grained chert lithics, and <1% fine-grained carbonate lithics.

Large amounts of fine-grained sparry calcite cement is present; few voids filled with large sparry calcite grains.

09NAH14: Pink, immature, pebble and granule-sized quartz- and chert-lithic, calcite-cemented conglomerate.

Very course-grained to fine-grained sand, granule, and pebble-sized quartz grains; largely fractured grains; strongly undulose; no grains with normal extinction. Some metamorphic polycrystalline quartz grains. Few plagioclase feldspar grains; medium to fine-grained sized with minor albite twinning. There were populations of chert grains; small population of mudstone grains; both a large range in grain size (fine- to coarse-grained sand).

<<1% muscovite, but it's very fine-grained. This indicates a very local source and supports the hypothesis of it being derived from the Stansbury uplift.

15NAH14: Medium to dark grey, medium- to fine-grained, submature to mature, calcite-cemented quartz arenite with faint crossbedding.

Rounded to very well rounded quartz grains; medium- to fine-grained; some undulose extinction, rarely strongly undulated grains, most grains have normal extinction. Feldspar are scattered, but are mostly k-spar; overall, the feldspars are the larger grains in the sample & are mostly medium-grained (rarely fine-grained); subrounded to subangular. <<1% very fine grained chert lithics present.

Large proportion of calcite cement, some sparry.

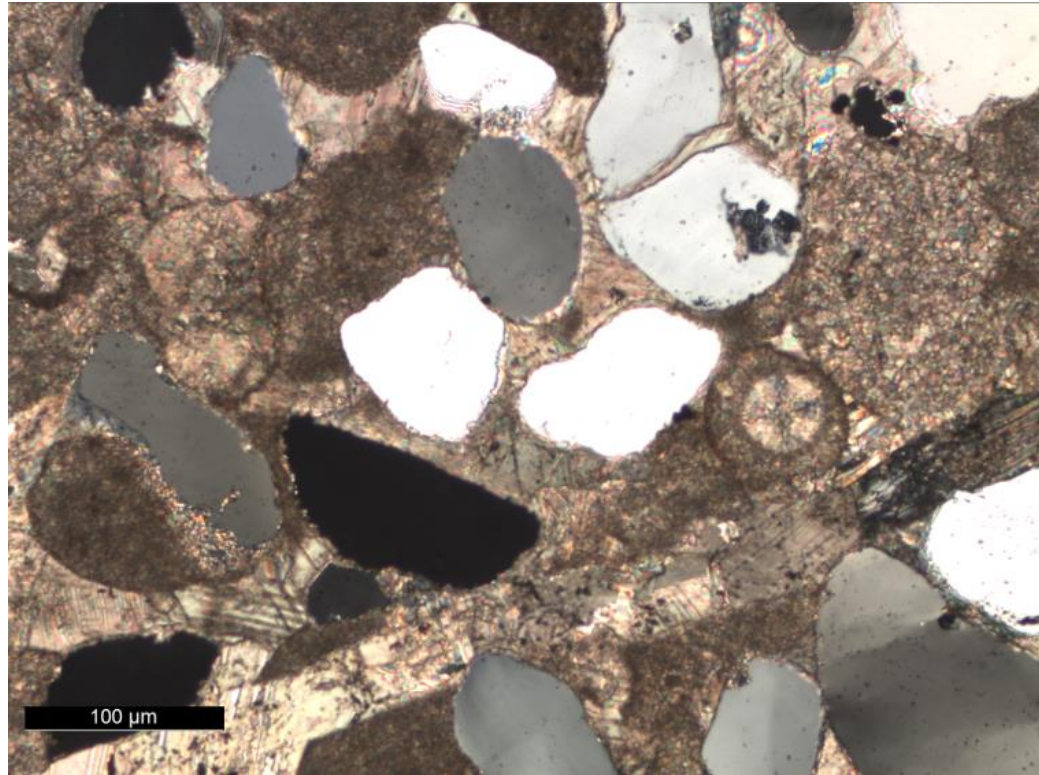
16NAH14: Light grey, very fine-grained, mature, calcite cemented quartz arenite.

Very well sorted; fine- to very fine-grained; subrounded to subangular; rarely undulose, most normal extinction. Very rare plagioclase and k-spar present; very fine-grained; subangular. Fine-grained subrounded to angular mudstone lithics. The mudstone mineralogy appears similar,

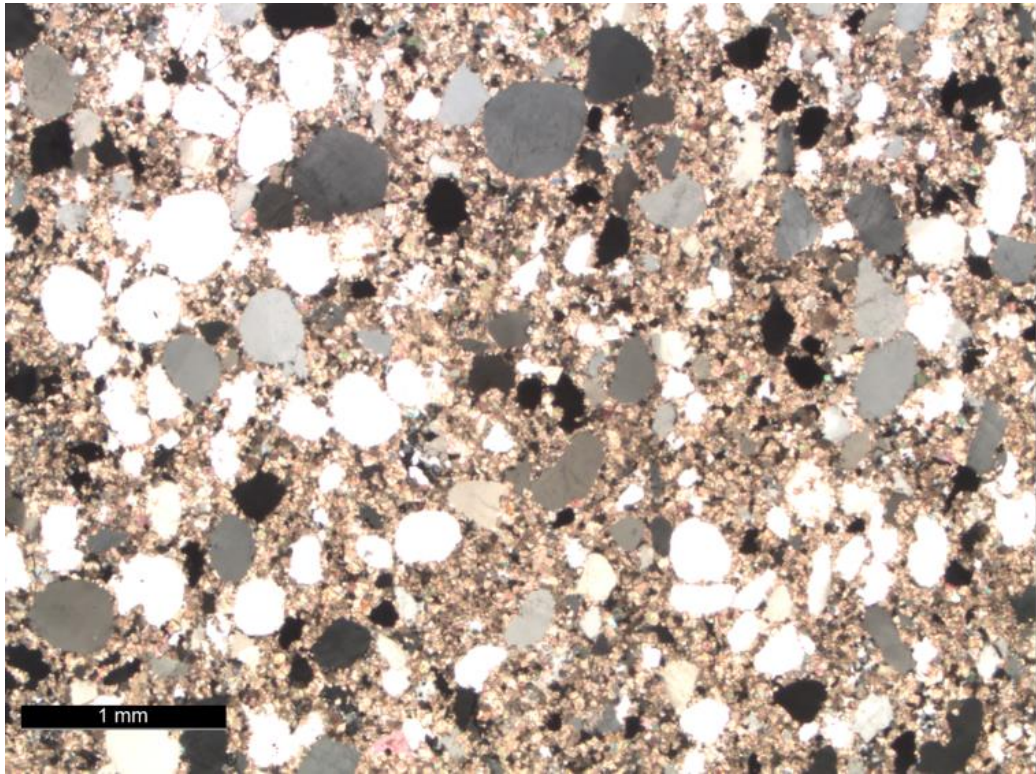
but due to range in angularity, there may be two different sources of mudstone. One fine-grained chert lithic found in sample.

Large proportion of secondary calcite cement, and a few voids filled with sparry calcite.

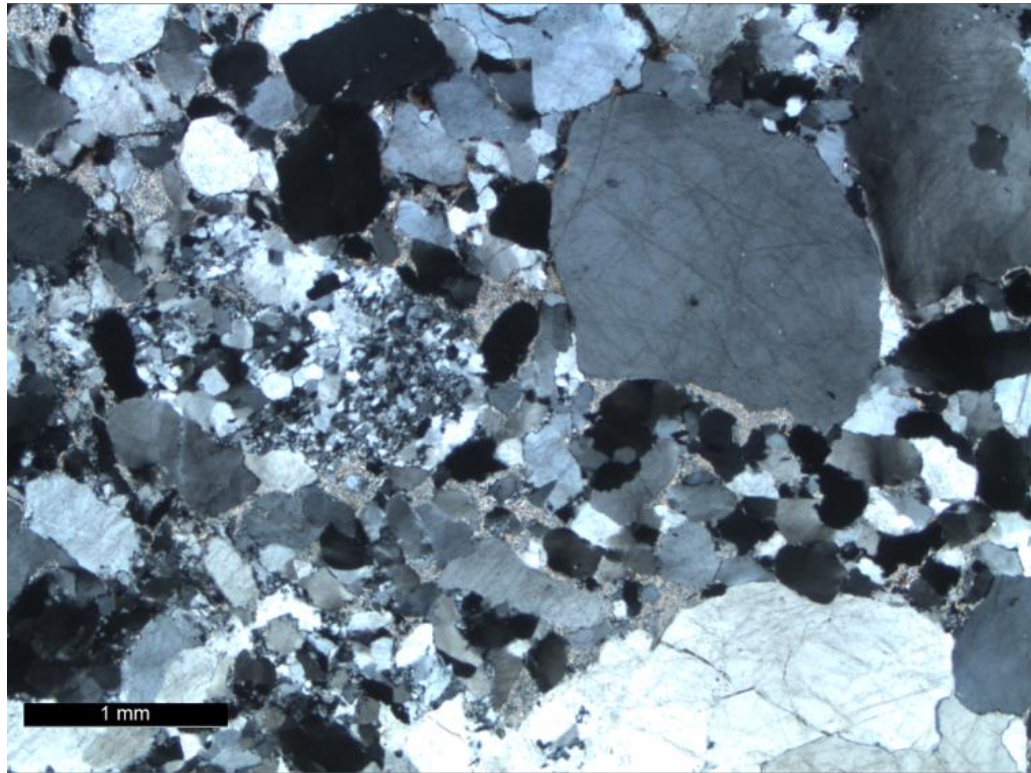
Appendix IV: Photomicrographs



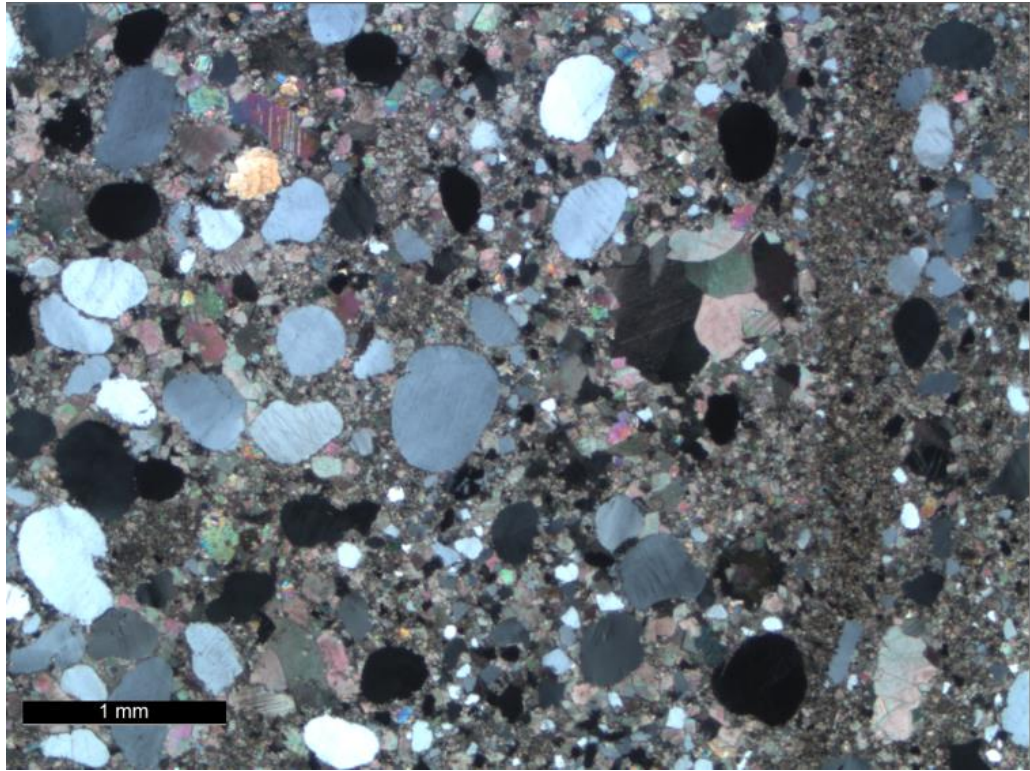
01NAH14: Showing rounded quartz grains, in sparry calcite cement, two squished peloids, an ooid, a calcite vein, and a grain of quartz with an isopached calcite rim.



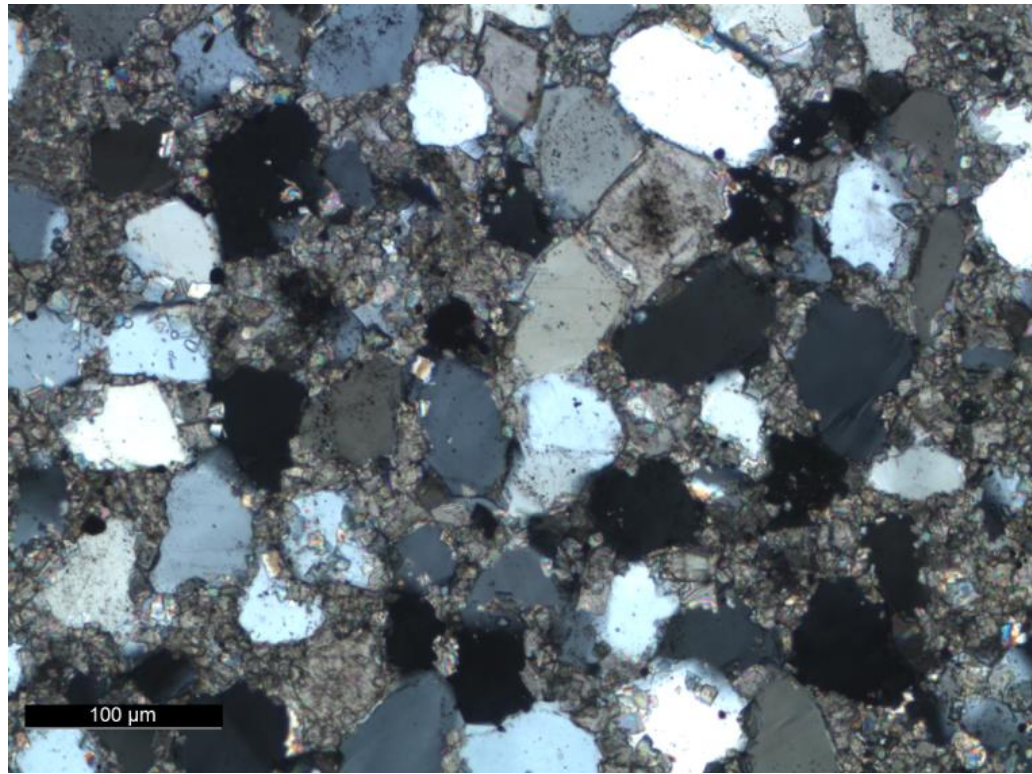
04NAH14: Showing rounded quartz grains, very minor populations of chert lithics, in a calcite cement.



09NAH14: Showing large ($>1\text{mm}$) undulose quartz grains, smaller populations of medium- to fine-grained rounded quartz grains, and chert lithics in a calcite cement.



15NAH14: Showing bedding dictated by different grain size changes and compositions. Rounded quartz grains, subrounded feldspars, and sparry calcite in a fine-grained calcitic matrix.



16NAH14: Showing subrounded to subangular quartz, subangular feldspar, and mudstone lithics in a calcite cemented matrix.

Appendix V: Foreland Basin Modeling Parameters

	Volume of Load (kg)	Load Density (kg/m ³)	Height of Crust (km)	α (km)	D (Nm)	ρ_{sediment} (kg/m ³)	$\rho_{\text{asthenosphere}}$ (kg/m ³)	Young's Modulus	Poissons Ratio
Antler	7.64×10^7	2600	3	119522	4×10^{23}	2500	3300	7×10^4	.25
Sevier	1.10×10^9	2800	40	267000	1×10^{21}	2500	3300	7×10^4	.25